

**THE GEOLOGICAL EVOLUTION
OF A PART OF THE
PONGOLA BASIN,
SOUTHEASTERN KAAPVAAL CRATON**

by

DIGBY JAMES COMRIE GOLD

*Submitted in partial fulfilment of the
requirements for the degree of
Doctor of Philosophy
in the
Department of Geology and Mineralogy
University of Natal*

Pietermaritzburg

September 1993

ABSTRACT

A stratigraphic and structural study of the Archaean Pongola Sequence on the southeastern Kaapvaal Craton centred on the area around the Klipwal Gold Mine is described. The lower predominantly volcanic Nsuze Group is overlain with a gradational transition by the upper clastic Mozaan Group in which six formations are recognized. The Sinqeni, Ntombe, Thalu, Hlashana, Odwaleni and the Kulphiso Formations. The Sinqeni and Hlashana Formations are predominantly arenaceous while the Ntombe and Kulphiso Formations are mainly argillaceous. The Odwaleni Formation contains a diamictite which is interpreted as a tillite, and is therefore the oldest glacial rock on record. The stratigraphic position of the Kulphiso Formation is problematic. The Mozaan Group was deposited in a deepening epeiric sea which was invaded periodically by storm generated deposits. Dolerite and ultramafic dykes and sills of various ages are represented.

Three phases of deformation are recognized in the Klipwal area. Early compression from the south-southeast initiated a major zone of bedding-parallel shear, the Izermijn shear zone, along the Nsuze-Mozaan contact and an oblique ramp, the Klipwal shear zone, at a higher stratigraphic level. An extensional phase caused reactivation of the Klipwal shear zone and the development of a major low-angle normal fault, the Gunsteling fault, above the Sinqeni Formation. The main phase of deformation, related to northeast-southwest compression is the most complex and most widely developed. Early northwest-trending subhorizontal upright folds were disrupted by contemporaneous north-striking dextral or dextral reverse shearing and northwest-striking sinistral or sinistral normal shearing. The obtuse relationship of these shear zones to the compression direction is probably the result of reactivation of basement structures with similar orientations. Northwest-trending folding continued during and after the shearing.

The structural styles and orientations observed in the Klipwal area are recognized regionally in the main Pongola basin, highlighting the need for further detailed studies before basin-wide correlations are made.

PREFACE

I, DIGBY JAMES COMRIE GOLD, hereby declare that this thesis
and its accompanying maps are my own original work,
that all assistance and sources of information have been acknowledged,
and that this work has not been presented to any other university
for the purpose of a higher degree.

A handwritten signature in blue ink, reading "Digby Gold", written over a horizontal line.

CONTENTS

CHAPTER 1: INTRODUCTION	1
OVERVIEW OF THE PONGOLA BASIN	1
Nsuze Group	1
Mozaan Group	4
Structural Evolution	4
Geochronology	5
PREVIOUS WORK	5
PRESENT STUDY	6
CHAPTER 2: STRATIGRAPHY AND SEDIMENTOLOGY	8
REGIONAL STRATIGRAPHY	8
Main Pongola Basin	10
Mfolozi Area	12
Kubuta Area	13
Mahlangatsha Area	14
Amsterdam Area	14
STRATIGRAPHY OF THE STUDY AREA	15
Upper Nsuze Group	15
Sedimentological Interpretation	17
Mozaan Group	21
<i>Singeni Formation</i>	25
<i>Ntombe Formation</i>	33
<i>Thalu Formation</i>	34
<i>Hlashana Formation</i>	36
<i>Odwaleni Formation</i>	40
<i>Kulphiso Formation</i>	45
Sedimentological Interpretation	50
<i>Singeni Formation</i>	56
<i>Ntombe Formation</i>	58
<i>Thalu Formation</i>	59
<i>Hlashana Formation</i>	60
<i>Odwaleni Formation</i>	62
<i>Kulphiso Formation</i>	64
Geochemistry	65
INTRUSIVE ROCKS	67
Geochemistry	67

CHAPTER 3: STRUCTURE	73
REGIONAL OVERVIEW	73
Main Pongola Basin	74
Mfolozi Area	76
Kubuta Area	77
Mahlangatsha Area	79
Amsterdam Area	80
THE STUDY AREA	80
North-northeasterly trending sinistral compressional shear zones and folds	83
<i>Izermijn Shear Zone</i>	83
<i>Ngwenya Syncline</i>	84
<i>Klipwal Shear Zone</i>	86
<i>Meander Shear Zone</i>	99
South-southeast directed normal faulting and associated folding ..	100
<i>Gunsteling Fault</i>	100
<i>Gunsteling anticline and syncline</i>	105
North-northwesterly trending folds	105
<i>Bethu Anticline</i>	108
<i>Mfeno Syncline and Anticline</i>	108
<i>Nombela Anticline</i>	110
<i>Prudentie Syncline</i>	111
Northerly trending dextral shear zones and faults	111
<i>Mkhuzwa Shear Zone</i>	112
<i>Qumeni Shear Zone</i>	113
<i>Altona Shear Zone</i>	113
<i>Sinqeni Shear Zone</i>	120
<i>Mhlope Shear Zone</i>	122
<i>Dwaleni Fault</i>	123
<i>Nkolotsheni-Bumbeni Shear Zone System</i>	125
<i>Nkolotsheni Shear Zone</i>	125
<i>Bumbeni Shear Zone</i>	126
<i>Khuphulangwenya Fault</i>	127
Northwesterly trending sinistral shear zones and faults	128
<i>Delft Shear Zone</i>	128
<i>Nkosetsha Shear Zone</i>	129
<i>Vergenoegheid Shear Zone</i>	129
<i>Mzamba Shear Zone</i>	130
<i>Duduka Fault</i>	130
Enigma of the conjugate shear zones	130
<i>Models for the conjugate relationship</i>	133

CHAPTER 4: SUMMARY AND CONCLUSIONS	139
GEODYNAMIC SYNTHESIS	139
SUMMARY	141
Stratigraphy	141
<i>The Study Area</i>	141
<i>Regional correlations</i>	142
<i>Depositional setting</i>	143
Structure	143
<i>The Study Area</i>	143
<i>Regional structure</i>	144
Concluding Statement	145
 REFERENCES	 146
 APPENDIX 1 : Thin section descriptions.	 159
 APPENDIX 2 : Geochemistry analyses	 163
 APPENDIX 3 : Locality sites	 166
 APPENDIX 4 : Sample preparation and analytical techniques	 167

ACKNOWLEDGEMENTS

This project went through various stages involving three supervisors. I would like to thank Dr Dawie Strydom for nurturing my interest in mapping and helping me with my fieldwork. I am indebted to Dr Mark Von Veh who assisted during the final phase and who took an interest in both the project and me as a person. Prof D.R. Hunter supervised the project during its middle phase.

This project forms part of the research undertaken by the Archaean Studies Research Group of the University of Natal, Pietermaritzburg, for which funding by the FRD and Anglo American Corporation is gratefully acknowledged. Financing for the computer on which this manuscript was prepared was contributed by the Klipwal Gold Mine and Lonrho (South Africa). The provision of a landcruiser by Dave Hill of Hillson Drilling is also greatly appreciated. Prof Allan Wilson and Mark Von Veh arranged funding during 1993.

James McKay, who entertained and encouraged the author while in the field, is thanked for initiating this study along with Dawie Strydom.

Roy Seyambu, Pat Suthan and Mukesh Seyambu contributed expert technical advice, including the preparation of samples for XRF, thin sections and developing of photographs.

The community at Klipwal are thanked for their hospitality. In particular Pete and Jenny McGaw (as well as Belinda and Mandy) who made my numerous field trips to Klipwal so enjoyable. Others I wish to thank are Rich and Chris Hobbs, Ian Jacobs, the Russells, the McEnerys, the Walkers and Dunlop van Rooyen.

Dieter Bührmann arranged the XRD analyses of the diamictites.

Numerous people contributed to this study through valuable discussions. Some of them are Profs V. Von Brunn, D.R. Hunter, Drs Dawie Strydom, Mark Von Veh, Roric Smith,

Marc Watchorn, Gary Gray, Bob Thomas, as well as Angela Riganti, Rich Hatfield, Alan McKenzie, Warwick Bullen, Julian Verbeek, Bruce Groenewald and Mbongeni Mabuza.

Anton Dlodlu is acknowledged for his assistance and witty companionship during the two years of fieldwork.

Olive Anderson proficiently draughted the numerous diagrams and maps and patiently carried out the vast number of alterations and corrections.

Dave Hill and Prof Norman Pammenter altruistically proof read the first and second editions of this manuscript respectively.

Leonie Berjak is thanked for her assistance and forbearance during the compilation of the manuscript in the final stages of preparation, along with Olive Anderson, Vicky Short and Lisa Cavé.

Finally, I wish to express my gratitude to my parents and sisters for their continued encouragement and support throughout my protracted career as a student.

CHAPTER 1: INTRODUCTION

OVERVIEW OF THE PONGOLA BASIN

The Pongola Sequence¹ constitutes an Archaean supracrustal succession on the southeastern Kaapvaal Craton and is exposed in northern Natal, southeastern Transvaal and in southern Swaziland (Figure 1.1). It is of considerable scientific interest because it is one of the earliest known cover sequences to have developed on a stabilized craton (Beukes, 1973). It contains the oldest recognized examples of tidalites (Von Brunn, 1974; Von Brunn and Mason, 1977), Superior type banded iron-formation (Beukes, 1973), palaeosols (Matthews and Scharrer, 1967; Watchorn and Armstrong, 1980) and diamictite (Von Brunn and Gold, 1993; this study). The sequence is subdivided into a lower volcano-sedimentary Nsuzi Group and an upper sedimentary Mozaan Group. The Nsuzi - Mozaan contact within the study area is gradational and is defined by the first appearance of orthoquartzite.

Nsuzi Group

The Nsuzi Group consists of extensive mafic to felsic volcanic rocks with subordinate sedimentary beds. The sedimentary component is largely restricted to a basal quartzite and to the uppermost beds, comprising mostly reworked tuffaceous volcanic rocks.

¹ Certain authors refer to the Pongola Sequence as a supergroup (e.g. Von Brunn and Hobday, 1976; Von Brunn and Mason, 1977; Watchorn, 1978, 1980; Laskowski and Kröner, 1985; Wronkiewicz and Condie, 1989; Matthews, 1990; Beukes and Cairncross, 1991a) whereas others assign group status to it (e.g. Button and Tyler, 1979; Button, 1981). Following the work of Hunter and Wilson (1988), Linström (1987) and Hatfield (1990) and in accordance with the recommendation of SACS (1980), the term sequence is adopted here. This term embraces major stratigraphic units of greater rank than group or supergroup traceable over large areas of a continent and bounded by unconformities of wide extent (SACS, *op. cit.*).

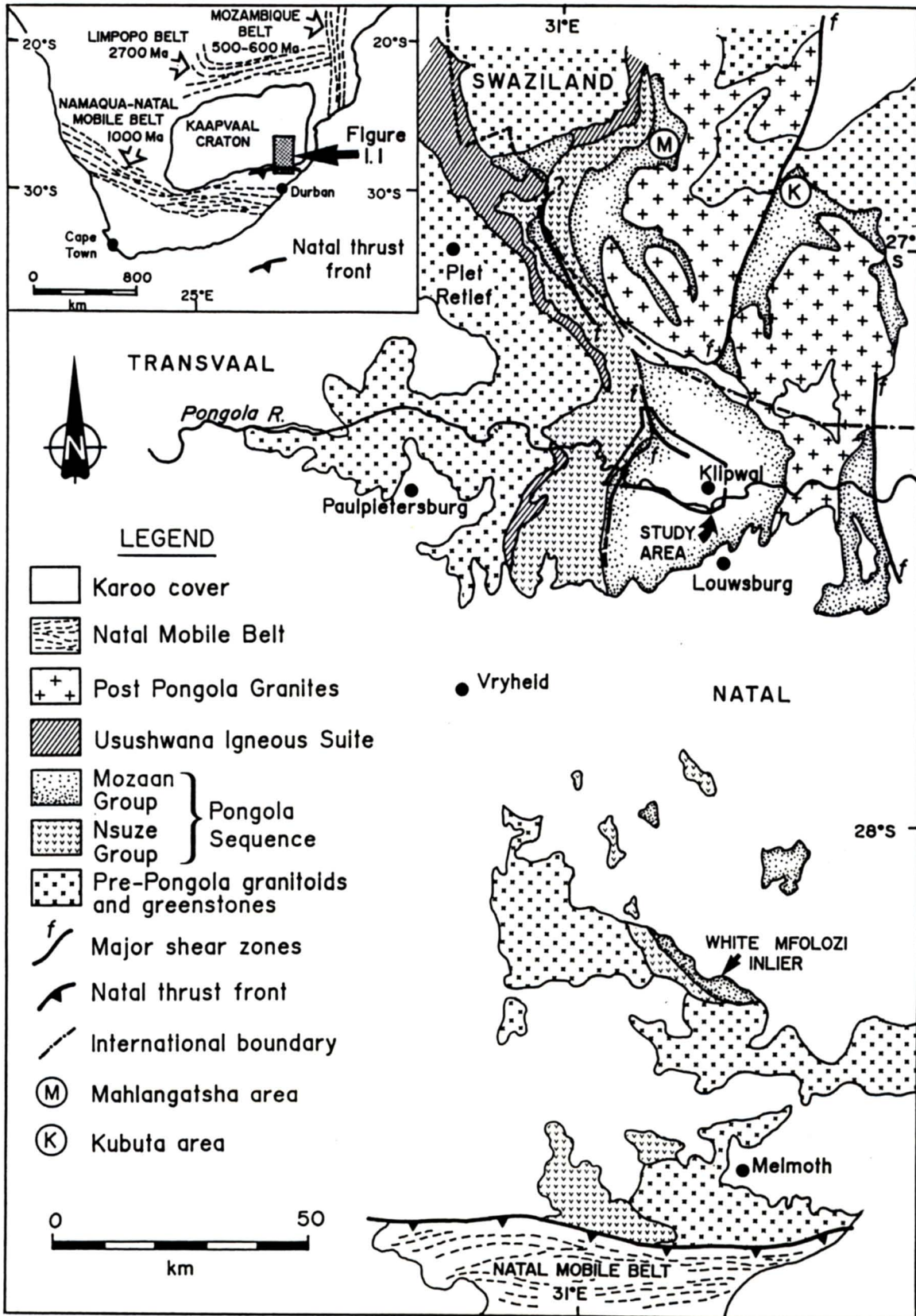


Figure 1.1: Simplified map showing the distribution of the Pongola Sequence (after Geol. Surv. Swaziland, 1982; Wolmarans, 1988).

An 8 m thick basal saprolite indicates that initial subaerial exposure and weathering of an extensive area resulted in the formation of a palaeoregolith (Watchorn and Armstrong, 1980). Braided streams draining to the south and southeast deposited immature clastic sediments to form the ~500 m thick basal Nsuze quartzite (Hunter and Wilson, 1988). Minor lava flows contemporaneous with this sedimentation preceded a major period of volcanism, characterized by a complex interdigitation of lavas of variable composition (ranging from basalt and andesite to rhyolite: Armstrong, 1980; Hunter and Wilson, *op.cit.*; Hatfield, 1990). The absence of pillowed lavas negates a marine environment. Magmatism associated with rifting is commonly alkaline, but the Nsuze rocks are uniformly tholeiitic (Hunter and Wilson, *op. cit.*). No modern day analogue for the environment of eruption is known (Armstrong *et al.*, 1986). The final stages of Nsuze volcanism is characterized by a decrease in volcanic rocks (including pyroclastics) and a concomitant increase in sedimentary rocks. The measured thickness of the Nsuze Group east of Paulpietersburg is nearly 10 000 m (Armstrong, 1980).

The lower part of the Nsuze Group in the Piet Retief area and in Swaziland (Figure 1.1), comprises mainly felsic volcanic rocks (Hatfield, 1990). The upper part is dominated by volcanic rocks of intermediate composition. These two volcanic rock types are separated by a thin, but laterally persistent volcanoclastic unit.

In the White Mfolozi inlier, southeast of Vryheid, the Nsuze Group is only 2000 m thick and is mostly made up of quartzitic sandstone. The southernmost Nsuze exposures are found near Nkandla (south and west of Melmoth) where they attain a maximum thickness of about 4000 m (Groenewald, 1984). The arenaceous and argillaceous sediments account for approximately 3000 m here.

Mozaan Group

The Mozaan Group is made up predominantly of arenaceous and argillaceous sedimentary rocks. In the White Mfolozi inlier, there is a marked unconformity at the contact between the Nsuze and Mozaan groups, where progressive overstep has eliminated approximately 1200 m of Nsuze stratigraphy.

The basal contact is gradational in the area east of Paulpietersburg. The transition is marked by an upward decrease in pyroclastics and development of sandstones (Watchorn, 1978, 1980; Armstrong, 1980). The contact with the Mozaan Group is defined by the first dominantly sedimentary horizon.

Initial deposition appears to have been the result of sedimentation on a braided alluvial plain resembling the modern Platte River (Miall, 1977; Watchorn, 1979a). The overlying sediments resemble progradational shelf sediments in a gently subsiding basin in which some chemical precipitation was occurring (Watchorn, *op. cit.*). They are in turn overlain by black massive or laminated mudstones with occasional intercalated sandstone interpreted as high-tidal-flat deposits and storm deposits respectively. Sedimentation was terminated by an episode of intermediate to felsic volcanism (Watchorn, 1980).

Structural Evolution

Two regional folding phases have been recognized in the main Pongola basin (Watchorn, 1978; Matthews, 1991). The earlier northwesterly trending phase was followed by a northeasterly oriented phase. The resulting fold interference led to the development of perisynclinal fold structures. The structure in the eastern part of the main Pongola basin has been influenced by several phases of granite intrusions (Matthews, 1985). Matthews (1991) interpreted the western margin to be undeformed, except for a major fault system

(his "Mahamba fault-belt"; Matthews, 1990). Hatfield (1990) studied its apparent northwestern extension to the east of Piet Retief.

In the Nkandla area, the Nsuzi beds are deformed by east-west trending folds and thrust faults (Matthews, 1990; Weilers, 1990). The southern margin of the Kaapvaal Craton is deformed by the ca 1000 Ma Namaqua-Natal tectonothermal event, which may have affected these beds (Groenewald, 1984; Figure 1.1).

Geochronology

The Nsuzi Group rests nonconformably on the Lochiel granite (Visser *et al.*, 1947; Hunter, 1974), dated at 3028 ± 14 Ma (Rb-Sr; Barton *et al.*, 1983) and 3107 ± 6 Ma (U-Pb; Kamo *et al.*, 1990). The Nsuzi lavas have yielded ages of 3090 ± 90 Ma (^{207}Pb - ^{206}Pb ; Burger and Coertze, 1973) and 2940 ± 22 Ma (U-Pb; Hegner *et al.*, 1984). The minimum age of the Pongola Sequence is defined by the intrusive Usushwana Igneous Suite, dated at 2871 ± 30 Ma (Sm-Nd; Hegner *et al.*, *op. cit.*) and 2813 ± 30 Ma (Rb-Sr; Davies *et al.*, 1970). The age of the Pongola Sequence is therefore bracketed between 2813 and 3107 Ma.

PREVIOUS WORK

Previous work on the Pongola rocks south of Swaziland has concentrated chiefly on the depositional environments of the sedimentary rocks and on the geochemistry of the volcanic rocks (e.g. Von Brunn, 1974; Von Brunn and Hobday, 1976; Watchorn, 1978, 1979a, 1980; Watchorn and Armstrong, 1980; Armstrong *et al.*, 1982, 1986; McLennan and Taylor, 1983; Eriksson and Soegaard, 1985; Laskowski and Kröner, 1985; Grandstaff *et al.*, 1986; Hunter and Wilson, 1988; Wronkiewicz and Condie, 1987, 1989; Dia *et al.*, 1990). Attempts at establishing the structural evolution of the basin

have been made (Humphrey and Krige, 1931; Carter, 1964; Matthews, 1985, 1987, 1990; Hatfield, 1990).

Studies in the vicinity of the present investigation have included a geochemical analysis of the Nsuzze Group east of Paulpietersburg (Armstrong, 1980), a general geological study of the area between the Pongola and Mozaan Rivers (Carter, 1964), a sedimentological analysis of the Mozaan Group (Watchorn, 1978), a study of the gold mineralization associated with the Klipwal shear zone (Russell, 1985), mapping projects (Mendonidis, 1979; Isherwood, 1979) and an economic investigation of the banded iron-formation (Carney, 1984).

PRESENT STUDY

The present study was initiated to address a number of aspects of the geology of the Pongola basin. The subdivisions of the Nsuzze and Mozaan Groups are still contentious with a number of formation schemes being described by various authors. The establishment of detailed stratotype sections with palaeoenvironmental interpretations in well-exposed areas is essential in order to characterize the regional variations more precisely and to allow for intrabasinal correlations. A contribution towards the achievement of this objective is aimed at in this study. Little consideration has been given in the past to the effects of structural complications on observed stratigraphic sequences as evidenced by the paucity of detailed structural studies. The recognition of extensive low-angle thrusts and normal faults has considerable implications for the repetition and elimination of stratigraphy.

The study area, which is situated in the vicinity of the Klipwal Gold Mine in the southeastern Transvaal (Figure 1.1), lends itself to this type of study because of the good exposure and the presence of a number of shear zones passing through it. The study area

is ~250 km² and has a triangular shape with the southern boundary defined by the Pongola River, the western side by the Nsuze - Mozaan contact and the northeast by the access road to the Klipwal Gold Mine. The area is underlain mainly by the Mozaan Group with small outliers of tillite of the Carboniferous Dwyka Group of the Karoo Sequence.

The study area is topographically rugged. Deep gorges are common, the most spectacular of which is along the Pongola River. The Sinqeni Mountain rises ~700 m above it to an elevation of ~1200 m a.m.s.l. The extreme topography coupled with the underground workings in the Klipwal Gold Mine offer good three-dimensional control on the structural geometry.

This study forms part of an on-going research programme at the University of Natal, Pietermaritzburg, into the Precambrian rocks of northern Natal, southeastern Transvaal and Swaziland. A detailed stratigraphic and structural study of the area was made through the compilation of lithological and structural maps (Maps 1 to 3 in the annexure) and stratigraphic columns, the collection and analysis of structural orientation data, the analyses of small- and large-scale structures in shear zones and the correlation of stratigraphy across shear zones.

The area was mapped using aerial photographs at a scale of 1:30 000. An aero-sketchmaster was used to convert the field data to a scale of 1:50 000 and to correct for radial distortions. The more structurally complex areas were mapped using aerial photographs at a scale of 1:10 000. The various rock types were sampled for purposes of microscopic identification of minerals and lithologies (Appendix 1), and for geochemical analyses of some of the intrusions as well as the mudstone and diamictite (Appendix 2). Primary and secondary planar and linear structural elements were measured with a Brunton compass and processed by computer to obtain vector statistics and stereographic projections, which are presented as equal area lower hemisphere projections. Contouring is at 5% intervals, unless otherwise stated.

CHAPTER 2: STRATIGRAPHY AND SEDIMENTOLOGY

REGIONAL STRATIGRAPHY

A two-fold subdivision of the Pongola basin into northern and southern sub-basins has been recognized (Groenewald, 1984). In the southern sub-basin, immediately north of the Natal Mobile Belt, only the Nsuzi Group is preserved. It is lithologically somewhat different from the Nsuzi strata in the northern sub-basin. The southern inliers are characterized by interbedded sedimentary and andesitic volcanic rocks, whereas the Nsuzi Group to the north comprises predominantly volcanic rocks with sedimentary rocks being developed only at the base and at the top of the succession (Armstrong, 1980).

The main distribution of the Pongola Sequence in the northern sub-basin in the southeastern Transvaal, northern Natal and southern Swaziland is found in the following areas (Figure 2.1):

1. the main Pongola basin,
2. Mfolozi Area in northern Natal,
3. the Kubuta area in southern Swaziland,
4. Mahlangatsha area in southern Swaziland, and
5. the vicinity of Amsterdam in the southeastern Transvaal.

The stratigraphic sequences in each of these five areas is briefly summarized below.

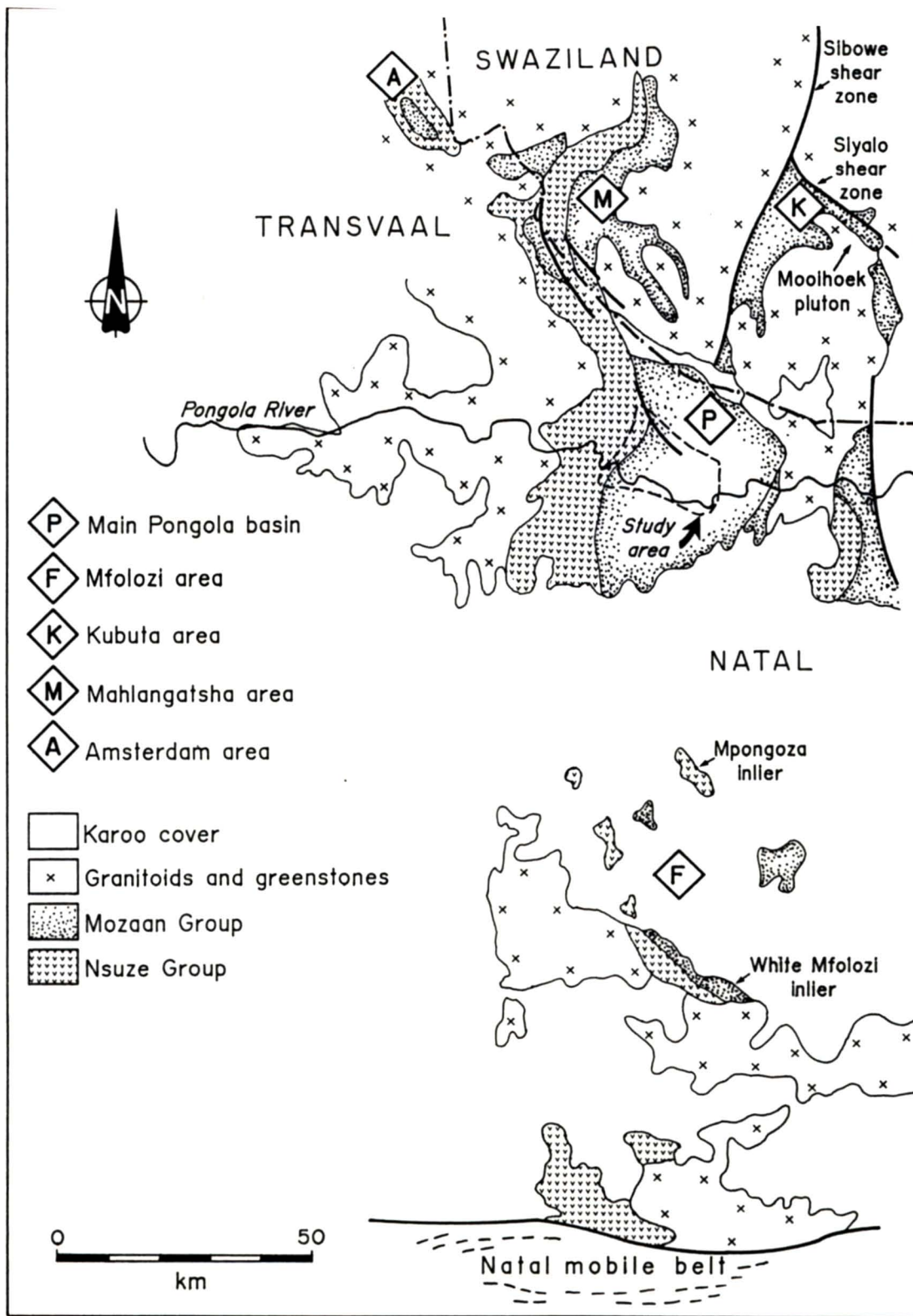


Figure 2.1: Simplified map showing the distribution of the Pongola Sequence and the five areas under discussion.

Main Pongola Basin

In the main basin, the Nsuze Group is made up of a ~10 000 m thick sequence of andesitic and basaltic lavas (Armstrong, 1980). The uppermost unit in the Nsuze consists of a banded siltstone which characteristically weathers to a reddish/pink colour. The overlying basal Mozaan succession, the Sinqeni Formation, is widely distributed along the western limits of the main basin. It consists of a very thick lower sandstone (~400 m), a marker iron-formation, which is in turn overlain by a second upper sandstone unit. The basal sandstone contains a polymict, matrix-supported conglomerate of variable thickness up to 20 m near its base.

A ~900 m thick sequence of mudstone interbedded with subordinate sandstone, referred to as the Ntombe Formation (SACS, 1980), overlies the Sinqeni Formation in the western parts of the main basin. The succeeding Thalu Formation comprises sandstone, mudstone and ferruginous mudstone including a banded iron-formation. It is overlain by the arenaceous Hlashana Formation.

In the central part of the main basin on both flanks of the intrusive Spekboom granite (Figure 2.1) a sequence of thick sandstone, including conglomerate and an internal iron-formation, may be correlated with the Sinqeni Formation (columns B and D in Figure 2.2). The underlying andalusite-bearing banded siltstone on the eastern side of the granite has been referred to as the Mkuzane Formation while the overlying sandstone has been called the Mkaya Formation (SACS, 1980; Beukes and Cairncross, 1991). On the west side of the granite, in the Itala Game Reserve, the equivalent units were designated as the Langfontein Formation. These three formations have been placed nearly two-thirds of the way up the Mozaan stratigraphic column with the sandstone package being correlated with the Hlashana Formation (SACS, 1980; Beukes and Cairncross, *op. cit.*). The Mkaya Formation has a closer affinity with the Sinqeni Formation while the Mkuzane and Langfontein Formations resemble the upper Nsuze Group.

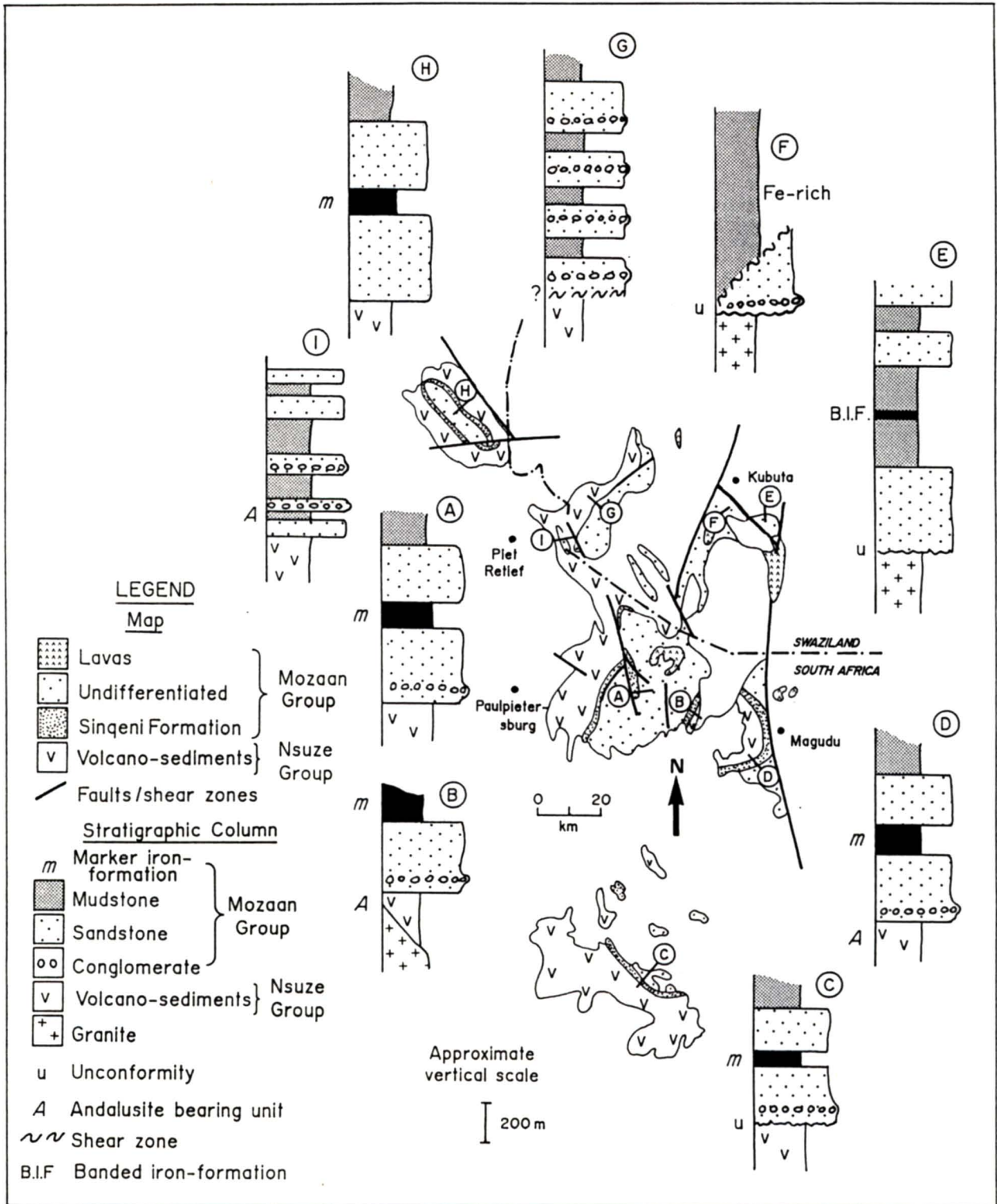


Figure 2.2: Simplified map showing the distribution of the Sinqeni Formation and the Mozaan Group basaltic lavas, with schematic representations of the stratigraphy at the base of the Mozaan. Stratigraphic columns modified after Hunter (1961), Geol. Surv., Swaziland (1980) and Weilers (1990).

The uppermost formation in the study area is the Odwaleni Formation comprising alternating sandstone and mudstone (some of which is ferruginous) and interbedded diamictite.

The uppermost units within the main Pongola basin comprise a series of lavas and volcanoclastics interbedded with sedimentary rocks. These volcanic rocks are found in the closure of the Tobolsk syncline as well as to the east in inliers near Magudu (Figure 2.2) and have been assigned to the upper parts of the Odwaleni Formation and the Nkoneni Formation (SACS, 1980).

Mfolozi Area

The Mozaan Group rests unconformably on the Nsuze Group here (Matthews, 1967). SACS (1980) divided the Mozaan stratigraphy of the White Mfolozi inlier into the Mandeva, Mpunga and Qwasha formations. Beukes and Cairncross (1991) considered the Mandeva Formation to be the lateral equivalent of the Sinqeni Formation.

The volcanic rocks in the Mpongoza inlier probably represent the terminal volcanic event of the Nsuze Group (Preston, 1987). A sandstone remnant 1 km west of the main inlier was correlated with the Mozaan Group.

A lithological sequence identical to the Sinqeni Formation is preserved on the farm Beverson, west of the Mpongoza inlier (Figure 2.1). Because of the westerly dips, this supports the correlation of the Mpongoza volcanic rocks with the Nsuze Group. Correlation of lithologies in the other small inliers is constrained by lack of continuity of exposure and marker beds.

Kubuta Area

Beukes and Cairncross (1991) considered the basal sandstone from this area to belong to the Sinqeni Formation, although no marker iron-formation is present (column F in Figure 2.2) nor is there any Nsuzi Group present. A well developed conglomerate occurs in the northernmost exposure to the northeast of the Siyalo shear zone (Figure 2.1). The only similarity that the basal sandstone in the Kubuta area has with the Sinqeni Formation of the type area is its ~500 m thickness (Hunter, 1961, 1963). It is lithologically more similar to the Ntombe Formation. A thick argillaceous succession which is interlayered with a number of relatively thin sandstone units overlies this basal sandstone. The sequence is capped by an amygdaloidal basaltic lava (Hunter, 1963), which may correlate with the Tobolsk lavas described by Beukes and Cairncross (*op. cit.*).

A basal sandstone overlain by mudstone and thick iron-formation crops out east of the Siyalo shear zone in its southeastern extension. Although originally correlated with the succession west of the shear zone (Hunter, 1961, 1963), the validity of this correlation is questionable due to the greater abundance of sandstone in the eastern exposures. Neither of the successions on either side of the Siyalo shear zone are comparable to the Sinqeni Formation (columns E and F, Figure 2.2). The stratigraphy to the northeast of the Siyalo shear zone is lithologically similar to Ntombe Formation.

Basaltic lavas with interbedded sandstone and andalusite schist occur to the southeast of the Mooihoek pluton (Figure 2.1). The dominance of volcanic rocks led Hunter (1963) to correlate this sequence with the Nsuzi Group, but an upper Mozaan correlation on the basis of their geochemical signatures which distinguish them from the basalt-andesite-rhyolite assemblage of the Nsuzi Group in the west is more likely.

Mahlangatsha Area

The Mozaan succession in the Mahlangatsha area differs from the Kubuta area in that the Mozaan Group comprises dominantly sandstone and conglomerate with only minor intercalations of mudstone (Figure 2.2). Hunter (1963) mapped seven sandstone beds and six thin interbedded mudstone units. The basal sequence comprises a thick sandstone with thin interbeds of sandy mudstone, in which andalusite is locally present.

The southernmost Mahlangatsha exposures, east of Piet Retief, are separated from the main Mahlangatsha exposure by two northwest-trending faults (Figure 2.2). The Mozaan Group southwest of the southwestern fault resembles the stratigraphy described by Hatfield (1990) in the area west of the Mahamba fault (column I, Figure 2.2). In both areas a ~ 10 m thick basal arenite is overlain by andalusite schists which might be correlatives of the banded siltstone unit of the upper Nsuze Group. Humphrey and Krige (1931) placed these lithologies at the base of the Mozaan Group as did Hunter (1963) in Swaziland. The andalusite schists are overlain by a thicker sandstone unit which does not contain an interbedded iron-formation (Hatfield, *op. cit.*).

Amsterdam Area

The upper Nsuze Group units in the Amsterdam area are reported by Van Vuuren (1965, *cited in* Weilers, 1990) to consist of andesitic and tholeiitic lavas. The Mozaan Group consists of a thick sandstone unit with an interbedded iron-formation (the Madola Shale Member (Humphrey and Krige, 1931)). This succession resembles the Sinqeni Formation of the type area, although banded siltstones are absent from the underlying Nsuze Group.

STRATIGRAPHY OF THE STUDY AREA

Upper Nsuze Group

The Nsuze Group lithologies were not studied in detail as the contact between the Nsuze and Mozaan Groups constituted the approximate western boundary of the study area. They are however duplicated by shearing within the study area. Detailed work on this group to the west was carried out by Armstrong (1980).

The uppermost ~ 400 m are mainly reworked volcanic tuffs marking a transition from the dominantly volcanic nature of the lower Nsuze Group to the sedimentary character of the Mozaan Group.

The lowest Nsuze unit in the area is an andesitic lava containing amygdaloidal layers (Figure 2.3). It is overlain with a sharp contact by a very dark, fine grained, 40 m thick sandstone unit characterized by planar cross-bedding and plane bedding. Individual beds are up to 40 cm thick. Within this sandstone unit are two polymict clast-supported conglomerates consisting largely of volcanic clasts (Figure 2.4). Clasts are elongated and 2-20 cm in length. The upper contact of the lower conglomerate is irregular due to loading. The upper conglomerate is more mature in character and is mainly clast supported. These two conglomerates are best developed south of the Pongola River becoming less well developed further northwards on the farms Vergenoegheid and Altona. The overlying sandstone contains rare clasts similar to those in the conglomerates.

The uppermost Nsuze lithology is a ~ 40 m thick banded siltstone made up of laterally continuous 1-3 cm thick alternating light and dark laminations. Micro-cross laminations are locally observed. The coarser-grained lighter bands have a sharp basal contact but grade up into the darker ones. The siltstone consists mostly of very fine-grained quartz, with the larger quartz grains displaying a high degree of rounding and sphericity. A greenschist facies metamorphism is indicated by the presence of biotite, muscovite and chlorite.

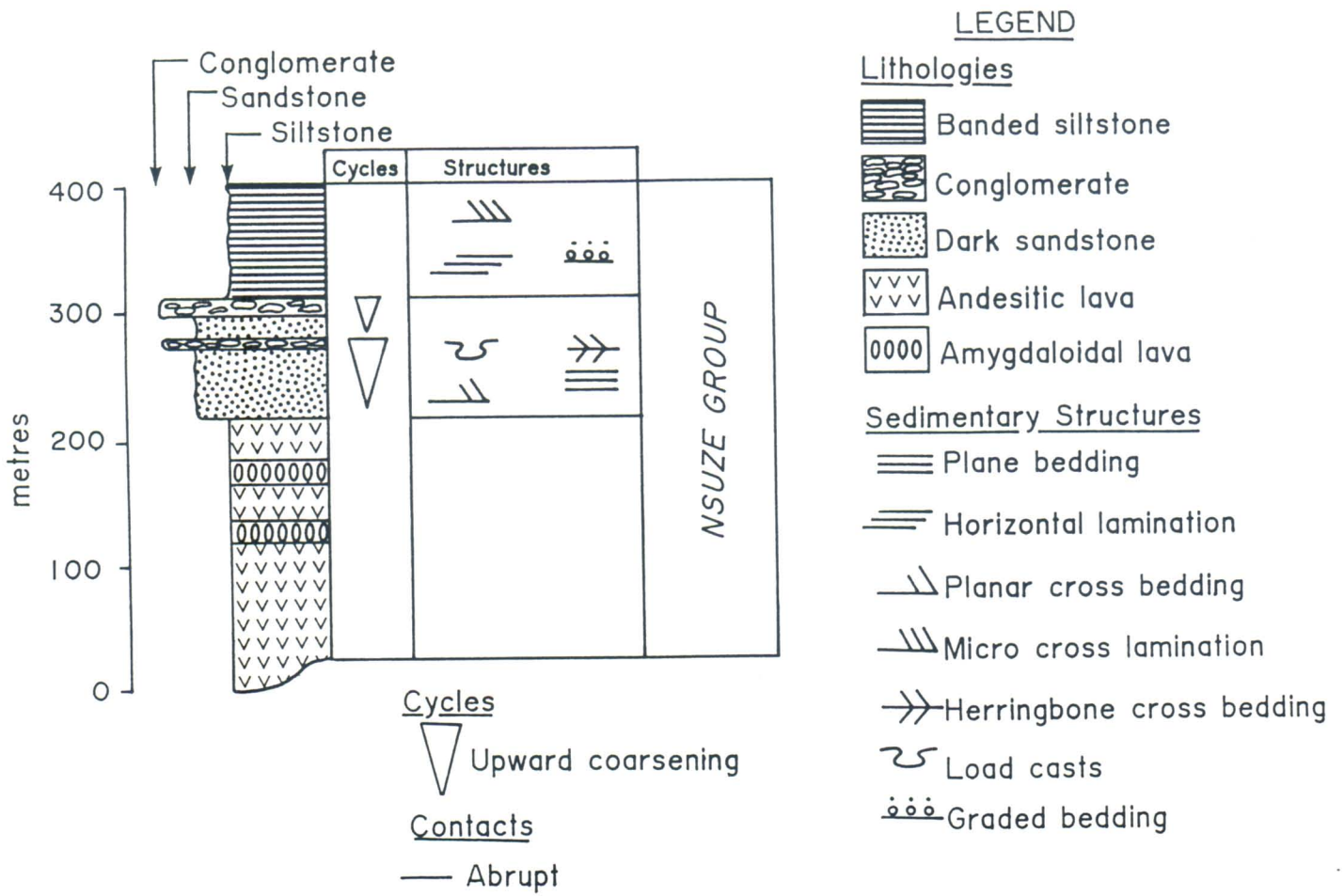


Figure 2.3: Stratigraphic column for the upper Nsuze Group.



Figure 2.4: Polymict clast supported conglomerate in the upper Nsuze Group (Ntombe Stream).

Sedimentological Interpretation

The andesitic lavas near the top of the Nsuze Group represent the penultimate stage of Nsuze volcanism. Lavas were extruded subaerially (Armstrong, 1980) and covered vast areas. Thin, impersistent, amygdaloidal lava flows indicate that only minor amounts of gas-charged magma were extruded during the waning phases of volcanism.

The overlying volcano-sedimentary facies represent deposition during the terminal phase. The dark Nsuze sandstone possibly represents the reworking of eroded iron-rich volcanics. This sediment was then reworked by wave action in a shoreface setting resulting in the development of cross-bedded and evenly laminated fine-grained sandstone.

The conglomerates were interpreted by Armstrong (1980) as laharic breccias (i.e. water-laid volcanic breccias and volcanic breccias). Lapidus (1990, page 316) defines a lahar as "a destructive landslide or mudflow of hot volcanoclastic material on the flanks of a volcano, formed when water from any source combines with the hot volcanic debris and slides downward, under its own weight, resulting in poorly stratified volcanoclastic beds". The source of the water may have been from torrential downpours of rain, rapidly melted ice or snow from subglacial eruptions, or from the ejection of water from a crater lake. The poor sorting of the conglomerate, along with the large variation in clast size, suggests a debris flow rather than a fluvial origin. However, the high degree of rounding of the clasts implies that the debris was transported over a great distance. The lack of bedding suggests that it was dumped rapidly in an aqueous environment (Figure 2.5). Given the appropriate submarine topography, volcanoclastic gravity-flows may move over very long distances without much admixture of extraneous sediment. A modern example of the above is given by the Roseau ash debris-flow which crossed the Grenada Basin over a distance in excess of 250 km (Carey and Sigurdsson, 1980; *cited in* Heinrichs, 1984).

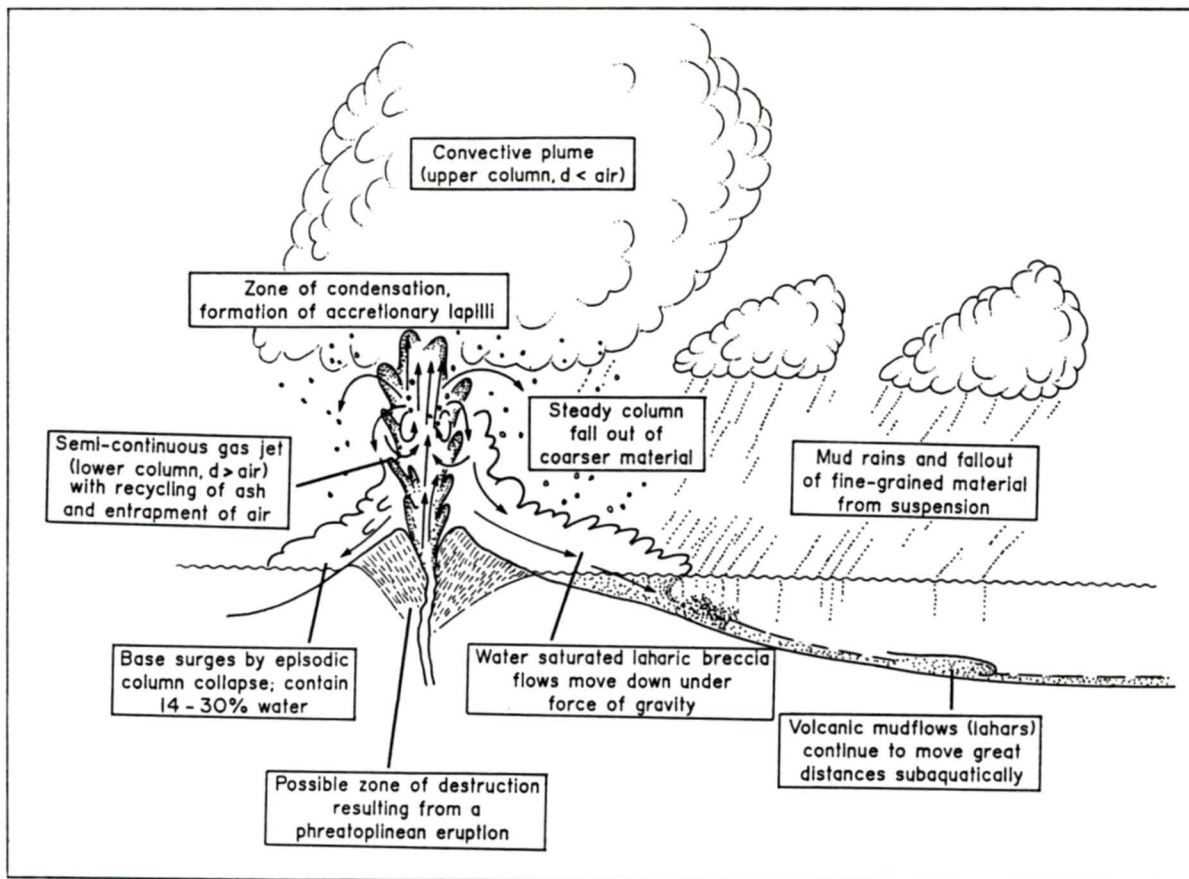


Figure 2.5: Diagrammatic model of volcanoclastic gravity-flows generated by a high-discharge phreatomagmatic eruption (modified after Heinrichs, 1984). Density is abbreviated as d .

Armstrong (1980) reported accretionary lapilli tuffs on Roodewal, some 15 km south of the Pongola River, which provide valuable clues as to the depositional environment during accumulation of the uppermost Nsuzi units;

1. they are related to explosive volcanism and deposited from the air (Heinrichs, 1984);
2. the lapilli may be carried in suspension by an aerosol, which is defined by Lapidus (1990, page 10) as a colloidal system in which the dispersion medium is a gas, and the dispersed phase consists of liquid droplets or solid particles. An extremely low aerosol viscosity allows this suspension to be spread very far from the eruptive vent. However, any aerosol should tend towards an isotropic expansion (i.e. horizontally as well as vertically) and

this would result in a rapid deposition of the suspended particles (Tazieff, 1970);

3. they are believed to form through the accretion of ash and dust by condensed water in a moisture-rich eruption column. The nucleus may be a solid particle or a condensing water droplet. Accretionary lapilli may be produced by rain flushing through the eruption column or the ash cloud accompanying a pyroclastic flow, or result from a phreatomagmatic eruption (Lapidus, 1990);
4. according to Moore and Peck (1962), it is likely that such deposits accumulate within a few kilometres of the vent, and that the vent was above water or in very shallow water during eruption.

The model proposed by Armstrong (1980, based on Moore and Peck, 1962) ties in with the envisaged environment of deposition for the banded siltstone in the study area. These fine-grained deposits may have been generated by explosive volcanic activity as evidenced by the lapilli. Accumulation took place some distance from the vent (inferred from the lack of accretionary lapilli). Collinson and Thompson (1989) suggested that volcanic ash and dust can be transported great distances by air currents, and that bed thickness is controlled by rainfall and wind patterns rather than distance from the volcanic vent. Each layer may thus represent a renewed episode of volcanism, resulting from extrusion of ash from the vent, transport by wind currents, and deposition within a shallow aquatic environment.

The sharp base and clear definition of the coarser-grained layers suggest that they represent relatively sudden events superimposed upon the background of quieter, more constant sedimentation of the finer grained, lighter layers. The internal grading and gradational tops of the coarser-grained layers indicates settling of the suspended load. The bases of the coarser layers are sometimes slightly irregular with a relief of a few millimetres.

In summary, the upper units of the Nsuze Group mark the termination of Nsuze volcanism. This late stage was characterized by explosive volcanic activity accompanied by the deposition of abundant air-fall and pyroclastic material (Figure 2.6). Subsidence, in response to the accumulation of great volumes of lava, resulted in the formation of depressions within the Pongola depository which accumulated sediments from pyroclastic ejecta and erosion of the surrounding volcanic terrane (Armstrong, 1980).

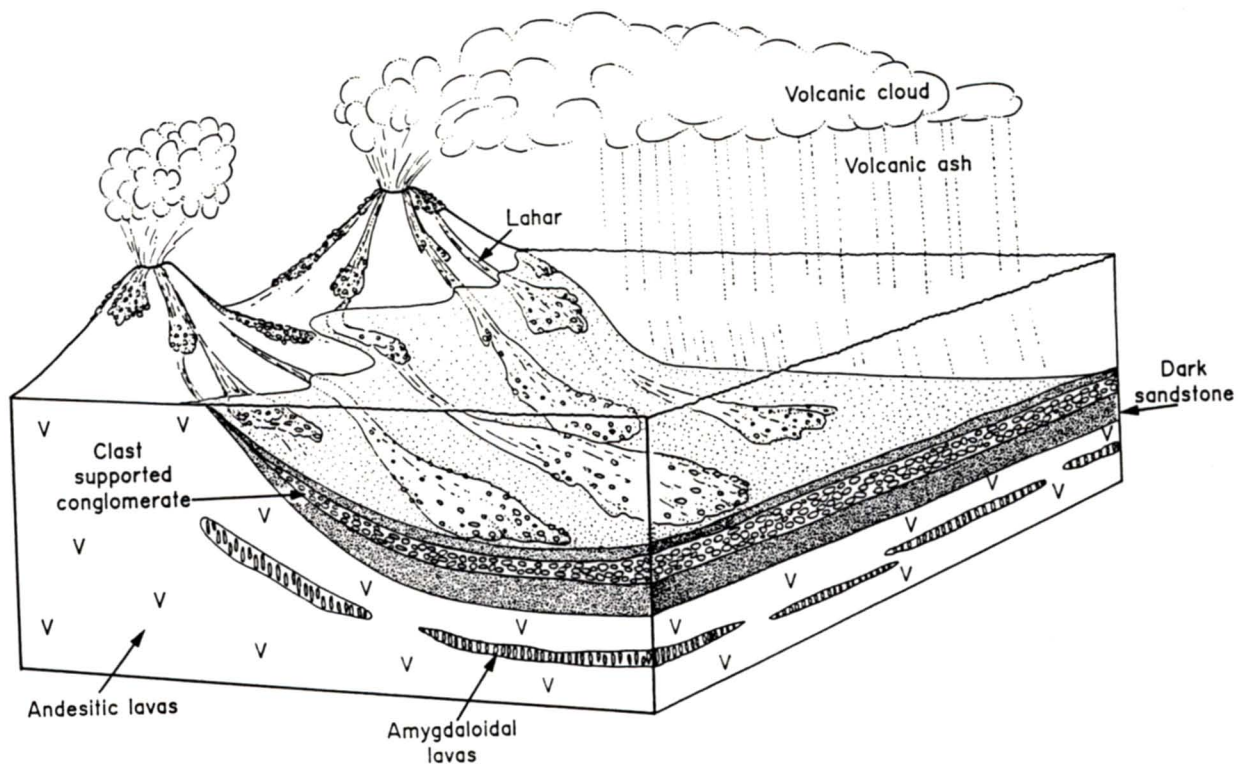


Figure 2.6: Diagrammatic model showing the accumulation of the upper Nsuze volcano-sediments.

Coarse, pyroclastic debris and talus breccia and rubble accumulated on the unstable slopes of the volcanoes. Movement of these deposits was initiated by tremors aided by the addition of water, loss of cohesion and gravity (Armstrong, 1980). The coarse-grained pyroclastic flows moved downslope and were dumped rapidly in shallow aquatic environments which were continually undergoing subsidence.

When the magma chambers were exhausted, volcanic activity ceased, but wind blown ash and dust continued to accumulate in the shallow depressions, where it formed graded, laterally persistent beds which were reworked locally by weak, possibly wind generated, currents. A period of quiescence followed the major episode of Nsuze volcanism during which time the depository deepened due to continued subsidence. A large, shallow basin, possibly an epeiric sea, developed. It was fed by fluvial systems which brought in vast amounts of clastic material, initiating the accumulation of the Mozaan Group sediments.

Mozaan Group

The stratigraphic subdivisions that have been applied to the Mozaan Group are confusing with different terminology being adopted for the various packages identified in the field. According to SACS (1980), there are seven subdivisions of the Mozaan Group in the main Pongola basin while Beukes and Cairncross (1991) propose nine different formations in the same area (Figure 2.7). An attempt is made in this work to correlate the stratigraphic units of the study area with the formations described in the literature. Unfortunately recent previous attempts to establish stratigraphic sequences (Watchorn, 1978; SACS, *op. cit.*; Beukes and Cairncross, *op. cit.*) have paid little attention to the structure of the Pongola Sequence regarding it as relatively undeformed. The presence of a number of major inter- and intraformational shear zones eliminating or duplicating stratigraphy is demonstrated in this study.

The stratigraphy of the Mozaan Group in the study area has been divided into six Formations; these are the Sinqeni, Ntombe, Thalu, Hlashana, Odwaleni and Kulphiso Formations (Map 1A and Figure 2.7). All these names were coined by SACS (1980) with the exception of the Kulphiso Formation which gets its name from a prominent mountain where the formation is located.

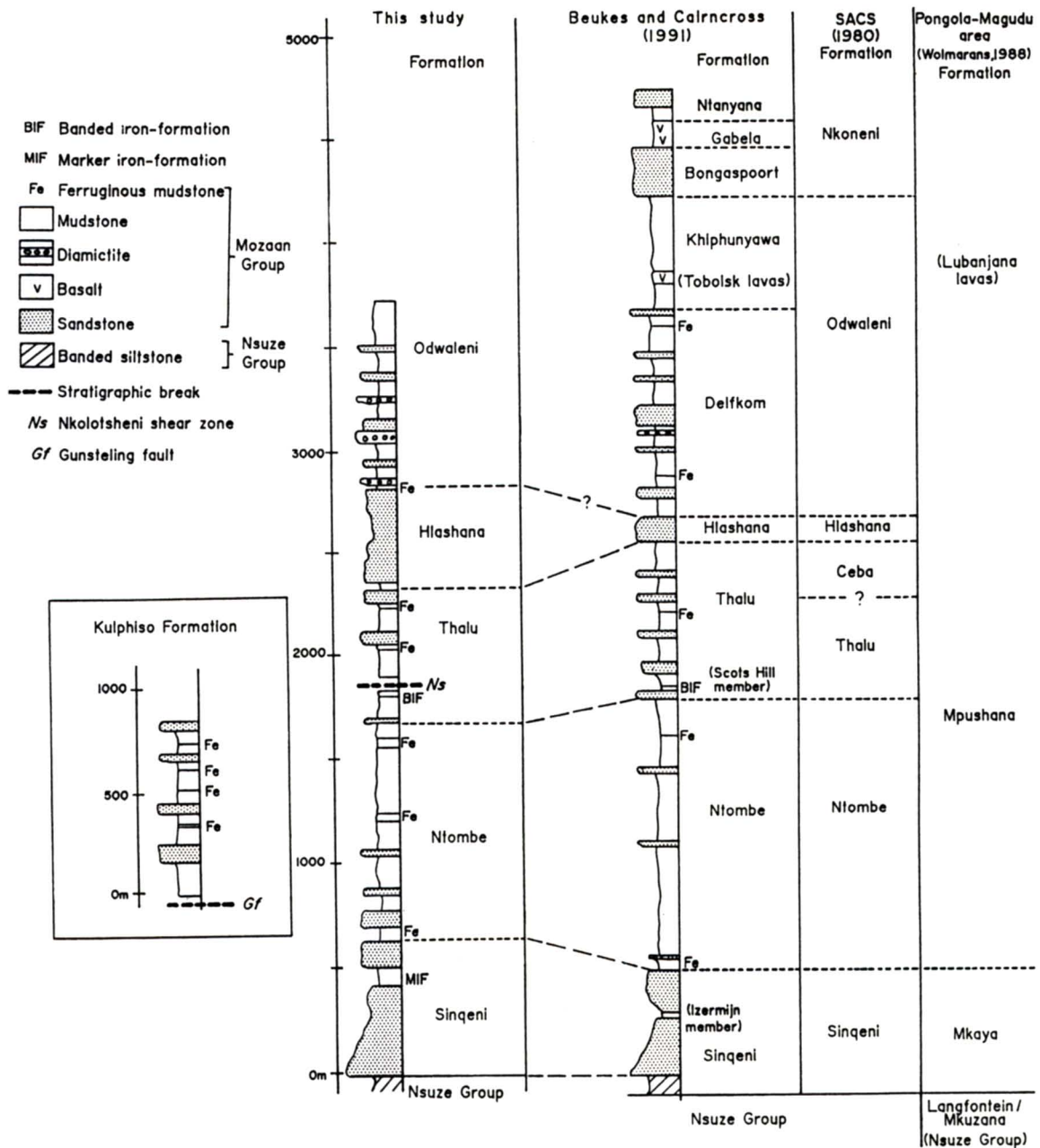


Figure 2.7: Comparative stratigraphic columns between this study and previous workers for the main Pongola basin.

Stratigraphic correlations within the Pongola basin are constrained by structural complications. Only two stratigraphic units can be used for correlation over long distances, namely the sediments comprising banded siltstones at the top of the Nsuzze Group along with the succeeding 650 m thick Sinqeni Formation which includes a basal conglomerate and an interbedded marker iron-formation, and the basaltic lavas of the Nkoneni Formation (SACS, 1980) at or near the preserved top of the Mozaan Group (Figure 2.2). The latter formation is not exposed in the study area.

No major unconformities are recognized in the area, although the complete succession is not preserved. Loss of ground across several bedding-parallel shear zones may have occurred.

The Mozaan Group in the study area is made up entirely of sedimentary lithologies, comprising predominantly mudstone and sandstone with lesser amounts of conglomerate, iron-formation and diamictite. They are discussed below in order of decreasing abundance. Basaltic lavas occur at the top of the succession beyond the limits of the study area (Figure 2.2).

Mudstone - The mudstone is extremely fine-grained and consists mostly of quartz with lesser amounts of biotite, muscovite and carbonate. Some samples contain a high percentage (40-50%) of opaque minerals.

Sandstone - There is a considerable variation in the types of sandstone from quartz-arenite to arkosic sandstone. Grain sizes vary from very fine-grained to very coarse-grained.

The basal quartz-arenite, which is also the thickest one, displays a high degree of recrystallization. In particular the lowest parts are locally totally recrystallized to the extent that the rock here consists almost entirely of quartz. The original grain shapes are destroyed with the exception of chert grains where the original, well-rounded shape can still be observed. The texture within this sandstone is isogranular and triple junctions are common. Locally muscovite, biotite and chlorite are present and the matrix may be extensively sericitized.

Iron-formation - The iron-formation is associated with mudstone with the exception of the lower marker iron-formation which is situated within the Sinqeni Formation. The iron-formation is fine-grained and the units are largely magnetite-rich and

can be banded, with individual bands being made up of chert, jaspilite and iron-oxides (predominantly magnetite). Only minor amounts of quartz can be discerned (in thin section), while the major constituents are opaque minerals.

Diamictite - The diamictite is a black, homogeneous, massive rock containing sparsely dispersed clasts (<5% by volume). Clast sizes range from 2 mm granules to boulders up to 75 cm in diameter. Clast shapes are angular to sub-rounded and the clasts are randomly oriented.

The matrix is extremely fine-grained and dark and contains minute opaque ferruginous grains. The results of X-ray diffraction analysis of two samples are given below:

	DMS 1	DMS 8
Magnetite	15	20
Grossular	4	2
Plagioclase	6	3
K-feldspar	0	8
Quartz	34	28
Chlorite	22	27
Illite	11	6
2.91Å	0	6
12.11Å	<u>8</u>	<u>0</u>
	100%	100%

Quartz, unaltered feldspar and lithic fragments in the matrix are sub-angular to rounded. Sand-sized grains display high sphericity, whereas the finer-grained particles are angular.

Conglomerate - The clasts within the conglomerates consist mostly of vein-quartz and chert, the latter consisting of black, white and banded varieties. The rock is polymict and typically matrix-supported but locally clast-supported. The clasts comprise from 20

to 50% of the rock but sometimes up to 80%. The matrix is poorly sorted and immature. The thickest (5-10 m) and best developed conglomerate is found several metres above the base of the Mozaan Group and is made up predominantly of vein-quartz clasts. The conglomerates higher up in the succession are much thinner and consist largely of chert clasts which are more angular than the quartz-vein clasts in the basal unit.

Sinqeni Formation

The transition between the Nsuzi and Mozaan Groups is defined by an upward decrease in pyroclastics and reworked volcanic material and an increase in sandstone. Evidence for a regional unconformity between the Nsuzi and Mozaan Groups as reported by Beukes and Cairncross (1991) could not be confirmed. The ~650 m thick Sinqeni Formation is characterized by two major sandstone units separated by an 80 m thick iron-formation (Figure 2.8A) and gets its name from the prominent Sinqeni mountain in the study area.

The basal orthoquartzite is upward fining, although subordinate arkoses are present towards its top. It is about 400 m thick and is typically medium- to coarse-grained but locally very coarse-grained to granular. The original well-rounded grain-shapes are sometimes preserved.

Prominent conglomerate lenses are developed between 5 and 30 m above its base. They vary in thickness from a few centimetres to 20 m (as for example on the farm Nooitverwacht). As many as five or six thin conglomerate units may be developed over a total thickness of about 25 to 30 m as can be seen at Altona. The conglomerates are not persistent as they tend to lens out laterally. The long-axes of clasts are typically aligned north-south in the plane of bedding. Imbrication is locally developed. The conglomerate lenses contain erosive bases and are commonly upward fining.

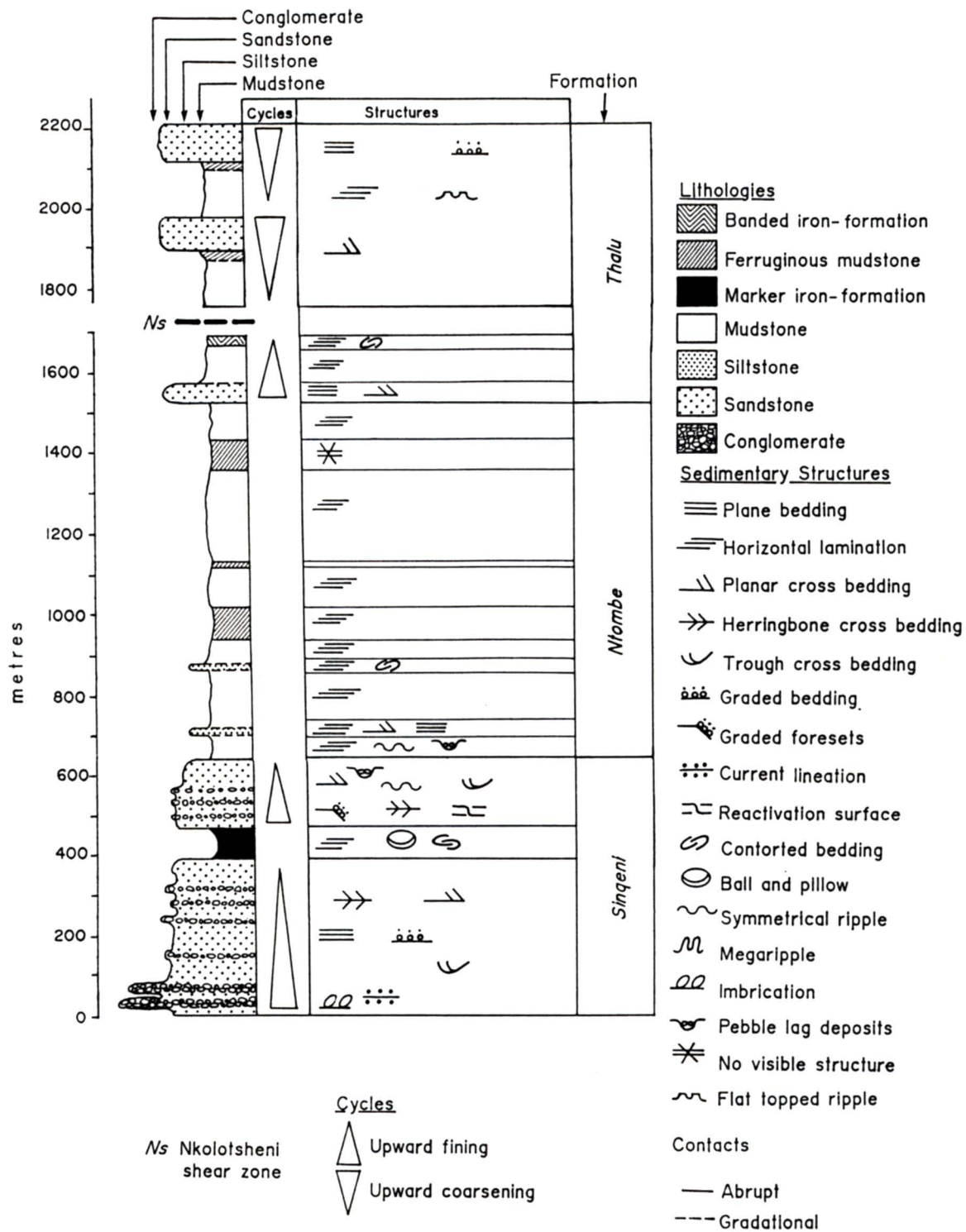


Figure 2.8A: Stratigraphic column for the Sinqeni, Ntombe and Thalu Formations. Locality sites for measured sections given in Figure 2.10. Symbols used in the stratigraphic columns are generally in accordance with Johnson (1987).

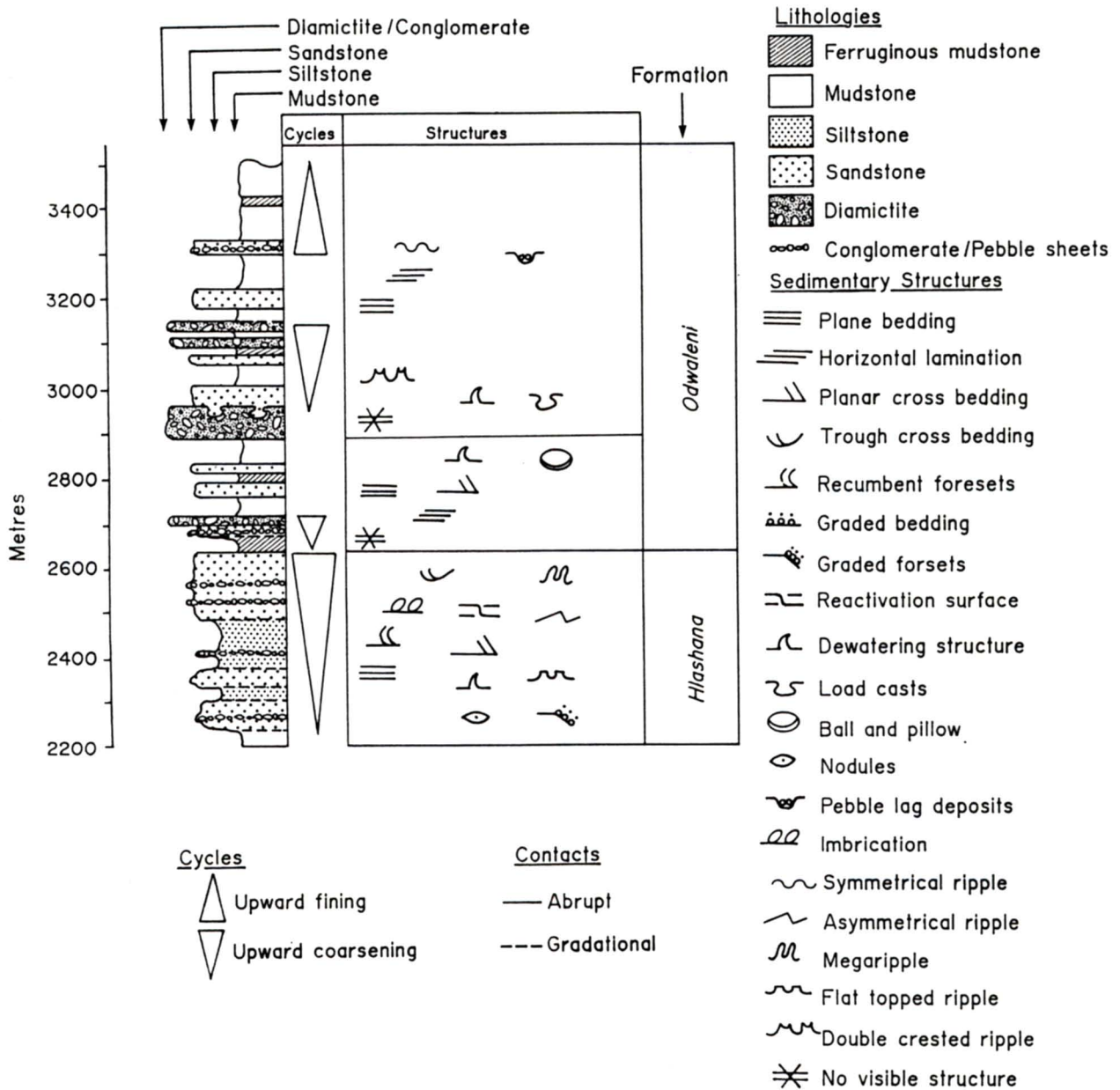


Figure 2.8B: Stratigraphic column for the Hlashana and Odwaleni Formations.

Internal bedding structures in the orthoquartzite consist of planar cross-beds, herringbone cross-stratification (Figure 2.9), and less often trough cross-beds. Planar cross-bedding, which may be bidirectional, is usually graded and is associated with coarse-grained sediments. The orthoquartzite becomes very coarse-grained towards its top.



Figure 2.9: Herringbone cross bedding in the basal Sinqeni Formation sandstone (Sinqeni mountain).

The marker iron-formation (MIF; equated with the Izermijn Member of Beukes and Cairncross (1991)), has a thickness of 60 to 80 m. It lies with an abrupt contact on the basal orthoquartzite, but gradational where arkose is developed. Gradation involves an upward fining (over a thickness of no more than 5 m) from arkose through siltstone and mudstone to ferruginous mudstone and finally into iron-formation.

The marker iron-formation may grade along strike into a banded iron-formation containing soft-sediment deformational structures. The banded iron-formation is made up of laminated jaspilite and iron-oxides; the latter predominantly comprising magnetite. The

magnetite-rich layers have a sharp lower contact, but grade upward into jaspilite. Individual bands are 0.5 to 3 cm thick. Locally, the unit is non-magnetic, indicating a higher content of haematite.

The overlying sandstone unit, which is 170 m thick, is a medium- to coarse-grained quartz-wacke. It is poorly sorted and granular with all grains being less than 5 mm in diameter. Oligomictic conglomerates consisting almost entirely of white vein quartz with subordinate white and black chert pebbles are common. The pebbles are angular to sub-rounded and vary in size from 10 to 25 mm. They are typically concentrated in layers up to 5 cm in thickness. Randomly dispersed clasts are often found in the enclosing quartz-wacke sometimes on the avalanche faces of planar foresets. Coarse-grained conglomerates up to 50 cm thick and containing of well rounded quartz pebbles up to 8 mm in diameter, are locally developed.

Sedimentary structures include planar and trough cross-bedding typically with pebble lag deposits. Ripples marks are uncommon, but where present, are usually symmetrical. Locally coarser-grained sediments are preserved in the troughs. Evidence for current reversals is suggested by herringbone cross-stratification. Prominent reactivation surfaces cut across bedding.

Palaeocurrent indicators within the Sinqeni Formation display a prominent southerly trend with a less well developed trend towards the north-northeast (Figure 2.10).

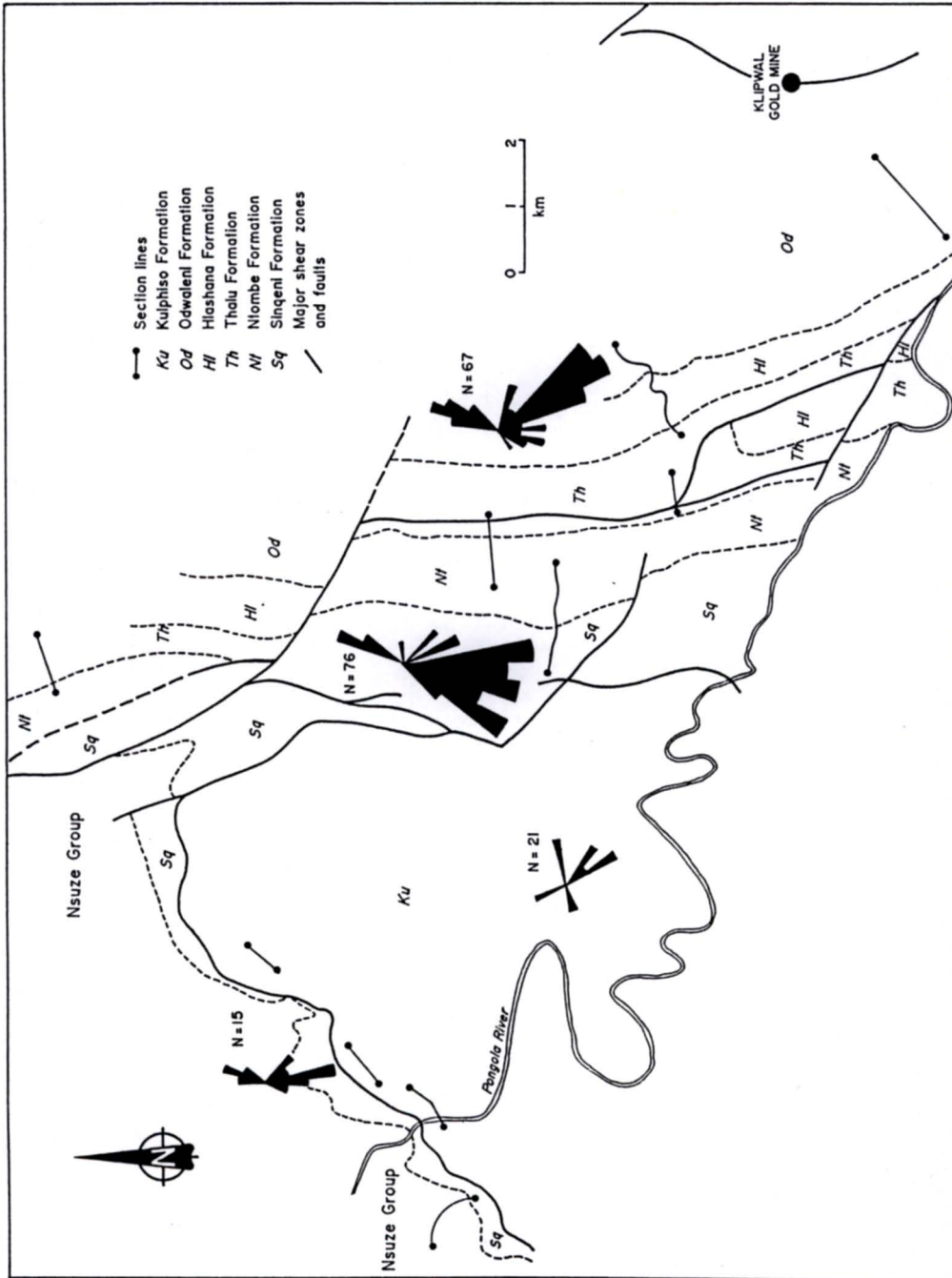


Figure 2.10: Palaeocurrent indicators within the study area. Measured profile localities also shown.

Associated mineralization

Basal Conglomerates

Prospecting of the conglomerates for gold has occurred sporadically since the end of the last century as evidenced by prospecting pits on the farms Altona, Gunsteling and Vergenoegheid and sample sites on the farm Nooitverwacht. Since the mid-1960's, and particularly in the last few years, several mining companies have analysed the conglomerates for gold. These conglomerates resemble the Witwatersrand banket, but no economic concentrations of gold have been located to date.

Marker Iron-Formation

Gold mineralization occurs in the marker iron-formation together with disseminated pyrite and is commonly associated with brittle fault zones (Figure 2.11). An attempt at mining this gold between the Sinqeni and Delft shear zones was made in the early-1980's by the Lonrho Corporation. The mine (Altona mine), was abandoned due to the structural complexities and the fractured nature of the iron-formation in the hanging wall (J.C. McKay, pers. comm., 1991).

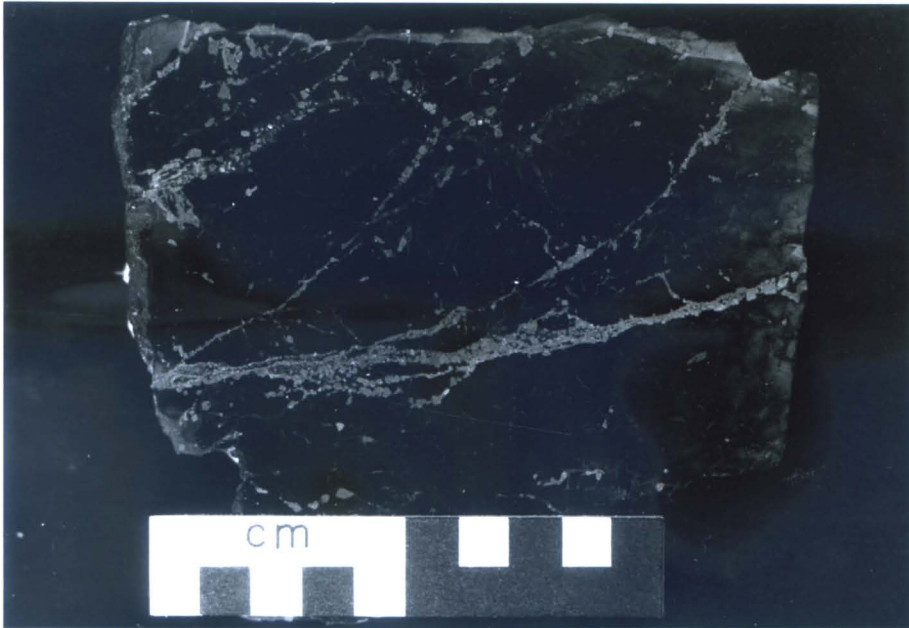


Figure 2.11A: Pyrite in small-scale listric faults in the marker iron-formation. Sample collected from the ore dump at the Altona Mine.

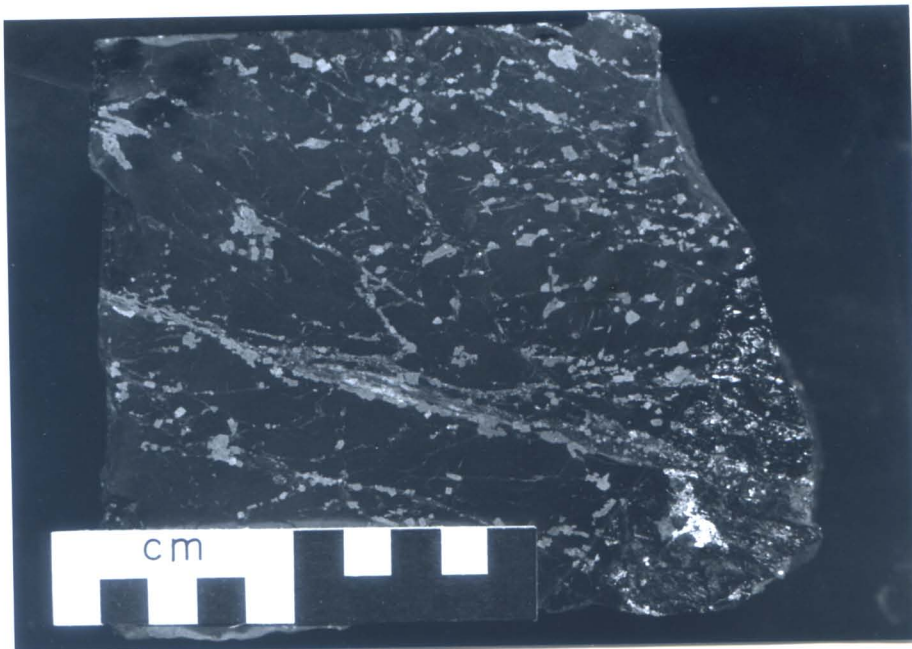


Figure 2.11B: Disseminated pyrite in the marker iron-formation. Sample collected from the ore dump at the Altona Mine.

Ntombe Formation

The ~900 m thick Ntombe Formation overlies the Singeni Formation and is named after the Ntombe stream to the south of the Pongola River. This formation is composed of ferruginous and non-ferruginous mudstone and siltstone (Figure 2.8A).

The lower mudstone is medium- to fine-grained and ferruginous, and has a banded appearance due to the presence of alternating ferruginous and non-ferruginous beds which have a maximum thickness of 30 cm. Small symmetrical ripple marks, with a wavelength less than 1 cm are developed in the mudstone (Figure 2.12). Interbedded with the ferruginous mudstone are graded lenses of siltstone. Locally lensoid pebble lag deposits (1-3 cm thick), consisting of well rounded vein quartz and chert pebbles up to 1 cm in diameter, are associated with the siltstone.

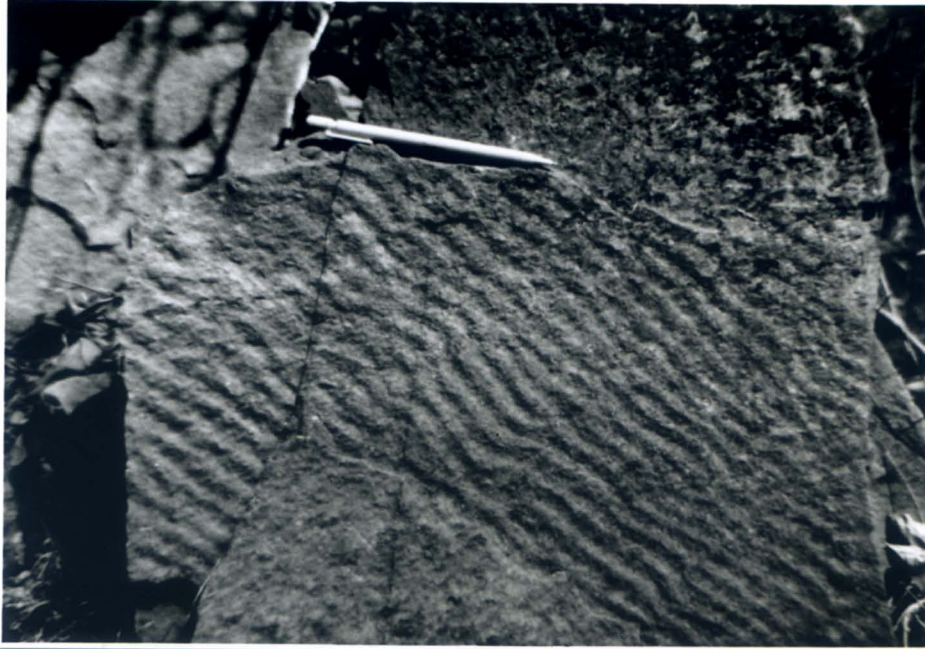


Figure 2.12: Small-scale symmetrical ripple marks in the Ntombe Formation (Duduka valley).

The ferruginous mudstone is gradationally overlain by a 15 m thick siltstone exhibiting delicate plane-lamination and planar cross-lamination which grades upwards into a finely laminated 140 m thick mudstone. This siltstone-mudstone cycle is repeated. The siltstone is also about 15 m thick but differs from the lower one in that it is characterized by contorted bedding. An overlying ferruginous mudstone is ~50 m thick and locally displays well-developed banding. The iron content diminishes as the unit grades into another overlying mudstone. This mudstone is relatively thick (500 m) and is generally very fine-grained and finely laminated. A number of fine- to medium-grained sandstone lenses, 10 to 15 cm thick, and two ferruginous mudstone interbeds are present in the lower portion. The latter are similar in character to the lower ferruginous mudstone.

The combined Sinqeni and Ntombe Formations make up an upward fining succession, with arenites dominating the lower third and argillaceous sediments the upper portion.

Thalu Formation

The Thalu formation is some 600 m thick and is characterized by alternating mudstone, ferruginous mudstone and sandstone with a near basal banded iron-formation. It commences with a moderately mature 50 m thick sandstone characterized by 20 to 30 cm thick beds that are plane-bedded and planar cross-bedded. The sandstone grades up into a fine-grained laminated mudstone, which in turn grades into a very fine-grained banded iron-formation (BIF; Figure 2.8A). The BIF comprises rhythmically interlaminated iron-oxide (magnetite and haematite) and grey chert or jasper. Pods of replacement chert commonly occur in the silica-rich laminae. Micro-laminations in this chert continue across the pods. Individual beds range in thickness from 2 mm to 3 cm. Irregular contortions of bedding are attributed to soft sediment slumping (Figure 2.13). This BIF can be correlated with the Scots Hill Member of Beukes and Cairncross (1991; Figure 2.7).

A bedding-parallel strike-slip shear zone, the Nkolotsheni shear zone, is situated above the BIF. The upper part of the Thalu Formation and a thick basal sandstone of the overlying Hlashana Formation appear to be tectonically duplicated by the Bumbeni shear zone, a splay of the Nkolotsheni shear zone.



Figure 2.13: Contorted bedding within the banded iron-formation of the Thalu Formation (Vergenoegheid farm).

The two units above the Nkolotsheni shear zone are both upward coarsening cycles with a mudstone grading upward through a black iron-rich mudstone into a poorly sorted sandstone. The mudstone is horizontally bedded and commonly contains lenses of sandstone 1-20 cm thick. Flat topped ripple marks frequently occur within the mudstone. Within the lower iron-rich mudstone is an approximately 1 m thick iron-poor mudstone which locally contains sandstone and mudstone clasts up to 5 cm in size. The two sandstones are generally fine-grained and commonly contain angular clasts of black chert with their long axes lying in the bedding plane. Where the original sedimentary structures are not obscured, planar cross-bedding, graded plane-bedding, flat topped ripple marks and poor sorting are observed.

Associated iron ore deposits

The largest concentration of iron ore in the study area is located within the BIF of the Thalu Formation. In a viability study carried out by ISCOR (Carney, 1984) the iron content was quoted as being 38 wt% and therefore not of economic grade. Other ferruginous shales are not as iron-rich as the BIF and were not considered as potential economic deposits.

Hlashana Formation

The ~400 m thick Hlashana Formation is dominated by sandstone and siltstone and is an upward coarsening succession (Figure 2.8B). A structureless mudstone at its base grades up into a fine grained sandstone. In this transitional zone lenses of sandstone 5-20 cm thick commonly occur as drapes (Figure 2.14). Occasionally clast-supported conglomerate beds are present. The constituent pebbles are 5-10 mm in size, well-rounded and well-sorted, and consist of black and white chert. These conglomerates comprise laterally extensive lensoid beds that can be traced for hundreds of metres.

The sandstone is overlain by a 70 m thick medium-grained orthoquartzite that does not contain any internal conglomerate beds. This unit is in turn overlain by a sequence consisting of a 30 m thick siltstone, a 40 m thick sandstone, a 100 m thick siltstone and a 150 m thick sandstone. The latter sandstone is fine- to medium-grained, well-sorted, very mature and is characterized by plane-bedding and angular and asymptotically-based planar cross-bedding (Figure 2.15). The planar cross-bedding is often graded (Figure 2.16), and in some cases, recumbent foresets are developed (Figure 2.17). Trough cross-bedding is rare (Figure 2.18). Ripples, including interference and flat topped bedforms, are common and range in amplitude from about 5 mm to 4 cm. Although palaeocurrent direction is predominantly southward, there is abundant evidence for variable flow

direction and current reversals (Figures 2.10 and 2.15). Dewatering structures become common towards the top of the sequence.



Figure 2.14: Sandstone drapes at a mudstone/sandstone contact in the Hlashana Formation.



Figure 2.15: Plane bedding and asymptotically-based planar cross-bedding showing current reversals in the Hlashana Formation (Madaga stream).



Figure 2.16: Graded foresets in sandstone of the Hlashana Formation (Madaga valley).



Figure 2.17: Recumbent foresets in sandstone of the Hlashana Formation (Bumbeni valley).



Figure 2.18: Plan view of well-developed trough cross-bedding in the Hlashana Formation (Bumbeni valley).

Conglomerates (up to 20 cm in thickness) and pebble sheets (Figure 2.19) are developed throughout the sandstone facies. Clasts are angular, composed of black and white chert and sometimes banded chert and vein quartz as well, and are up to 5 cm in diameter. The matrix is usually poorly sorted and consists predominantly of sub-rounded quartz grains. Imbrication of clasts supports a southward transport direction.

The siltstone in the Hlashana Formation is immature, poorly sorted and contains sandstone, conglomerate and mudstone interbeds. The conglomerates are commonly made up of angular rip-up clasts of mudstone. Sedimentary structures are similar to those in the sandstone. Asymmetric ripples are common and locally develop into mega-ripples with amplitudes of 20 cm and wavelengths of 45 cm.



Figure 2.19: Pebble sheet in the Hlashana Formation near the Pongola River - Bumbeni Stream intersection.

Odwaleni Formation

The Odwaleni Formation is some 900 m thick (Figure 2.8B) and is distinguished from the underlying Hlashana Formation by interbedding of mudstone, ferruginous mudstone and diamictite with sandstone. There is an abrupt upward transition from the underlying Hlashana Formation into the Odwaleni Formation, the base of which is marked by a 40 m thick structureless ferruginous mudstone. This grades upwards into a feldspathic quartz-wacke overlain in turn by a finely laminated siltstone and a second quartz-wacke. Five to 8 cm thick pebble lag deposits occur within the quartz-wacke. A 10 to 12 m thick diamictite bed rests disconformably on the second quartz-wacke. It is massive and contains only small clasts no larger than 2 cm in diameter. The overlying 20 m thick

mudstone is overlain with a sharp contact by a quartz-wacke which contains an intraformational iron-formation approximately two-thirds of the way up. This 30 m sandstone - iron-formation assemblage constitutes a useful marker in that it is easily recognised, and can be mapped along strike for several kilometres in the footwall as well as in the hanging wall of the Klipwal shear zone. The sandstone is characterized by plane-bedding and planar cross-bedding with beds up to 75 cm in thickness. Soft sediment deformation is common and is manifested by dewatering, dish, and ball and pillow structures (Figure 2.20).

The overlying 50 m thick stratified mudstone displaying flame and ball and pillow structures underlies an 80 m thick indurated, black diamictite. Clast rock types are very diverse being made up of quartzite, vein quartz, chert, banded iron-formation, mudstone, gneiss (Figure 2.21), granite and volcanic rock. The clasts range in size from less than 1 cm to about 75 cm in diameter. They are randomly dispersed and show little preferred orientation, except for a weakly developed parallelism with faint horizontal stratification. Some faceted and striated clasts were observed (Figure 2.22). The diamictite differs from all rudites in the Pongola basin in that they display an exceptional diversity in clast size and composition.

The diamictite is overlain by a 30 m thick sandstone, which in turn is overlain by a 40 m thick mudstone and another 15 m thick sandstone. The lower sandstone displays soft sedimentation dewatering features and load structures that extend into the subjacent diamictite (Figure 2.23).

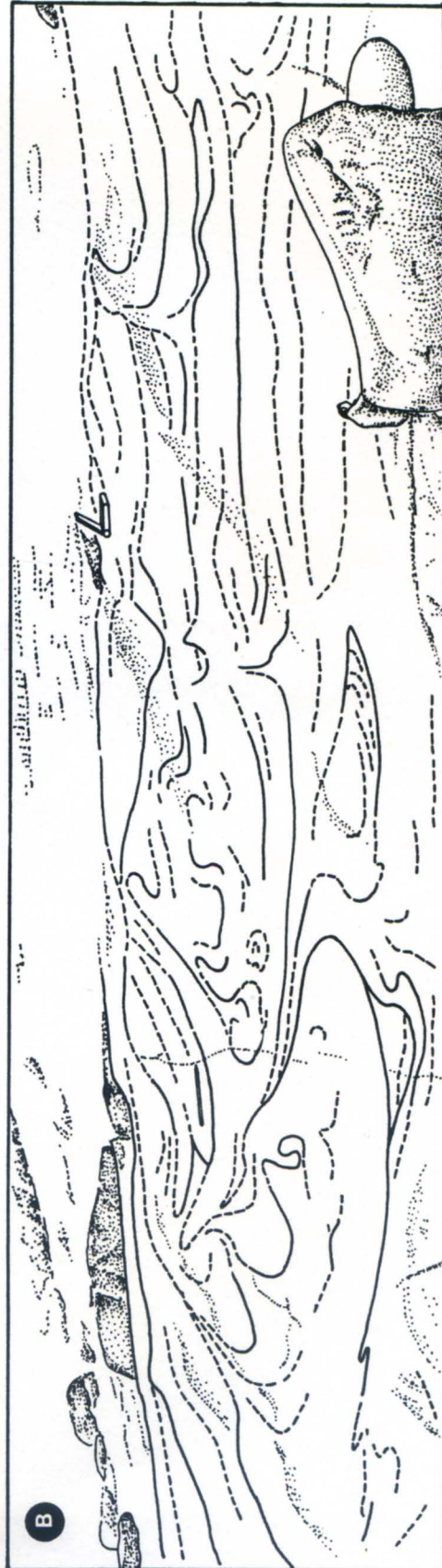


Figure 2.20: Soft sediment deformation in an Odwaleni Formation sandstone east of the Meander shear zone. Photographic (A) and diagrammatic (B) representations.



Figure 2.21: Gneiss clast in diamictite of the Odwaleni Formation (Madaga Stream).



Figure 2.22: Striated clast set in diamictite within the Odwaleni Formation (Mageza stream).

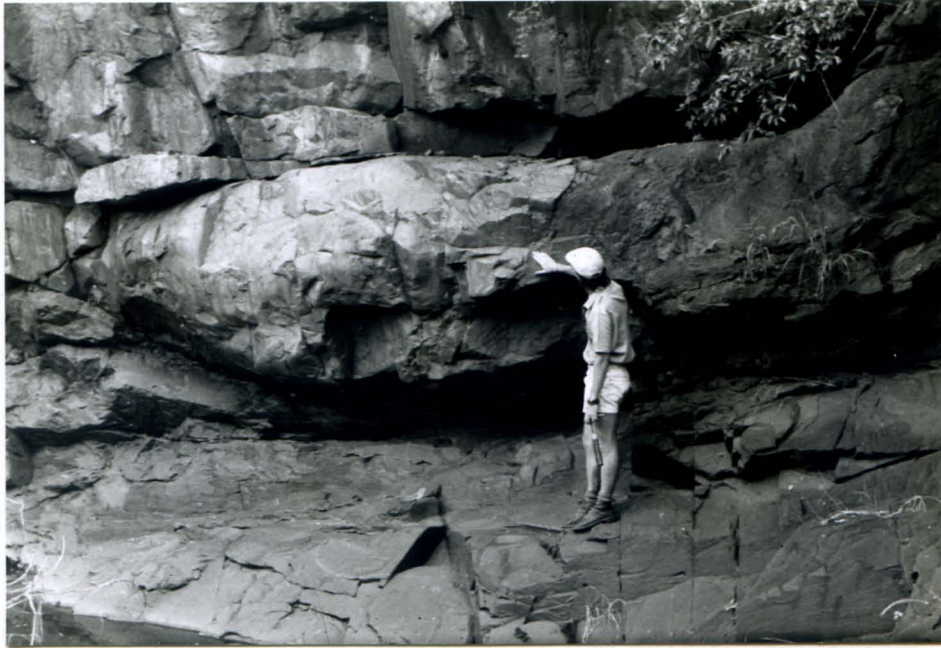


Figure 2.23: Load casting of sandstone into subjacent diamictite of the Odwaleni Formation (Mageza Stream).

The upper sandstone is medium-grained and plane-bedded. It is finely laminated and contains rip-up clasts (up to 5 cm long) near its base. Double crested ripples are occasionally developed (Figure 2.24). At higher levels it becomes fine-grained, locally structureless and grades up into a mudstone which becomes ferruginous upwards. This is overlain by two massive diamictites, with clasts up to 2 cm, that both grade up into laminated mudstone. The top of the formation is defined by two quartz-arenites, each overlain by mudstone. The lower sandstone has planar cross-beds, ranging in thickness from 1-40 cm, which indicate southward palaeocurrent directions. Symmetrical ripple marks with wavelengths less than 1 cm are developed. Immediately above the lower sandstone-mudstone contact are lensoid beds of sandstone less than 10 cm thick that become progressively thinner and less well-defined upwards.



Figure 2.24: Double crested ripples in sandstone of the Odwaleni Formation (Namkhuzwa valley).

An upward fining quartz-arenite overlies the mudstone with a sharply defined contact. Near its base, the sandstone contains pebble sheets with grains 0.5 to 1 cm in size. Higher up in the sequence symmetrical ripples become common. The sandstone grades upwards into a mudstone, locally containing iron-rich units. The latter constitute the topmost lithology of in the formation.

Kulphiso Formation

The Kulphiso Formation is located in the hanging wall of the Gunsteling normal fault and is best exposed on Prudentie (Map 1A). It consists of alternating sandstone, mudstone, ferruginous mudstone and a banded iron-formation near its base. The stratigraphic position of this ~ 800 m thick succession (Figure 2.25) is uncertain. Its constituent units

cannot be matched with those of the Ntombe Formation. It does however have similarities with the upper parts of the Ntombe Formation and the lower units within the Thalu Formation.

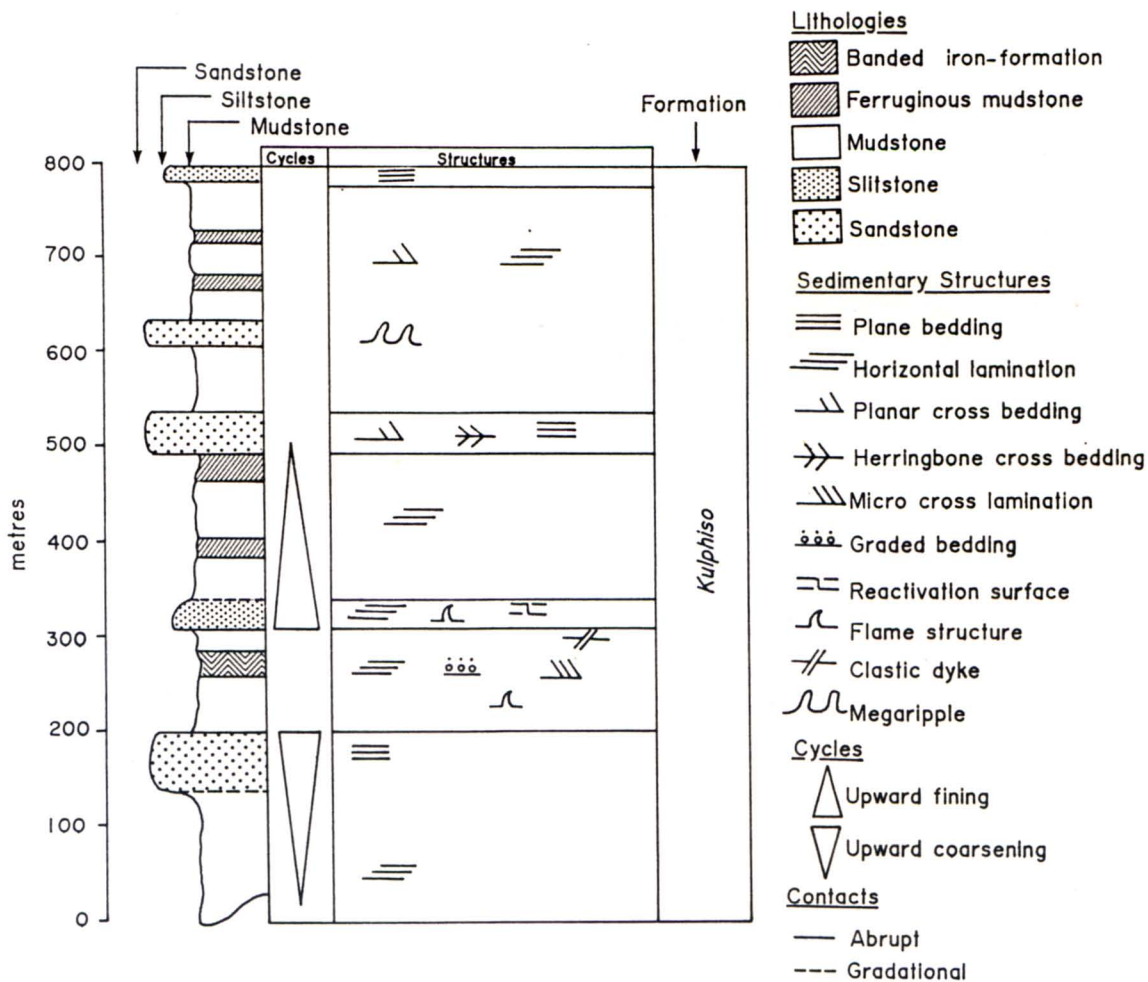


Figure 2.25: Stratigraphic column for the Kulphiso Formation.

The Kulphiso Formation is regarded here as a separate entity of uncertain stratigraphic position, either above the Odwaleni Formation if the displacement on the Gunsteling fault is large, or equivalent to the Ntombe Formation if small. The Kulphiso Formation is unlike the other Mozaan formations in that it comprises a higher proportion of argillaceous sedimentary rocks.

The lowest mappable unit is a horizontally laminated mudstone that is at least 140 m thick. Interlayered siltstone marks the gradational contact with an overlying sandstone. The sandstone varies in thickness between 30 and 70 m. Discontinuous sandstone beds about 1 m thick are developed near the base of the overlying 110 m thick mudstone. The mudstone is characterized by fine laminations, graded bedding, micro-cross-lamination, water escape structures (Figure 2.26), rip-up clasts and clastic dykes (Figure 2.27). It is locally magnetic and banded iron-formation is found near the top.

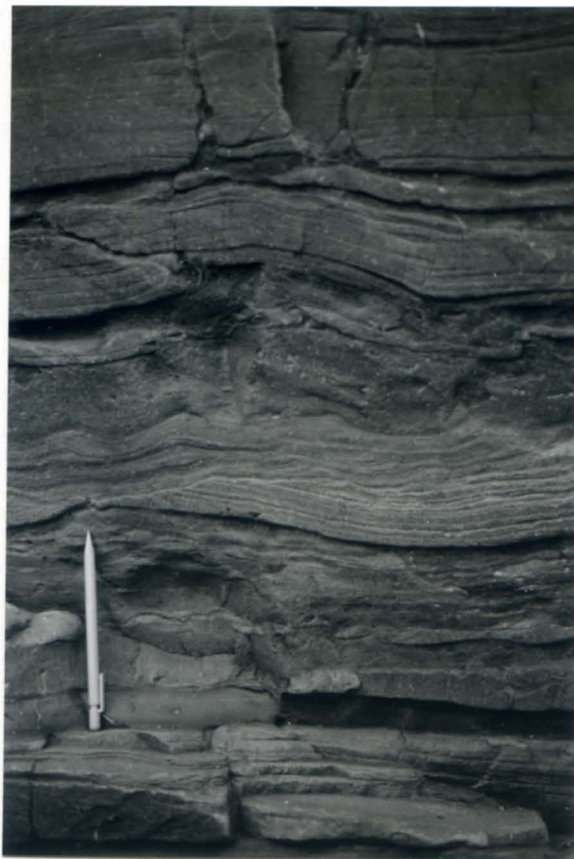


Figure 2.26: Laminated mudstone which locally displays dewatering structures found in the Kulphiso Formation (Mkhuzwa valley).



Figure 2.27: Micro-cross laminated mudstone intruded by a clastic dyke in the Kulphiso Formation (Mvumangwe stream).

A 35 m thick horizontally laminated siltstone separates this mudstone from a 160 m thick overlying one. Locally flame structures disrupt the alternating arenaceous and argillaceous laminations in the siltstone, and on a small scale, reactivation surfaces are developed. The upper mudstone is partly ferruginous.

The overlying sandstone varies in thickness from 20 to 40 m. Individual beds are ~ 30 cm in thickness and contain bimodal planar cross-beds and plane-beds. The medium-grained quartz-wacke passes unconformably up into a quartz-arenite locally containing coarse-grained beds with well rounded clasts. Overlying the sandstone is a mudstone. Classic mega-ripples, with amplitudes of 20 cm and wavelengths of 100 cm, are developed at the top of the overlying sandstone (Figure 2.28).



Figure 2.28A: Mega-ripples in the Kulphiso Formation to the west of Sinqeni mountain alongside the Pongola river.

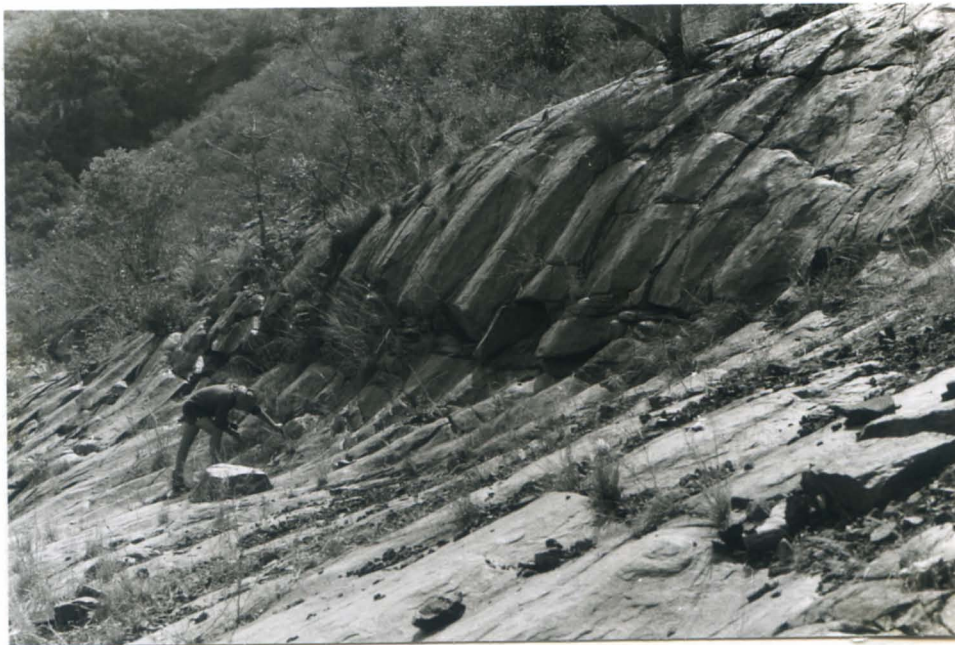


Figure 2.28B: Oblique view of mega-ripples in the Kulphiso Formation.

The formation is capped by a 150 m thick mudstone succession, containing sandstone interbeds up to 10 cm thick and two iron-rich units. This grades up into a 15 m thick siltstone with thin (5-20 cm) beds of quartz-wacke.

Sedimentological Interpretation

Following the final phases of Nsuze volcanism, the Pongola depository is believed to have undergone substantial subsidence with the development of a broad, relatively shallow, epeiric sea which covered an extensive area (Figure 2.29).

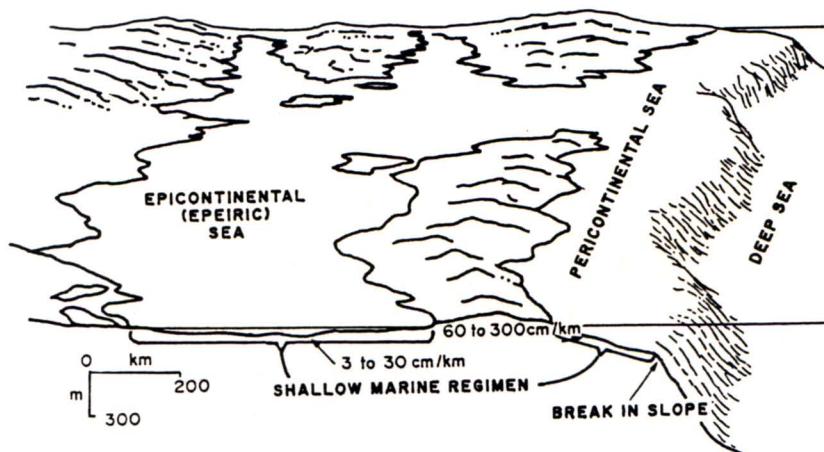


Figure 2.29: Diagrammatic model distinguishing between epicontinental and pericontinental seas (after Boggs, 1987).

There are no truly representative modern analogues for an epeiric sea, although the Baltic Sea, Yellow Sea, Bering Sea and Hudson Bay have been proposed as possible modern counterparts (Klein, 1982; Nio and Nelson, 1982; Fraser, 1989). Shallow marine models are based on pericontinental sea environments (Heckel, 1972; Fraser, *op. cit.*). It is assumed that similar sedimentological processes operate on continental shelves as they did in epeiric seas (Boggs, 1987), but the similarities of, and the differences between these two environments are not yet completely understood.

Epeiric seas differ from their modern counterparts chiefly in their broad lateral extent with a corresponding low gradient, and partial or complete isolation from deep oceanic basins. These factors, in turn, probably imposed major constraints on the processes which operated in the shallow waters of such epeiric seas, in that the introduction of wave-, tide- or climatically-induced currents from any deep marine basins into the shallow marine environment must have, to a degree at least, been prevented (Fraser, 1989).

The shallow depths and gradients in epeiric seas could extend the friction-dominated zone much farther offshore than present-day marginal seas. As a result of the dominance of these frictional forces, it is likely that the energy of most waves would be dissipated over broad areas of the basin and would have little effect on the substrate. The nearly flat gradients in epeiric seas meant that initial rates of progradation were faster than those occurring in marginal seas, and the volumes of sediment needed to maintain a constant rate of progradation did not need to increase geometrically. The result of low gradients, therefore, is that depositional systems can cover significantly wider areas than those on modern shelves. This effect is enhanced by the reduced ability of marine processes in epeiric seas to redistribute incoming sediment (Fraser, 1989).

According to Swift *et al.* (1971), the shelf is subjected mainly to such currents as tidal and storm-generated currents which rework and transport sediment. The currents resulting from tidal action on shelves are bidirectional, and usually asymmetric with respect to velocity. Symmetrical waves give rise to the development of comparatively small, intricately related, herringbone cross-bedding, while asymmetric currents shape sand waves with one side so steep that large-scale separation is inevitable. The asymmetric currents may result in sediment transport in one direction only if tidal velocity is near the threshold needed for erosion and transport (Boggs, 1987).

Unidirectional currents are generated by wind shear stress, usually during severe storms, as wind blows across the water surface, gradually entraining progressively deeper layers

of water, until, if wind velocity and duration are great enough, the moving column of water may extend to the seabed with enough velocity to transport sediment (Boggs, 1987). Where the wind forces water on shore, it creates an elevation of the water column and hence a seaward pressure gradient. Water particles experience the pressure gradient, as well as the Coriolis force, causing the initial seaward flow to be deflected to the left (in the southern hemisphere). This seaward flow will evolve into a geostrophic flow moving sub-parallel to the isobaths (Allen, 1984; Walker, 1984; Boggs, *op. cit.*; and Figure 2.30). During such storms sand may accumulate deeper within the basin as a response to transportation of sediment from the basin margins by geostrophic flow, which is induced by wind forcing, barotropic gradients and tide forcing. As a consequence the dominant transport directions are nearly parallel to the coastline. However, due to the shelf gradient, a small offshore component of transport may be present, and down-welling currents produced during storms may be particularly effective in transporting sediment away from the shoreface and depositing it deeper into the basin (Fraser, 1989).

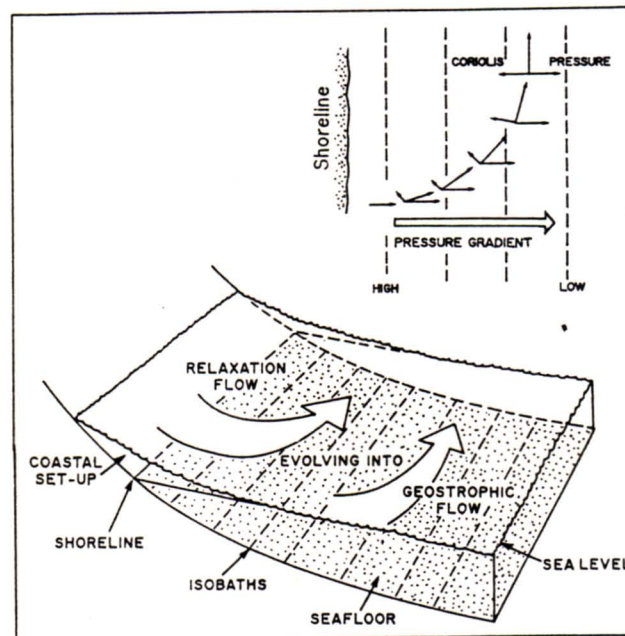


Figure 2.30: Model showing the evolution of geostrophic flows (after Boggs, 1987).

The storms may generate flows which result in the formation of current ripples and mega-ripples. Such currents with high velocities (in the order of 2 m/sec) may result in the development of plane-bedding if the water is not too deep (Winn, 1991), but if the water is too shallow, these plane-beds will be destroyed with the formation of dunes which are subsequently reworked into current ripples. The net result may therefore be an increment of sand transport, but no preservation of sedimentary structures other than ripple cross-lamination.

Two features characteristic of storm deposits are graded storm deposits and hummocky cross-stratification (Gadow and Reineck, 1969; Duke *et al.*, 1991; Monaco, 1992). Graded storm layers are found in somewhat deeper waters than hummocky cross-stratification and occur where the mean flow component is greater than the wave orbital component (Reineck and Singh, 1980; Aigner, 1982). Graded storm layers have long been recognised on modern shelves, but have been interpreted as turbidites, as they are similar to Bouma sequences (Fraser, 1989). It is more probable that graded layers represent the deposits of strong bottom flows generated by barotropic gradients set up by storms that transport sediments put into suspension by cyclic storm wave loading of the substrate (Nelson, 1982).

Hummocky cross-stratification (HCS) develops as flow transverse bedforms with no avalanche faces and represents sharp-crested mega-ripples that have been modified by complex storm currents where the wave orbital current component is greater than or equal to the mean flow component. They are best preserved on the inner shelf where fair weather wave and current activity is normally insufficient to remould the substrate (Fraser, 1989; Duke *et al.*, 1991).

Studies of modern shelves suggest that they may receive relatively small amounts of extrabasinal sediment during a transgressive phase (Fraser, 1989). Sediments are derived primarily from within the basin itself through shoreface bypassing, and these are spread

as a blanket of sands over the shelf as the sea level rises and the shoreface retreats. In shelf bypassing, the sediments eroded from the retreating shoreface are shifted down current by littoral drift, and by inner shelf storm currents during periods of strong onshore winds, and tend to be deposited just seaward of the shoreface, to form the leading edge of the shelf surficial sand sheet (Swift, 1975).

There is an enormous range in the size and geometry of sand bodies. First order features make up a sand sheet, or massif, comprising linear bodies of sand in the order of 100 km in length, 10's km in width, and trend perpendicular to depositional strike. Second order sand ridges which develop on the linear sand ridges may be up to 40 m high and 10's km long. These constructional features formed on the shelf by the interaction of tide- and storm-generated currents (Fraser, 1989) and are capable of being reworked by processes incipient on the shelf (Swift, 1976). Such ridges may migrate at a rate of 120 m/year (Swift and Field, 1981). Transport of sediment on the ridges may occur in the form of smaller scale bed forms as they migrated up and out of swales and onto the flanks of the sand ridges, commonly at an oblique angle to the ridge crests. The resulting internal structures consist of smaller scale cross-beds within larger scale, gently inclined beds. The migration of these second order features result in the formation of reactivation structures. Third order features which may be superimposed on the linear sand ridges are sand waves as much as 10 m high and 500 m long (Fraser, *op. cit.*). These form mainly in response to tide- and wind-driven currents and developed with their crests perpendicular to the resultant flow and are evidenced by reactivation surfaces. The internal structure of the sand wave is a result of the strength and degree of asymmetry of the governing currents (Allen, 1980). Reactivation surfaces as the result of migration of smaller bedforms over the larger ones.

Considerable information concerning the origin and dynamics of sand ridges and sand waves is available, but relatively little is known about their evolution (Fraser, 1989). Anderton (1976) proposed a model where sands are deposited in large sand waves under

fair-weather conditions at the upstream end of flow paths, producing thick, tabular sets of cross-beds. During moderate storms, however, sand wave crests are eroded, and sand is transported farther down the transport path, where it is deposited on small dunes, producing trough crosssets. At the same time, fine-grained sediments are carried to the distal ends of the transport paths, where they are deposited in storm layers.

The physical conditions of deposition of muds is more difficult to interpret than those of coarser grained deposits (Collinson and Thompson, 1989). There are two main reasons for this:

1. The range of different physical processes which operate during deposition of muds is much more restricted than for coarser grained sediments in that muds are mostly deposited by suspension settling processes.
2. Fine-grained sediments, particularly those rich in clay minerals, have a much higher initial porosity than most coarse-grained sediments, which makes them more susceptible to compaction on burial. This has the effect of distorting and compressing any structures (and initial thickness) to the point where they are completely obliterated. It is also not understood why fine-grained muddy sediments accumulate in high energy areas, such as the coastal zone (Hill and Nadeau, 1989).

The mud accumulates in areas of the basin which are not subjected to large shear stress, e.g. in deep water and at the end of tidal transport paths, or where rates of influx are so large that episodic shelf transport processes are unable to redistribute all the incoming sediment (Fraser, 1989). The presence of muds implies relatively weak tidal currents (Stride *et al.*, 1982). Density stratification may be intense in the basin as a result of warm river water flowing over cool ocean water. When combined with offshore wind-forced surface waters, cold, nutrient-rich waters may intrude on to the shelf until flocculation causes mixing (Boggs, 1987; Fraser, *op. cit.*).

It is common for mud substrates to lack bedforms other than ripples (Fraser, 1989), and the most common type of stratification present is caused by rhythmic alternations of coarse and fine layers produced in response to episodic transport induced by passing storms (Reineck and Singh, 1972).

Sinqeni Formation

An upward fining succession, such as the one observed in the Sinqeni Formation, is characteristic of a transgressive depositional cycle in a progressively deepening basin (e.g. Fraser, 1989) as is apparent from its great thickness (650 m). The amount of sediment delivered was large and apparently large enough to overcome the tendency of sediments to be trapped in the shore zone (as described by Fraser, *op. cit.*, page 300) during periods of rising water level.

The basal sandstone is interpreted to have resulted from the development of a broad sand sheet as a response to the accumulation of coarse-grained sediments in a rapidly subsiding basin. The abundance of both delicate herringbone cross-bedding and larger scale bidirectional cross-bedding within the sandstone implies that there was a variation in the symmetry of the currents operating within the basin. Shallow depths are characterized by large sand waves (Walker, 1984), which would have resulted in the formation of the large-scale cross-bedded units observed in the sandstone.

The polymict conglomerates near to the base of the Sinqeni Formation are the result of high current velocities. Two different, interacting mechanisms can be postulated for their formation. Initially high-density turbidity flows, representing a reworking of coarse material that was deposited at mountain flanks in fan-delta or beach environments, was transported and then redeposited in the deeper, more distal parts of the epeiric sea by debris flows. Alexander *et al.* (1990) maintain that such conglomerates are frequently

associated with sandstone packages, and this association, along with the sandy matrix and local clast imbrication, is suggestive of a turbidity flow (Lowe, 1982). Later, the turbidity flow deposits were winnowed by strong tidal-currents which removed much of the finer sand fraction to leave a lag of gravel. The sand would have been transported away in the form of sand-ribbons and asymmetrical sand waves (Stride *et al.*, 1982). Similar modern gravel sheets from around the British Isles have been reported by Stride *et al.* (*op. cit.*) and seem to be aerially extensive and, like the conglomerates of the Sinqeni Formation are very thin. The plane-bedded units associated with the conglomerates are possibly the result of deposition arising from storm-generated, pressure-gradient flows (Winn, 1991), which could have initiated the turbidity flows.

Deposition of the sand sheet (i.e. the basal sandstone) was abruptly terminated either by a rapid increase in water depth (due to a tectonic subsidence or a rise in sea level), or to a dramatic climatic change whereby river run-off abated resulting in clastic input into the basin being vastly reduced. It appears that deposition of the very fine-grained marker iron-formation (MIF) took place under essentially quiescent sedimentary conditions. The absence of sedimentary structures in the iron-formation, with the exception of bedding 2-25 cm thick, suggests that suspension settling of the fine ferruginous particles along with clay minerals occurred in waters removed from any current activity. Chemical precipitation accompanied suspension settling resulting in the formation of banded iron-formation. Depositional conditions were not consistent throughout the depository during deposition of the MIF which resulted in lateral variations in the iron content and nature of the facies, as well as its variation in thickness. Its lateral persistence militates against Watchorn's (1978, 1979a, 1980) interpretation of the MIF representing abandoned channel deposits.

Following this period of quiescence, the Mozaan basin was again subjected to transgression, where clastic sediment was contributed in vast amounts probably by inflowing fluvial systems. This resulted in the accumulation of the 170 m thick quartz-wacke. It appears that these sands were not reworked to the same degree as those seen

in the basal sandstone as is indicated by the upward decrease in maturity of the sandstone from the first to the second sandstone units, although similar depositional mechanisms for the two units are inferred.

Ntombe Formation

The initiation of the Ntombe Formation deposition indicates the onset of a brief respite in the subsidence rate of the basin as well as a decrease in sediment input into the Mozaan basin. These muds were the products of chemical weathering of unstable rock sources (e.g. basic igneous rocks) within the provenance area and extreme physical attrition. The fine-grained debris which was produced by chemical weathering comprised mainly clay minerals and chlorite. The physically derived sediment component had a mineral content dependent upon the rocks of the source area (Collinson and Thompson, 1989). The mud fraction of epeiric sea deposits was probably extrabasinal. Unlike shelf sands muddy shelf deposits represent slow settling of suspended sediments, and would be moulded by tides and storms (Galloway and Hobday, 1983). These siliciclastic muds and sands were contributed to the shelf by river outflow, and shoreline erosion, together with fine dust blown into the epeiric sea from a vegetation-free source area.

It is possible that the coarser fraction of incoming sediment was trapped in the foreshore zone in river mouths and distributaries as they become transformed into estuaries with the rapid rise in sea level. These areas then acted as sediment sinks, trapping riverine sediments on fringing tidal flats and bayhead deltas as described by Fraser (1989). The finer mud fraction bypassed the areas where sands were being trapped and continued in suspension into the central parts of the basin.

A considerable thickness (some 900 m) of mudstone and ferruginous mudstone makes up the Ntombe Formation. This succession represents a facies association indicative of a

prolonged quiet period during which time clastic sedimentation was not occurring on any significant scale. The only coarse-grained sedimentation led to the development of pebble and silt lenses within the mudstone and the two relatively thin siltstone units. It is apparent from the poor sorting of the coarser-grained beds, their immaturity and the evidence for soft sediment deformation, that they accumulated rapidly in an environment which was atypical of Mozaan sedimentation at the time. They may be related to deposition under storm induced conditions which initiated slope failure and movement into the basin under gravity.

Following the deposition of the silty units, a prolonged period of quiescence prevailed during which time some 500 m of argillaceous sediments accumulated. This interval was marked only by variations in the iron content of the accumulating muds, possibly related to a change in climatic conditions and different weathering processes of the provenance area.

Thalu Formation

The quiet conditions experienced during the deposition of the Ntombe Formation were terminated by the laying down of the basal plane-bedded and planar cross-bedded sandstone of the Thalu Formation. This sandstone is interpreted to have developed as a sand patch or a broad expanse of sand lacking large-scale surface morphology within the basin related to storm surge retention flow. Sand patches occur in areas where turbulence is sufficient to keep mud in suspension or to resuspend it episodically after it has been deposited, and where the amount of available sand is small or where current velocities are insufficient to maintain large bedforms (Fraser, 1989).

Deposition of sand within the sandpatch ceased following a gradual decrease in the input of coarse clastic sediment into the basin, until only deposition of muds from suspension

took place. When most of the mud particles had settled out from suspension, deposition of chemical precipitates in the form of banded iron-formation took place. This iron-formation closely resembles those of the Lake Superior-type (Eichler, 1976; Mel'nik, 1982; Cloud, 1983; Beukes, 1983), in that it is associated with clastic sedimentary rocks of shelf, epicontinental or eugeosynclinal environments, and does not have any direct spatial relationship to volcanic activity. Many of the Lake Superior-type deposits occur in basins lacking contemporaneous volcanism and which reflected conditions prevailing in restricted basins. Deposition of the iron-formation occurred in shallow and quiet water environments at depths of between 50 and 200 m (Eichler, *op. cit.*). The chert pods that are observed in the iron-formation, suggest that there was an early diagenetic compaction of the original sediment, while the prelithification slump structures indicate that both the chert and the iron-formation were deposited originally as a colloidal mass.

Deposition of the mudstone and iron-rich mudstone in the upper parts of the Thalu Formation must have occurred under quiescent conditions in relatively deep waters. Occasional storm deposits resulted in the accumulation of winnowed residual lag conglomerates. The gradational upper contact with the overlying sandstone is possibly the result of a transgression of a sandpatch in a gradually shallowing basin. Watchorn (1979a) attributed this facies change to a progradational shelf. The sandstone is not well sorted indicating relatively rapid deposition, typical of storm deposits. The black chert fragments in the sandstone facies possibly represent rip-up clasts eroded from tidal flat and beach environments. This transition from mudstone, through black mudstone to sandstone, is repeated indicating a facies sequence.

Hlashana Formation

During the deposition of the Hlashana Formation, the Pongola epeiric sea was probably relatively shallow and subjected to a transgressive phase again as indicated by the

accumulation of a vast thickness of arenaceous sediments.

There is much evidence within these sandstones and siltstones to suggest that they are the result of storm-induced conditions, such as pebble lag sheets, mega-ripples and poor sorting. Sand and silt may be transported from tidal flats and sand bars towards the centre of the basin by ebb currents during storm surges (Gadow and Reineck, 1969; Walker, 1984; Fraser, 1989). Deposition associated with large volumes of water would have resulted in the formation of soft sediment deformation structures as a result of slumping which are characteristic of this succession. Silts are also particularly susceptible to liquefaction during storms due to their low permeability (Cluckey *et al.*, 1985; *cited in* Hill and Nadeau, 1989).

In contrast to the poorly sorted siltstones, the sandstones are well-sorted and mature. Progressive sorting of sediments was not a continuous process, but instead occurred during short periods of intense current flow, interspersed with long periods of storage. Sorting can work to completion only where the influx of sediment does not overwhelm the ability of transport processes to redistribute and sort it (Fraser, 1989). The pebble sheets within the Hlashana Formation are probably the result of winnowing of sand waves and dunes during severe storms. Pebble beds occur at the upstream ends of flow paths, and the eroded sand is carried downflow, where it is deposited as storm layers (Fraser, *op. cit.*).

The lateral variability of cross-bedding within the arenaceous deposits is attributed to the onset and passage of storm waves and currents, and to near-bed flow variations related to the existence and migration of sand waves and dunes as well as to the multidirectionality of such currents (Allen, 1973). This results in highly variable wave energy conditions, dependent on the intensity and duration of the storm (Hill and Nadeau, 1989). It is possible that this effect was enhanced by asymmetric tidal currents, with the dominant direction aligned north-south. Furthermore, the development of plane-bedding and planar cross-bedding can also be attributed to episodic deposition from storm-generated, pressure-

gradient flows (Winn, 1991). The structureless topmost bed of the Hlashana Formation appears to have been the result of rapid deposition and can be attributed to storms eroding sands from the shoreface and redepositing them farther within the basin.

Odwaleni Formation

The sharp vertical transition from the predominantly arenaceous Hlashana Formation into the succeeding mudstone-diamictite assemblage of the Odwaleni Formation reflects a rapid transformation from a shallow-water environment to deeper water conditions in which current or wave activity and arenaceous sediment input was restricted. Such subsidence could be related to tectonic elevation along marginal faults associated with rifting of the depositional basin. Such synsedimentary tectonism may have contributed to the occurrence of diamictite. The diamictite may have originated as mudflows derived from a clay-rich deeply-weathered source area, similar to that envisaged by Stanistreet *et al.*, (1988) and Martin *et al.*, (1989) for a diamictite in the Archaean Witwatersrand Supergroup. The structureless nature of the Mozaan diamictite, and its predominantly argillaceous constitution, suggest that this lithotype was emplaced in an analogous manner, as subaqueous clast-bearing mudflows (Von Brunn and Gold, 1993). The occurrence of more than one diamictite can be attributed to an intermittent supply of debris, delivered to the basin by down-slope mass flows from a topographic high. Tectonic activity and associated gravitational instability also resulted in liquefaction of sand as indicated by the deformed sandstone above the main diamictite and related load structures that protrude into the Mozaan diamictite.

Whereas tectonically induced mudflows could have been a major factor in the emplacement of the diamictite, a contributory glacial influence cannot be ruled out. Under the appropriate climatic conditions, highland ice masses would have developed and expanded on tectonically-elevated ground (Von Brunn and Gold, 1993). Snow could have been

precipitated when humid air cooled adiabatically as it rose from the adjacent marine basin. Thus local mountain glaciation, envisaged as being a side effect of uplift and related erosion, could have contributed to a supply of detritus (cf. Schermerhorn, 1974, 1975) that was subjected to down-slope gravity flow. Clasts of the transported debris would have been abraded, rounded and comminuted in the tractional zone of the active glaciers (Boulton, 1978), and possibly during sediment gravity flow as well. Subaqueous emplacement would account for the sharp contact between the diamictite and the subjacent mudstone. An absence of dropstones in the associated argillites indicates that deposition of glaciogenic sediment by rain-out from floating ice is unlikely (Von Brunn and Gold, 1992, 1993).

Persuasive evidence pointing to a glacial association relates to the presence of striations and facets on some of the clast surfaces, as well as the varied composition of the clasts. An important aspect in this regard is the distinct difference of the diamictite from all other rudaceous units in the Pongola basin. Pebble conglomerates, consisting of only quartz and chert, are widespread in the sequence, but they never show the same diversity of clast size and composition as the diamictite. Furthermore, the Mozaan diamictite is lithologically similar to other diamictites of known glacial affinity, including the Late Palaeozoic diamictite of the Dwyka Group of southern Africa (e.g. Von Brunn, 1981, 1987; Visser, 1983, 1989; Gravenor *et al.*, 1984). A conspicuous feature of the Mozaan diamictite, which distinguishes it from the Dwyka diamictite, is the presence of well-rounded sand grains some of which display a high sphericity. The grains may have been of aeolian origin and were blown onto the glaciers (from a vegetation-free hinterland), such as those described by Squyres *et al.* (1991). Alternatively the rounded grains could reflect abrasion within the basal till during subglacial transport (Anderson and Molnia, 1989), or incorporation into the basal debris of the glacier as it passed over tidal deposits at the margins of the depository.

The remainder of the Odwaleni Formation is characterised by argillaceous mudstone and

ferruginous mudstone (indicative of a tranquil depository) with interlayers of sandstones typical of storm induced deposits.

Kulphiso Formation

It is evident from the fine grained lithologies within this formation that deposition took place in a deep, tranquil environment lacking the input of large amounts of clastic material and removed from any significant current activity. These stable conditions must have prevailed for a considerable length of time which enabled the accumulation of at least 140 m of mudstone. Initially deposition occurred in the form of suspension settling of fine-grained material. The horizontal laminations are probably the result of seasonal fluctuations of conditions such as water temperature. The quiet conditions were terminated by the influx of coarser grained material, probably as a consequence of storm-induced activity.

A return to quiescent conditions is marked by the accumulation of a thick argillaceous sequence. Sandstone lenses representing probable storm deposits and chemical precipitation of the banded iron-formation interrupted the dominant process of suspension settling.

The remainder of the Kulphiso Formation is characterised by thick mudstone units interrupted by storm deposits in the form of poorly sorted sandstone and siltstone, which typically include such structures as water escape structures and clastic dykes indicative of a rapid deposition rates.

Geochemistry

The results discussed in this section represent major and trace element analyses of 12 samples of mudstone and diamictite from the Mozaan Group. The analytical data are given in Appendix 2 and localities in Appendix 3. The purpose of the analyses is to provide geochemical data for typical examples of the various rock-types.

The geochemical analyses of mudstone, iron-formation and diamictite from the Mozaan Group allow a comparison to be made with other more extensive studies (e.g. McLennan and Taylor, 1983; Laskowski and Kröner, 1985; Wronkiewicz and Condie, 1989). Fine-grained terrigenous clastic sediments provide an important source of information on the composition, tectonic setting and evolutionary growth of the early continental crust (Wronkiewicz and Condie, *op. cit.*).

An interesting feature of the analyses is their very high Cr/Ni ratios (particularly for the diamictite) which distinguishes them from other Archaean sediments (e.g. McLennan and Taylor, 1983; Wronkiewicz and Condie, 1989). High Cr concentrations indicate sources with substantial mafic or komatiitic components (Laskowski and Kröner, 1985). Chromium can be enriched in weathering profiles (Wronkiewicz and Condie, *op. cit.*) such as in the deeply weathered Archaean profiles of the pre-Pongola basement (Matthews and Scharrer, 1967; Armstrong *et al.*, 1982). Studies of Cenozoic laterites indicate that Cr is retained in upper soil layers in Cr-rich chlorite (penninite), chromite and magnetite, whereas Ni is liberated during the breakdown of olivine and pyroxene or is leached from secondary clay minerals (Zeissink, 1971). Downward migration of Ni in these laterites causes increased Cr/Ni ratios in the upper levels. Thus erosion of the upper portions of Archaean laterites possibly accounts for the high concentration of Cr in these sediments.

An alternative explanation is that the Archaean oceans may have been enriched in Cr, relative to modern oceans, due to ocean-ridge or back-arc hydrothermal leaching of

komatiitic oceanic crust. Clay-particle scavenging of Cr in enriched Archaean seawater could thus explain the high Cr concentrations in the Mozaan mudstone (Wronkiewicz and Condie, 1989).

Two samples of mudstone (MS8 and MS11) collected from the Klipwal Mine are also enriched in Cr, probably associated with mineralizing fluids.

Results presented by Wronkiewicz and Condie (1989) suggest that the Pongola mudstone was derived from a source enriched in granite by a factor of 100 to 300% relative to other Archaean mudstone in southern Africa. Homogenous hood granites are favoured for the Pongola granite source component as their trace element and K₂O contents (Hunter, 1963) match the granite composition calculated in mixing models (Laskowski and Kröner, 1985; Wronkiewicz and Condie, *op. cit.*). These granites, the most extensive of which is the Locheil batholith, occur adjacent to and may underlie much of the Pongola basin. According to Wronkiewicz and Condie (*op. cit.*) the Pongola mudstone reflects derivation from the most fractionated and evolved sources.

The Chemical Index of Alteration (CIA of Nesbitt and Young, 1982) for Pongola mudstones generally falls near 78 (Wronkiewicz and Condie, 1989). These CIA values are transitional between those of the Moodies (CIA = 59, McLennan and Taylor, 1983) and Witwatersrand mudstones (CIA = 83, Wronkiewicz and Condie, *op. cit.*). The CIA data appears to record moderate to intense chemical weathering during the deposition of the Pongola Sequence. The CIA value of 68 calculated for the Mozaan diamictite is somewhat lower than that calculated for the mudstone indicating a lower degree of chemical weathering. This could be interpreted to be consistent with a glacial origin for the diamictite.

The geochemistry of the diamictite is remarkably consistent for the three samples (which were collected from sites some 8 km apart along strike). This points to homogenisation

of the parent rocks transported by the ice-sheets, as well as to a stable depository allowing the discharge from the ice-melt to accumulate under quiet conditions.

INTRUSIVE ROCKS

The only intrusive rocks in the study area are post Pongola dolerites and minor ultramafic bodies, most of which were sills intruded sub-parallel to the regional bedding. Several dyke-like intrusions cut across bedding but it was not possible to determine whether they are contemporaneous with the sills. Only one east-west striking dyke intrudes into Karoo Supergroup rocks between the Duduka and Bumbeni streams. Some of the intrusions are pre- to syn-tectonic, such as in the Klipwal, Altona, Sinqeni and Bumbeni shear zones. The phyllonitic dykes host the gold mineralization in the Klipwal shear zone.

The dolerites are generally recrystallized. Quartz, carbonate, chlorite and amphiboles (actinolite and tremolite) are common (see Appendix 1 for mineralogy). The undeformed dolerites are generally highly altered and display evidence of greenschist metamorphism.

Ultramafic intrusions made up primarily of cumulus olivine and to a lesser extent orthopyroxene and post-cumulus clinopyroxene are uncommon, but are found to the south and west of the Klipwal Gold Mine as isolated bodies (samples DB 5, DB 9, DB 13 and DB 14: Appendices 1 and 2).

Geochemistry

The geochemical characteristics of 30 dolerite and ultramafic samples were ascertained in an attempt to gain an insight as to their origin and to differentiate between Archaean and Karoo dolerites.

Interpretation of the analytical results is however tentative due to uncertainty concerning the age of the dolerite samples. All samples were analyzed for 10 major and 15 trace elements (presented in Appendix 2 with localities given in Appendix 3) by X-Ray fluorescence spectrometry. Details of the sample preparation are given in Appendix 4. Total-Fe is given as the ratio of ferric to ferrous iron changes with oxidation state and alteration, and is likely to be different in each sample.

Most dolerites have MgO contents ranging from 5 to 9 wt%, and SiO₂ content between 47 and 56 wt%. Sample DB 5 is unusual in this respect as its SiO₂ content (56.12 wt%) contrasts with its high MgO (17.22 wt%). Average values of major elements for these dolerites is comparable to the average compositions of dolerites reported by Maitre (1976).

The dolerites and ultramafics occupy distinct fields on a Jensen diagram (Figure 2.31). The dolerites lie in the tholeiitic field whereas the ultramafic intrusions are confined to the peridotitic komatiite field as defined by Jensen (1976). Similar geochemical subdivisions are observed for dykes in the southernmost outcrop of the Nsuze Group (Groenewald, 1984).

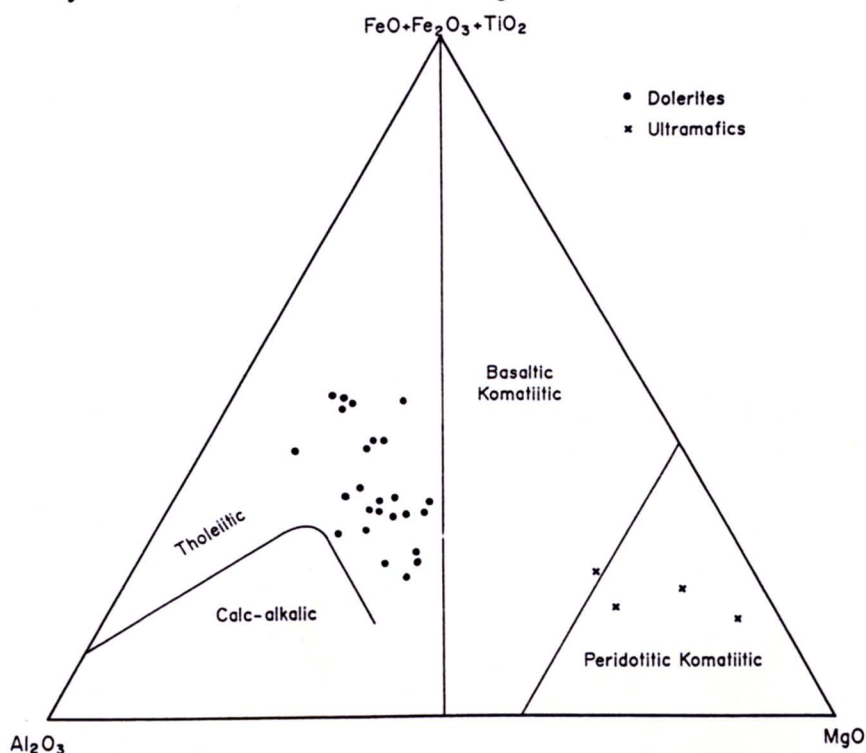


Figure 2.31: Jensen cation diagram for the intrusions into the Mozaan Group within the study area.

Inter-element correlations are generally highly significant in the study of mafic rocks (Armstrong *et al.*, 1984). The Mg-number ($\text{Mg}/(\text{Mg} + \text{Fe})$) is used as a reference parameter for the discussion of general geochemical features. The Mg-number of the analysed sample ranges widely from 40 to 86 (Figure 2.32) reflecting a range from ultramafic to tholeiitic. Most of the variation diagrams do not display well-defined trends. Datum points are more or less widely scattered, but tend to cluster in a single field, indicating an overall similarity in the geochemistry of the dolerites. However, Na_2O , Ti_2O and P_2O_5 become relatively depleted with increasing Mg-number. A marked increase in TiO_2 at Mg-numbers less than 55 is observed and could be related to the presence of Ti-bearing mineral phases (eg Ti-magnetite and ilmenite). Al_2O_3 has a linear trend at Mg-number < 70 but thereafter there is a relative decrease in Al. A possible explanation is that early fractionation of olivine resulted in the enrichment in aluminium in the residual liquid.

Samples DB 13 and DB 14 from two ultramafic intrusions to the south of the Klipwal mine are distinguished by their high MgO (29.73 and 36.52 wt% respectively) and low SiO_2 contents (46.85 and 44.28 respectively), reflecting the presence of olivine. The two bodies have similar element ratios to those of the other dolerites, however their absolute ratios are much lower (Figure 2.33). These samples may possibly reflect cumulates in a differentiated layered intrusion.

Samples from sheared dolerites show a greater variability with respect to the analytical data, which is probably related to "secondary" (silicification and sericitization) processes. The dolerites sampled from the Klipwal Mine do not show any marked variation with respect to their chemistry in comparison with undeformed dolerites, except for their relative depletion in Na_2O , MgO and MnO and enrichment in K_2O (Figures 2.31 and 2.32). Alteration of the dolerites does not seem to have been characterized by a significant mobilization of major elements.

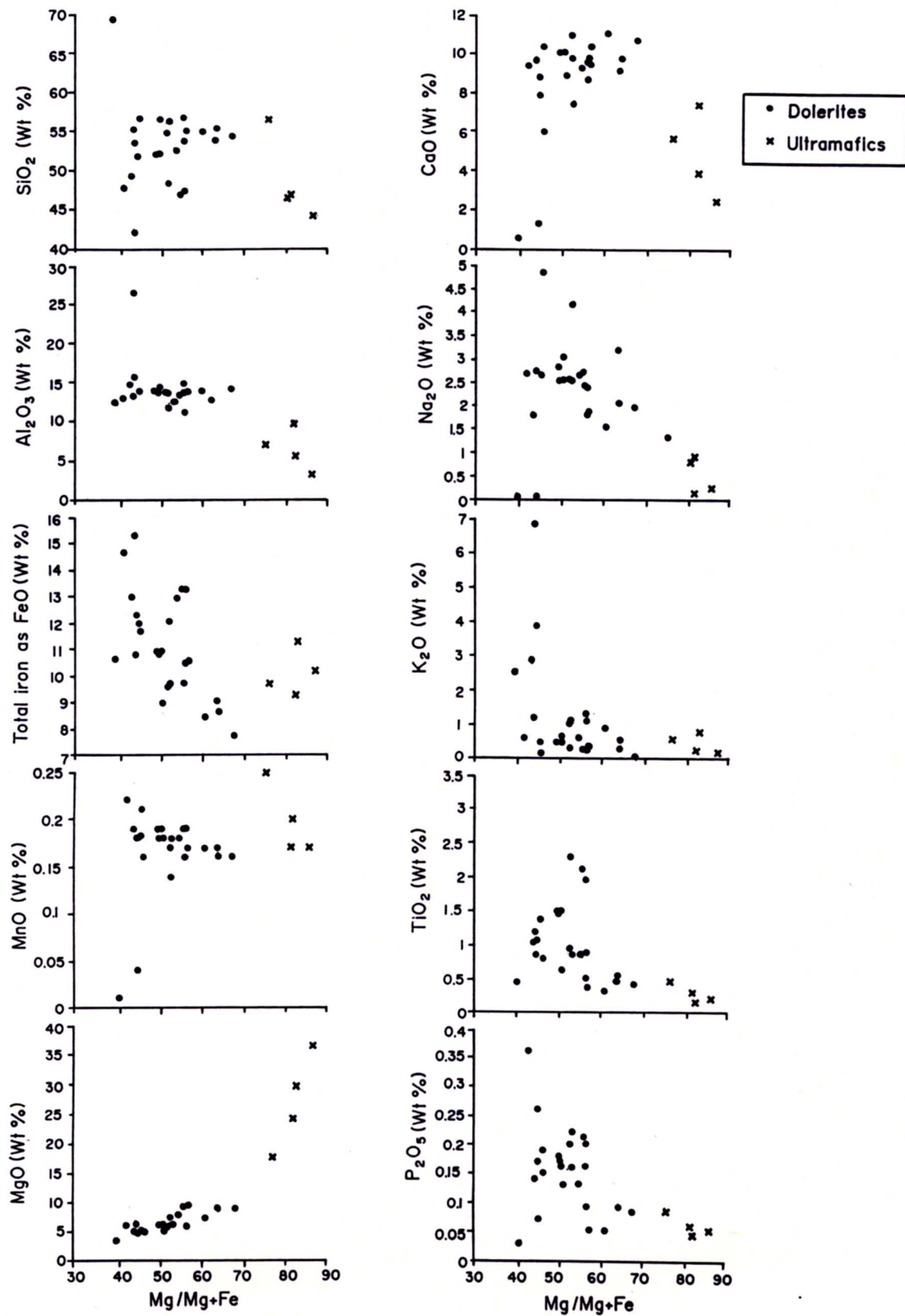


Figure 2.32: Mg-number variation with major elements for the intrusions.

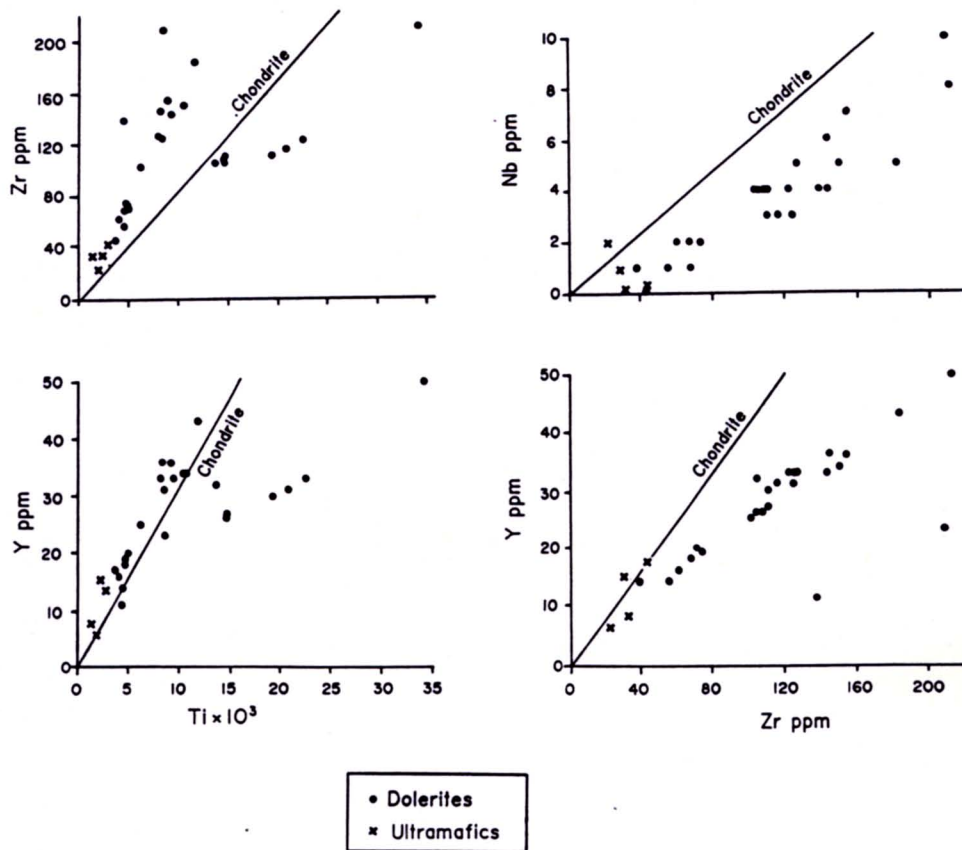


Figure 2.33: Incompatible element plots for the intrusions.

Plots of Zr and Y against Ti appear to define two distinct populations. One group has (Zr/Ti and Y/Ti) ratios greater than primordial mantle and the other lower ratios (Figure 2.33). The intrusive rocks having lower ratios than primordial mantle must either been derived from a Zr enriched source or alternatively the enrichment is the result of crustal contamination. Niobium and Y are both depleted relative to Zr having Nb/Zr and Y/Zr ratios less than in primordial mantle. This implies that the magmas were derived from a Zr-enriched source or that significant contamination occurred as the magma rose to higher crustal levels.

Spidergrams of four representative samples have similar patterns (Figure 2.34), but the sheared dolerites from the Klipwal Mine display enrichment in both K and Rb. This

presumably results from migration of mineralizing fluids accompanying gold mineralization.

It is clear from the evidence provided above that these intrusions have a diverse and complex geochemistry and the Karoo dolerites cannot be distinguished from older counterparts on the basis of geochemistry.

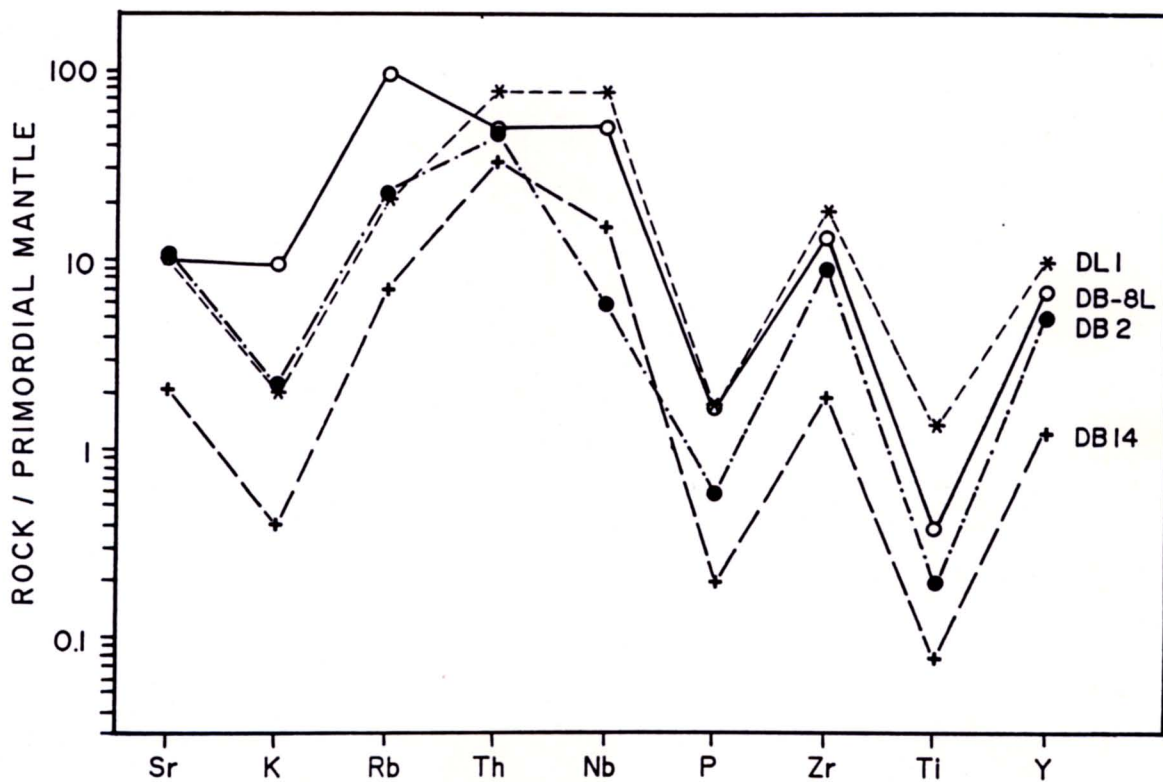


Figure 2.34: Normalized rock/primordial mantle spidergram plot for representative samples of the intrusions. DL 1 and DB 2 are typical dolerites, DB-8L was sampled from 8-Level in the Klipwal mine and DB 14 is an ultramafic sill.

CHAPTER 3: STRUCTURE

REGIONAL OVERVIEW

An overview of the major structures in the northern parts of the Pongola basin is provided in order to place the structures in the study area into the regional context. The dominance of northwest and northerly trends in the southeast Kaapvaal Craton is clearly observed on Landsat satellite imagery (Figure 3.1). This is also apparent from the structures observed in the northern parts of the Pongola basin.

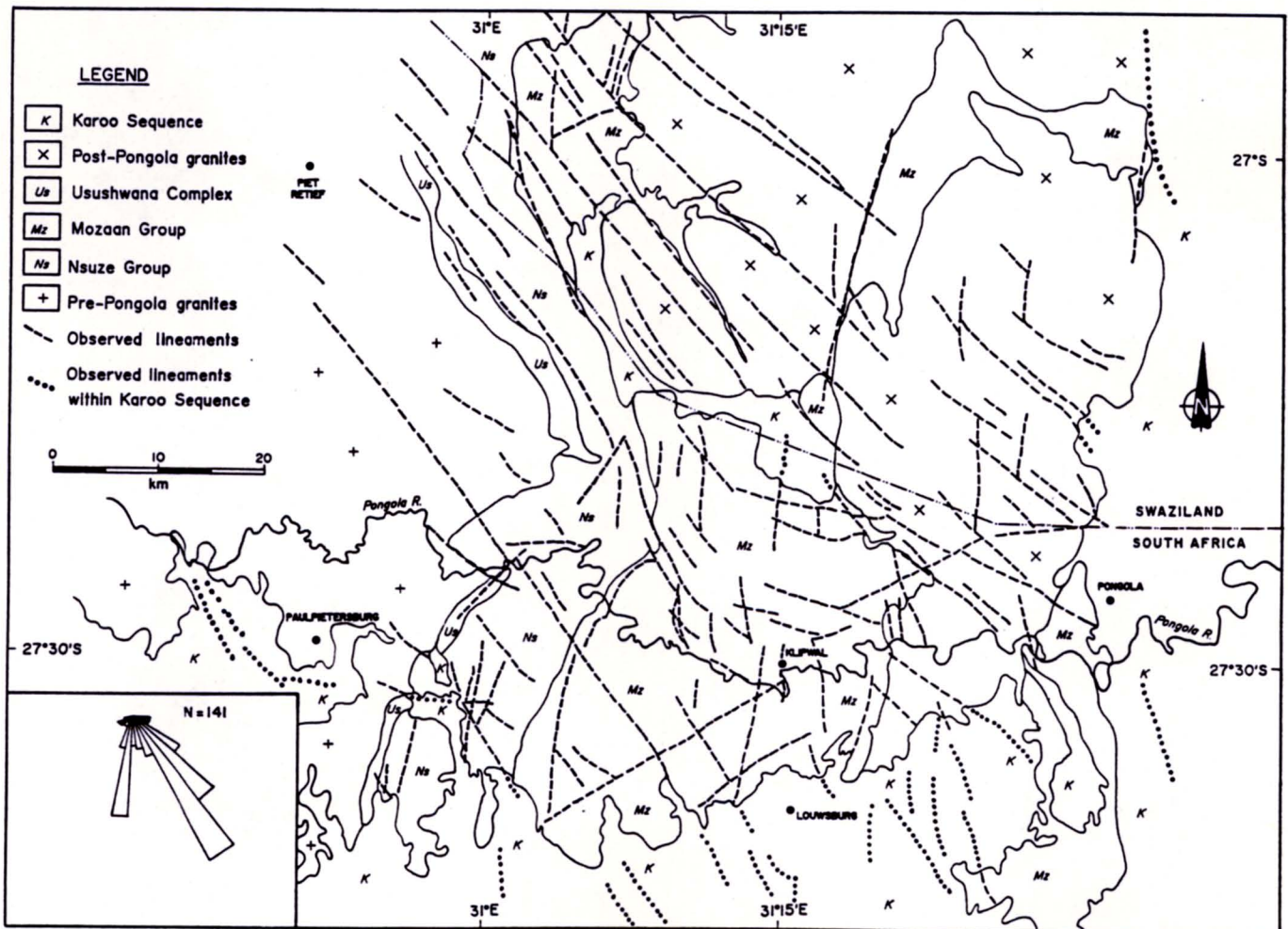


Figure 3.1: Lineaments in southeast Kaapvaal Craton observed from Landsat images. The inset is a rose diagram showing the dominant structural trends.

Main Pongola Basin

In the main Pongola basin (Figure 3.2) Watchorn (1978) recognized two major northwest-trending peri-synclinal sub-basins, a southwestern "Piensrand basin" and a northeastern "Hartland basin". The latter name is inappropriate as the geographical locality of Hartland is situated several tens of kilometres south of this sub-basin and has led to some confusion (e.g. Weilers (1990) who called the southwestern sub-basin the "Hartland basin"). The two sub-basins are referred to here as the Piensrand and Tobolsk synclines (Figure 3.2).

Both Watchorn (1978) and Matthews (1990) postulated that these peri-synclines were the result of interference folding of northwest-trending F_1 and east-northeast-trending F_2 folds. The intensity of the latter phase of folding is considered to decrease away from the intrusive contact of the extensive Spekboom granite (Matthews, 1985).

The Piensrand and Tobolsk synclines are separated by a shear zone, the northwest striking Delft shear zone which truncates the northerly trending Altona and Sinqeni shear zones to the south. The Delft shear zone appears to be the southeasterly extension of the Mahamba shear zone mapped by Hatfield (1990) to the east of Piet Retief (Figure 3.2). The Mahamba shear zone is interpreted by Hatfield (*op. cit.*) as a transpressional structure. In the Swaziland area sinistral transpression seems to be partitioned into an easterly dipping thrust and an adjacent sinistral shear zone. Hatfield postulated that the two structures were generated during the same D_1 deformational event. The ~15 km long Mahamba shear zone is associated with a ~40 km sinistral displacement, accompanying large-scale drag and attenuation of the Pongola strata, particularly the Nsuze Group (Hunter and Wilson, 1988). The regional shallow southeast to east-southeast dips change abruptly to steep (~60°) northeast dips northwards.

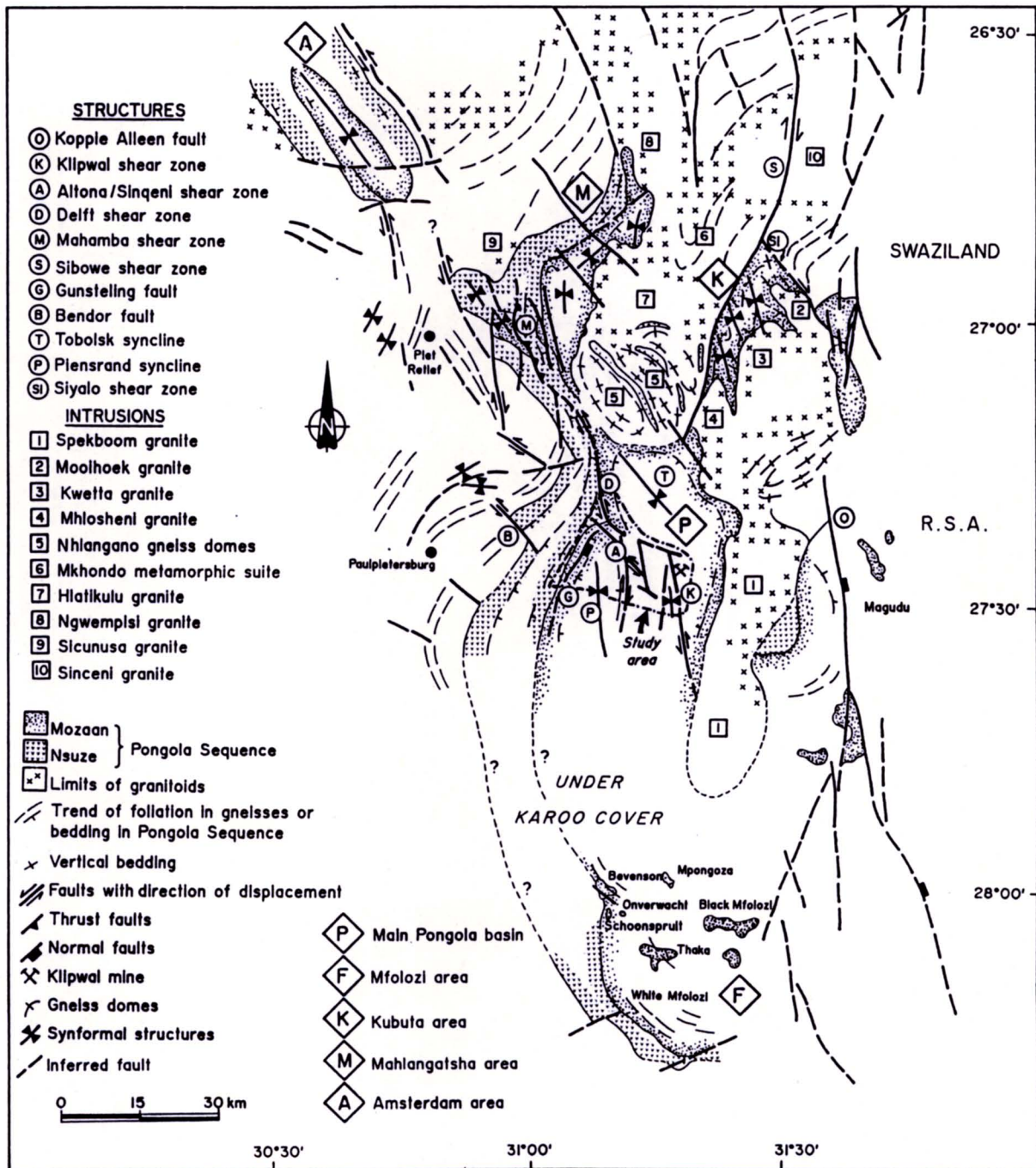


Figure 3.2: Simplified map showing the geology of the southeastern Kaapvaal Craton. International boundaries omitted for clarity. Map compiled from Hunter, 1968; Geol. Surv. Swaziland, 1968, 1980, 1982; Hammerbeck, 1977; Armstrong, 1980; Smith, 1987; Sleigh, 1988; Wolmarans, 1988; Hunter and Wilson, 1988; Hatfield, 1990; Verbeek, 1991 and this study.

It seems probable that pull-apart grabens formed during late stage transtension into which the Usushwana mafic suite intruded (Hunter and Wilson, 1988). The Usushwana suite has been dated at 2813 ± 30 Ma (Rb-Sr whole rock; Davies *et al.*, 1970) and 2871 ± 30 Ma (Sm-Nd; Hegner *et al.*, 1984). The intrusion is late syn-tectonic as it is itself deformed by northwest and north-trending shear zones.

Northerly trending structures have been described from both the Mahamba shear zone (Geol. Surv., Swaziland, 1968, 1980; Hatfield, 1990), and the pre-Pongola basement (Hunter, 1970a; Hepworth, 1973; Smith, 1987; Talbot *et al.*, 1987; Sleigh, 1988; Verbeek, 1991).

A major northward trending fault, the Koppie Alleen fault (Linström, 1987), marks the eastern margin of the main Pongola basin (Figure 3.2). Late movement on this fault has led to the downthrow of the Mozaan and Karoo rocks by ~ 130 m (Linström, 1987) so that the upper basaltic units of the Mozaan Group are preserved in a series of inliers (Wolmarans, 1988).

The Spekboom granite intrudes the Pongola basin post-tectonically, but has unfortunately not yet been dated (Linström, 1987). The intrusion is elongate in plan view with its long axis trending north-northeast. Updoming of the Pongola Sequence associated with the intrusion has resulted in the exposure of the Nsuzi volcanics and andalusite-bearing siltstone on the eastern and western flanks of the batholith (Figure 3.3). Only a thin slither of the Nsuzi Group is preserved in the west.

Mfolozi Area

Only a limited number of structural studies of the inliers between Beverson and the White Mfolozi (Figure 3.2) have been undertaken. Matthews (1990) reported that they have been

rotated into a series of tilted fault blocks. Unmapped northerly and northwesterly oriented shear zones are present in the Bevenson, Thaka, Schoonspruit, Onverwacht inliers and those along the Black Mfolozi River. The Mpongoza inlier is elongated in a northwest direction (Preston, 1987), possibly reflecting a structural control.

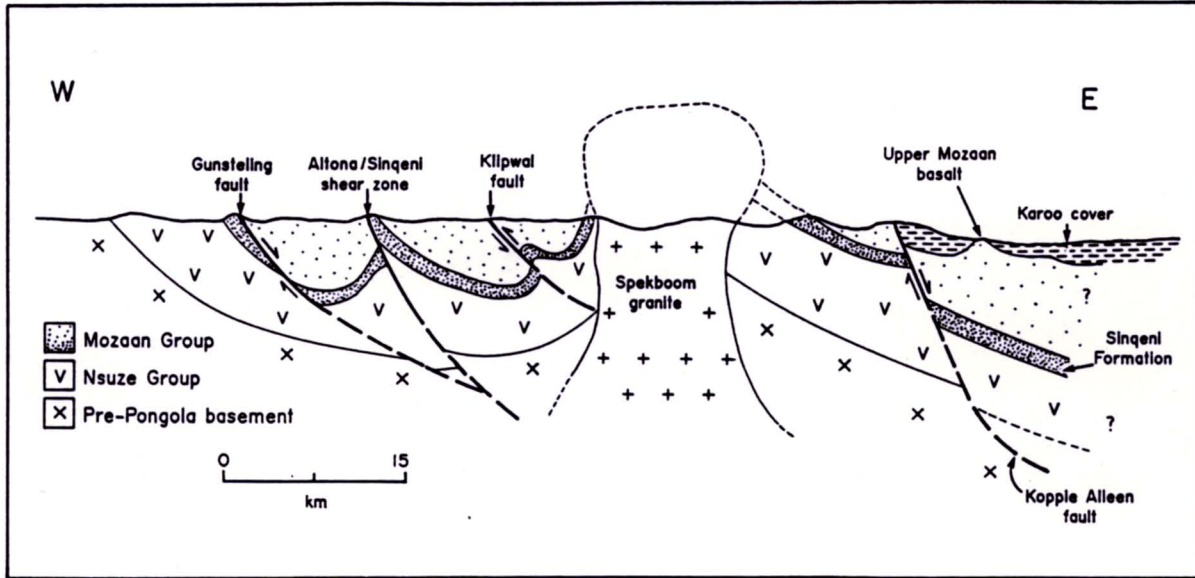


Figure 3.3: Schematic east-west cross-section through the main Pongola basin between Paulpietersburg and Magudu.

Kubuta Area

Although structures trending northwest are most commonly developed in Swaziland (Figures 3.1 and 3.2), the most intense deformation is displayed by northerly striking shear zones. Most of these shear zones display dextral senses of movement and have a very steep dip towards the east. The best developed example is the north-northeast striking Sibowe shear zone, which truncates the Mozaan strata in the Kubuta area (Hunter, 1953, 1991; Hepworth, 1973; Geol. Surv., Swaziland, 1968, 1980; Figure 3.4), the pre-Pongola gneiss basement, and the Sinceni pluton (which has yielded a Rb-Sr whole-rock isochron age of 2992 ± 44 Ma; Trumball, 1990). It is a broad mylonitized zone with

lineations and fold axes typically plunging towards the southeast (Hepworth, 1973). Large amplitude folds with axes also plunging towards the southeast deform the Mozaan Group to the east. According to Hepworth (*op. cit.*), early lineations plunging towards the northeast were re-oriented by progressive deformation into a southeasterly alignment.

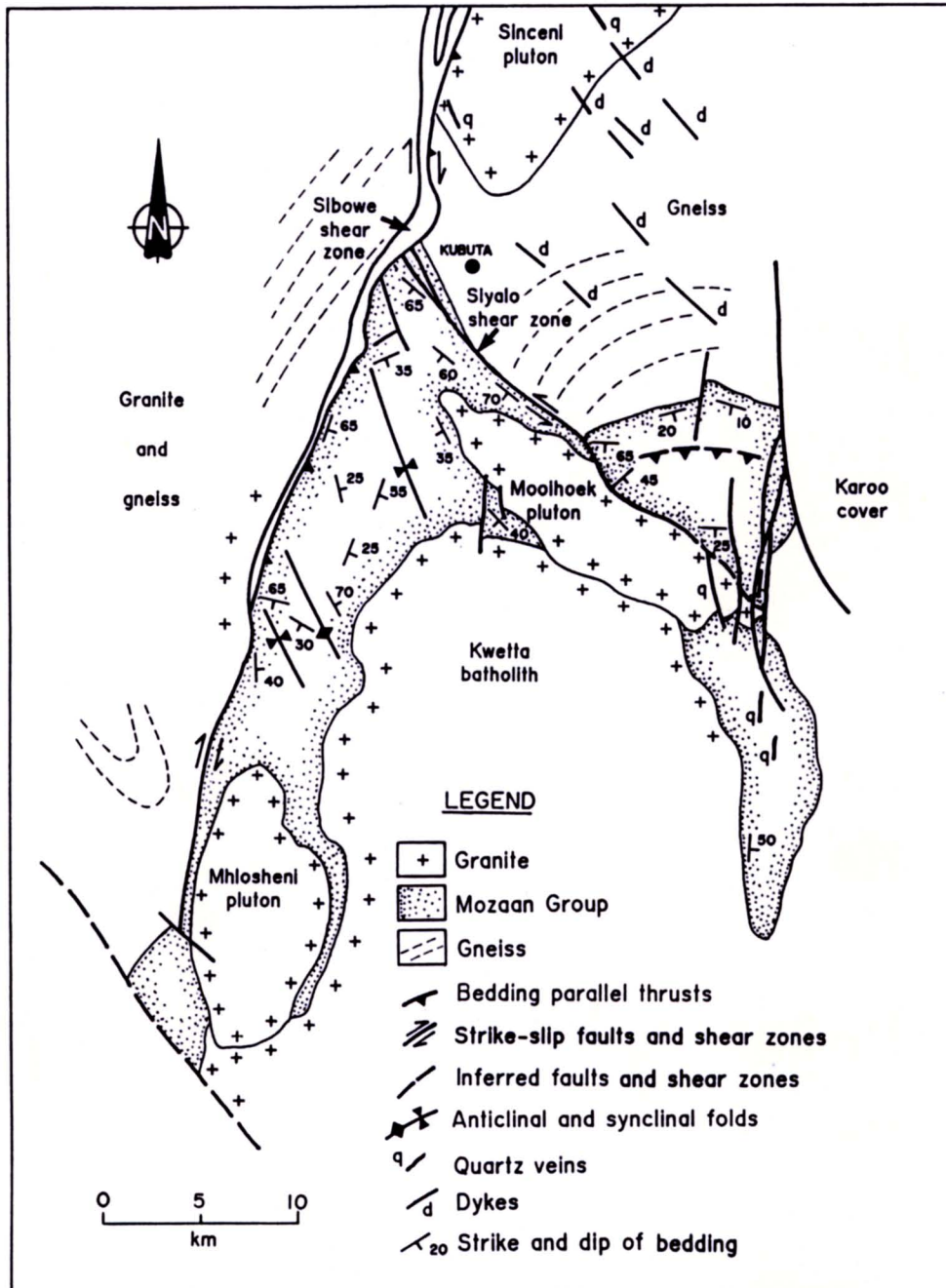


Figure 3.4: Geological map of the Kubuta area. Modified after Hunter, 1968; Geol. Surv., Swaziland, 1968, 1980, 1982.

The Mozaan Group sandstone to the east of the Sibowe shear zone is preserved within a broad synclinorium, the northeastern limb of which is truncated by the northwest-trending Siyalo shear zone. The Siyalo shear zone contains sinistral movement indicators and sub-horizontal lineations. The synclinorium has a sub-vertical northeastern limb, which Hunter (1961) attributed to the forceful emplacement of a granite plug on the northeastern flank.

The intrusion of both the Mooihoek and the Mhlosheni granites appear to have been structurally controlled, as the former pluton is aligned northwest and the latter has a northerly orientation (Figure 3.4) reflecting the two dominant structural trends.

A number of other megacrystic granite plutons (e.g. Kwetta batholith) intrude the Pongola strata in southern Swaziland.

Mahlangatsha Area

Several phases of deformation have been recognized in the northern Mahlangatsha plateau (Roering, 1968). A large northeast-trending synclinal structure resulted from two coaxial phases of folding. Later northeast-trending cross-folding produced a number of subsidiary basins (Roering, *op. cit.*). A final phase of deformation involved westward overthrusting. The post-tectonic Ngwempisi pluton provides a minimum age for the deformation, although no precise radiometric dates have been obtained.

An intense northwest dipping foliation is largely confined to a belt approximately 2 km wide overlapping the contact of the Nsuzi and Mozaan Groups in the northwestern flank of the regional synclinorium (Roering, 1968; Hunter, 1991). The contact between the Nsuzi and Mozaan Groups appears to be tectonic because Mozaan beds are truncated at the contact.

The regional strike of the Pongola Sequence swings southeast in the southernmost part of the Mahlangatsha area, where it is truncated by the Mahamba shear zone.

Whereas a substantial thickness of Nsuzi strata is preserved to the west of the Mahlangatsha plateau, it is not found on the eastern side of the regional syncline, where the Mozaan Group sandstone is intruded by the Hlatikulu granite batholith (Figure 3.2).

Amsterdam Area

The Pongola Sequence is preserved in a northwest-trending syncline in the Amsterdam district (Figure 3.2), the northeastern limb of which is sub-vertical. The pre-Pongola granitoid basement on this flank is extensively sheared. The southwestern dips gently northeast and shows no evidence of deformation.

THE STUDY AREA

Three episodes of folding, shearing and faulting can be recognized within the study area based on structural relationships. The first event resulted from compression from the south-southeast and is evidenced by transpressional shear zones (Izermijn and Klipwal) and a northeast-trending fold (Ngwenya syncline). An episode of normal faulting with extension to the south-southeast preceded or followed this event (Gunsteling fault). Finally a major deformation event produced early north-northwest folding and late conjugate north and northwest striking shearing (Gold, 1991).

The shear zones tend to be zones of ductile-brittle deformation so that the distinction between "shear zones" and "faults" is often blurred.

The original names given to the tectonic discontinuities that had been mapped by previous workers have been retained as far as possible, although some of them have been redefined, or new names have had to be introduced for various reasons (Table 3.1):

1. The Altona and Sinqeni shear zones were previously described as a single structure (the Keerom fault, Humphrey and Krige, 1931) or as part of the Mahamba fault belt (Matthews; 1987, 1990).
2. The Qumeni shear zone was originally called the Bethu fault by Carter (1964), but it was felt that the name Bethu should be reserved for the anticline situated in the Bethu hill.
3. The Bethu and Nombela anticlines were called the Altona anticline by Watchorn (1978), but they are separate folds. The original name of Humphrey and Krige (*op. cit.*) is retained here. The name Altona is reserved for the Altona shear zone (Carter *op. cit.*).
4. The Delft shear zone (Humphrey and Krige, *op. cit.*) was called the Oranjedal fault by Carter (*op. cit.*) and also forms part of Matthews' (1987; 1990) Mahamba fault belt. The original name has again been retained here.
5. The Duduka fault named after the nearby stream was originally called the Klipwal fault by Carter (*op. cit.*). The name Klipwal shear zone is however now associated with the shear zone containing the gold ore body at the Klipwal Mine, thus the term Duduka fault is preferred to Carter's original description.

Table 3.1: Names and brief descriptions of the various major shear zones, faults and folds, including the source of the names used. See Maps 1B, 1C, 2 and 3 for localities.

Name used in this thesis	Description	Source of name(s) and previous names
Klipwal shear zone	N-S striking sinistral transpression	unknown
Izermijn shear zone	NNE striking sinistral transpression	This study
Gunsteling fault	NNE striking dextral transtension	(Humphrey and Krige, 1931)
Altona shear zone	N-S striking dextral strike-slip	(Carter, 1964)
Sinqeni shear zone	N-S striking dextral strike-slip	This study
Mhlope shear zone	NNE striking dextral N-S strike-slip	This study
Mkhuzwa shear zone	N-S trending dextral strike-slip	This study
Qumeni shear zone	NW-SE and N-S striking dextral strike-slip	This study (previously Bethu shear zone; Carter, 1964)
Enyabisa shear zone	N-S striking dextral strike-slip	This study
Dwaleni fault	N-S striking dextral strike-slip	This study
Nkolotsheni shear zone	N-S striking dextral strike-slip	This study
Bumbeni shear zone	N-S striking dextral strike-slip	This study
Khuphulangwenya fault	N-S striking dextral strike-slip	This study
Delft shear zone	NW-SE striking sinistral strike-slip	(Humphrey and Krige, 1931), Oranjedal shear zone (Carter, 1964) and Mahamba fault belt (Matthews, 1987; 1990).
Vergenoegheid shear zone	NW-SE striking sinistral strike-slip	(Carter, 1964)
Duduka fault	NW-SE striking sinistral strike-slip	Klipwal fault (Carter, 1964)
Nkosetsha shear zone	NW-SE striking sinistral strike-slip	This study
Mzamba shear zone	NW-SE striking sinistral strike-slip	This study
Meander shear zone	NE-SW striking transpression	This study
Bethu anticline	NW-SE trending axial trace	Altona anticline (Watchorn, 1978)
Mfeno syncline and anticline	NW-SE trending axial trace	This study
Nombela anticline	NNW-SSE trending axial trace	Altona anticline (Watchorn, 1978)
Prudentie syncline	NW-SE trending axial trace	Watchorn (1978, 1979b)

North-northeasterly trending sinistral compressional shear zones and folds

Izermijn Shear Zone

This previously unrecognized northeast-trending shear zone is located at the western edge of the study area (Map 1B) and is best exposed on the Izermijn farm after which it is named.

Shearing occurs over a broad zone at least 400 m wide and involves both upper Nsuze and lower Mozaan Group stratigraphy. This shearing predates the northwest-trending shear zones to the northeast. A moderately well-developed southeast-dipping cleavage axial planar to tight folds occurs within amygdaloidal Nsuze lavas some 400 m below the basal Mozaan contact. The degree of deformation increases as the basal quartz arenite of the Mozaan Group is approached. A north-northwest vergence direction is indicated by slickenside striations and the long axes of elongated clasts and amygdales in the matrix-supported conglomerate and lavas (Map 1B). If this compression occurred before the regional folding which affected the Pongola basin, then it is probable that the Izermijn shear zone was a sub-horizontal structure.

Higher in the stratigraphy, flat-lying shear zones are developed with the hanging wall being displaced towards the north-northwest relative to the footwall. Furthermore, small-scale ramps (Figure 3.5) and folds are indicative of compression from the south-southeast.

The competency contrast between the Nsuze volcanics and the 650 m thick basal Mozaan sandstone resulted in the ductile deformation of the former, but little internal deformation of the latter, except for bedding-parallel slip along the basal contact. Recrystallization of the basal sandstone occurred during this deformation, further increasing its competency.



Figure 3.5: Footwall ramp in Mozaan Group sandstone at Prudentie. View towards the southwest.

Ngwenya Syncline

This south-southwest-trending syncline occurs in the footwall of the Klipwal shear zone (Maps 1C and 2). It developed prior to the shearing as the Klipwal shear zone cuts across its eastern limb. The fold is interpreted as initially forming at a high angle to the compression from the south-southeast, and then rotating into parallelism with the Klipwal shear zone because of the transpressional deformation along the shear zone. A number of east-west-trending open upright folds with half-wavelengths of ~ 150 m in the eastern limb of the Tobolsk syncline may have formed at this time (Map 2). Alternatively the buttressing effect of a large (kilometre scale) north-south trending pre-tectonic dolerite may have localized the deformation and influenced the fold axis orientation producing a major north-south overfold (Figure 3.6). As deformation continued, the upper limb of the developing fold became sheared out and a zone of north-south convergent wrenching was

initiated. The bedding in the hanging wall became overturned and tightly folded while the eastern limb of the Ngwenya syncline in the footwall steepened.

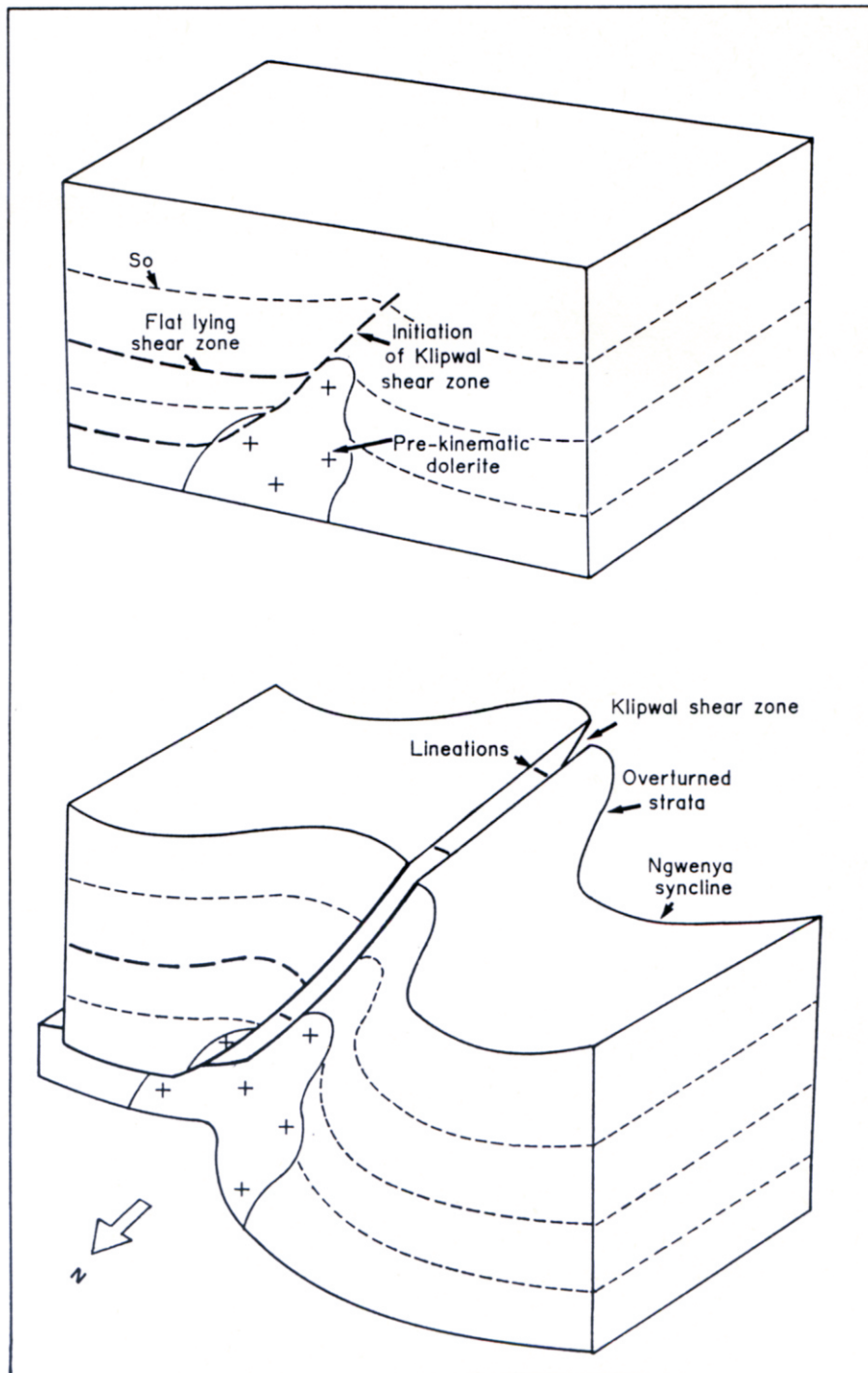


Figure 3.6: Schematic model showing the development of the Klipwal shear zone and the associated Ngwenya syncline.

Klipwal Shear Zone

Early ductile-brittle shearing

The Klipwal shear zone can be traced within the study area from the Nkwazane stream in the north where it is cut by the Nkosetsha shear zone to the Pongola River in the south (Map 2). It can be followed further south within the Itala Game Reserve for another 6 km before it disappears beneath the Karoo Sequence (Wolmarans, 1988). The strike changes from northeast north of the Klipwal Mine to south-southeast in the south and the dip is to the east or southeast. It cuts through the eastern limb of a pre-existing fold, the Ngwenya syncline. As the shear zone is approached from the west, the bedding steepens from a relatively shallow dip becoming overturned and parallel to the shear zone adjacent to it. The displacement along the shear zone, including later deformational events is ~ 3.3 km.

This shear zone has a poor surface expression (its relief is not apparent in Landsat images generally). Lithologies that are sheared include sandstone, mudstone and diamictite as well as pre- and, possibly, syn-tectonic dolerite intrusions.

The zone of deformation is about 100 m in width, with most of the movement being restricted to a zone which is between 0.5 and 2 m wide. This narrow zone can be mylonitic where the shear zone has deformed competent lithologies, but is predominantly represented by a fault gouge where mudstone or dolerite are deformed. The foliation within the shear zone in the Klipwal area dips 45° to the east and quartz fibre lineations plunge obliquely towards the southeast (average 140/38; Figure 3.7). The partial girdle on the stereoplot (Map 1B) is due to the presentation of late extensional lineations related to transtensional movements.

A sinistral reverse sense of movement is inferred in the southern part from shear sense indicators and reverse drag of bedding in the footwall (Figure 3.8). The pattern of the secondary shear zones also support a sinistral reverse movement. The rejoining splays commonly define hindward dipping duplexes.

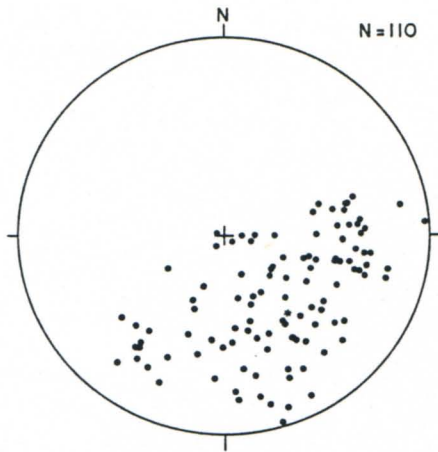


Figure 3.7: Lineations associated with transpression measured within the Klipwal shear zone.



Figure 3.8: Drag folding in the footwall of the Klipwal shear zone. View looking north.

The Klipwal shear zone assumes a reverse sense of movement where it strikes northeast. The transpression in the south thus defines an oblique ramp to a northeast-trending ramp.

Locally, late small-scale, non-cylindrical chevron folds and kink bands deform the shear-related foliation. Their axes are at high angles to the stretching lineation (Figure 3.9).



Figure 3.9: Fold axes in the Klipwal shear zone.

Bedding in the hanging wall dips shallowly northwards or northwestwards while the footwall bedding has been overturned and has an orientation sub-parallel to that of the Klipwal shear zone (Figure 3.10 and Map 1C). In the Itala Game Reserve to the south of the Pongola River the shearing has overturned the hanging wall strata.

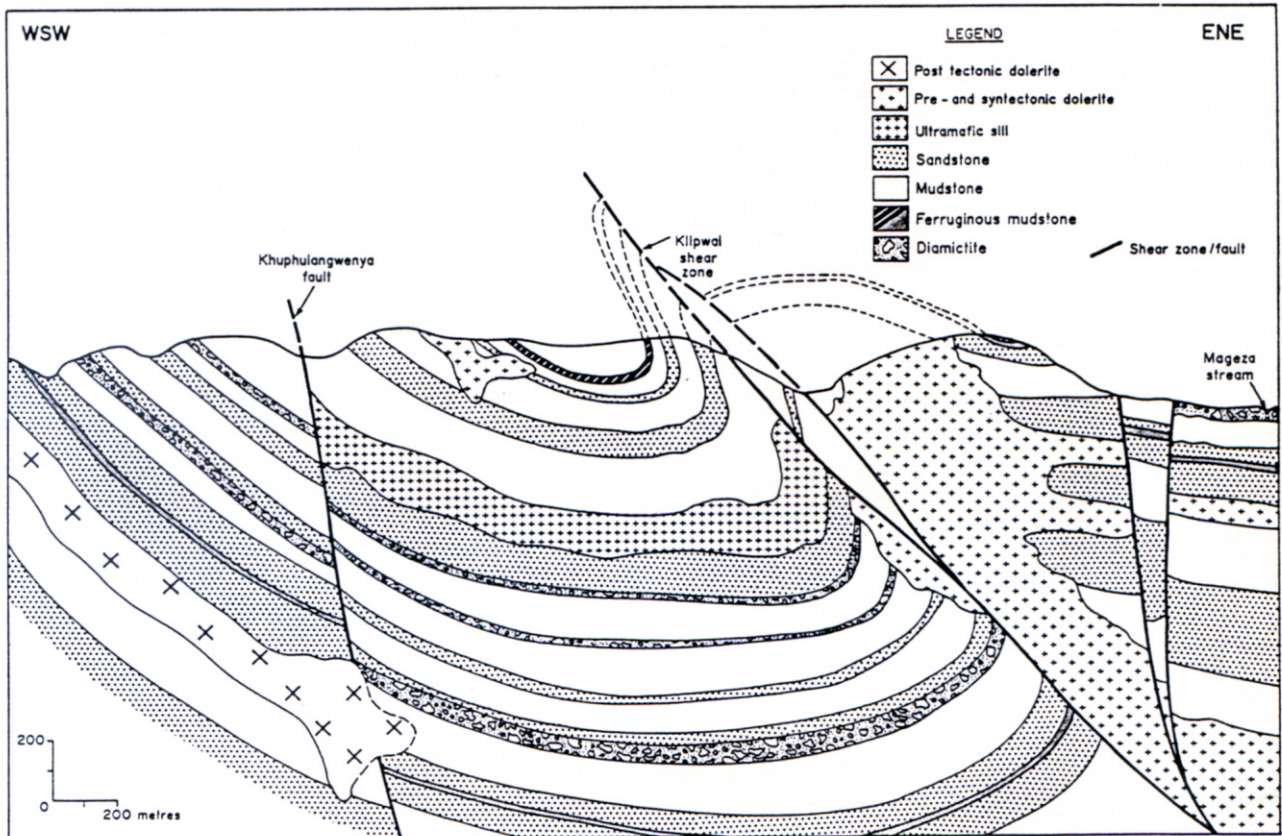


Figure 3.10: Cross-section through the Klipwal and adjacent shear zones. The topography in the area where the section was constructed is rugged and provides excellent three-dimensional control. See Map 2 for locality.

A significant amount of deformation occurred in both the footwall and hanging wall strata away from the shear zone in the form of discrete low angle thrust faults (Figures 3.11 and 3.12A). A thrust fault with a footwall ramp can be seen on the banks of the Pongola River (Figure 3.13). A system of fault splays is exposed in the underground workings of the Klipwal mine between levels 8-11 (Figure 3.14). The deformation here has exploited the lithological contact between sandstone and dolerite. Slickenside striations and tension-gash geometry show that movement along these faults was to the northwestward (Figure 3.12B).



Figure 3.11: Bedding-parallel faulting in the hanging wall of the Klipwal shear zone. Fault cuts upsection northwards to the right of the photograph. Note the southward dipping cleavage to the left of the photograph. View looking southwest.

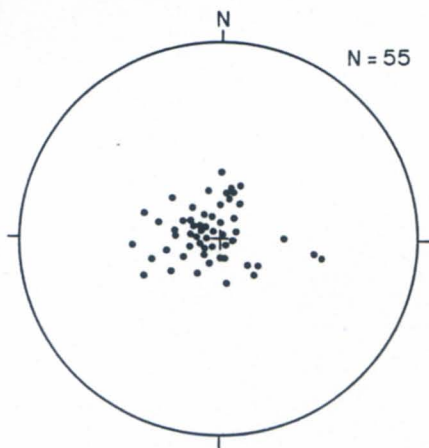


Figure 3.12A: Poles to fault planes in the hanging wall and footwall of the Klipwal shear zone.

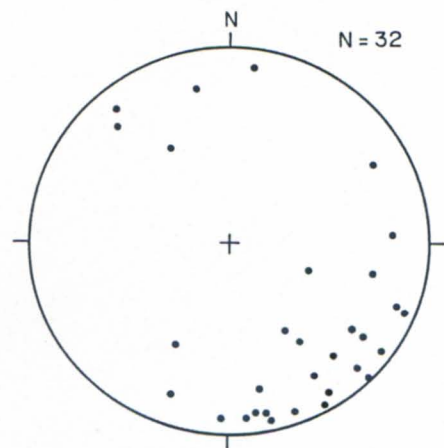


Figure 3.12B: Lineations in footwall and hanging-wall faults.



Figure 3.13: Footwall splay to the Klipwal shear zone along the Pongola River with cut-off of footwall stratigraphy. View looking north.

Late brittle deformation

The compressional phase which generated the Klipwal shear zone was followed by a transtensional phase, during which time its hanging wall moved down towards the northeast relative to the footwall. The relative timing of these events can be established from overprinting relationships. In contrast to the lineations which plunge to the southeast, the striations and quartz fibre lineations associated with this event plunge moderately to the northeast at 45° and partly obliterate the early lineations (Figures 3.15 and 3.16).

This phase is characterized by the development of steeply dipping normal sinistral faults (Figure 3.17), which dip towards the east and northeast, as well as fault drag in the hanging wall of the shear zone. The intensity of the faulting diminishes away from the shear zone, but is high in the dolerite.

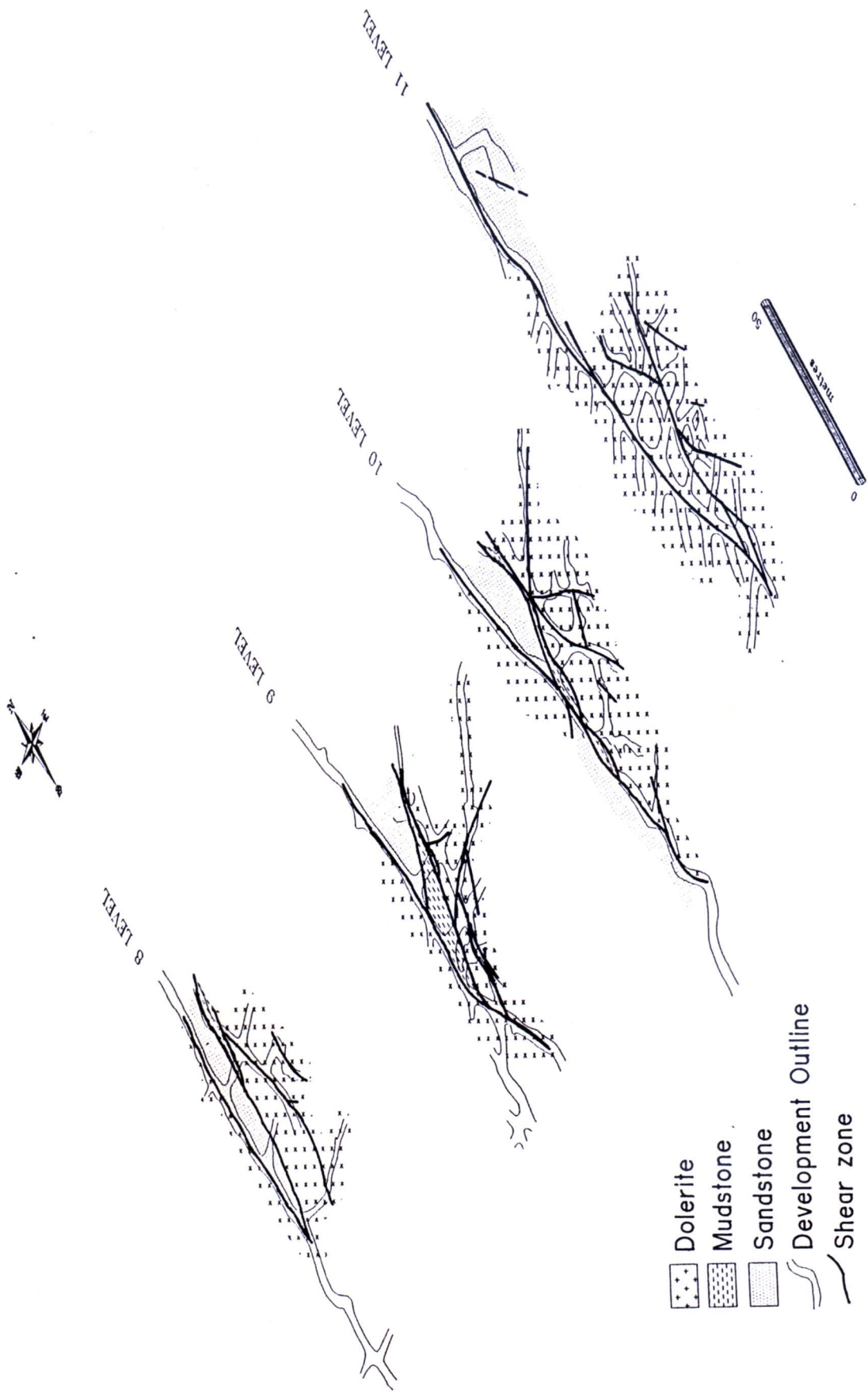


Figure 3.14: Three-dimensional plot of the hanging-wall ore body in the Klipwal Mine. View from the southeast, 30° above the horizontal.

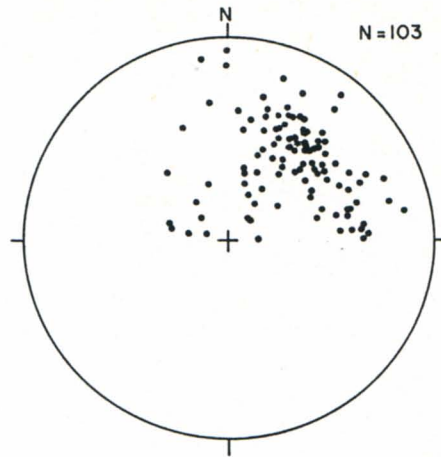


Figure 3.15: Stereoplot of lineations associated with transtension.

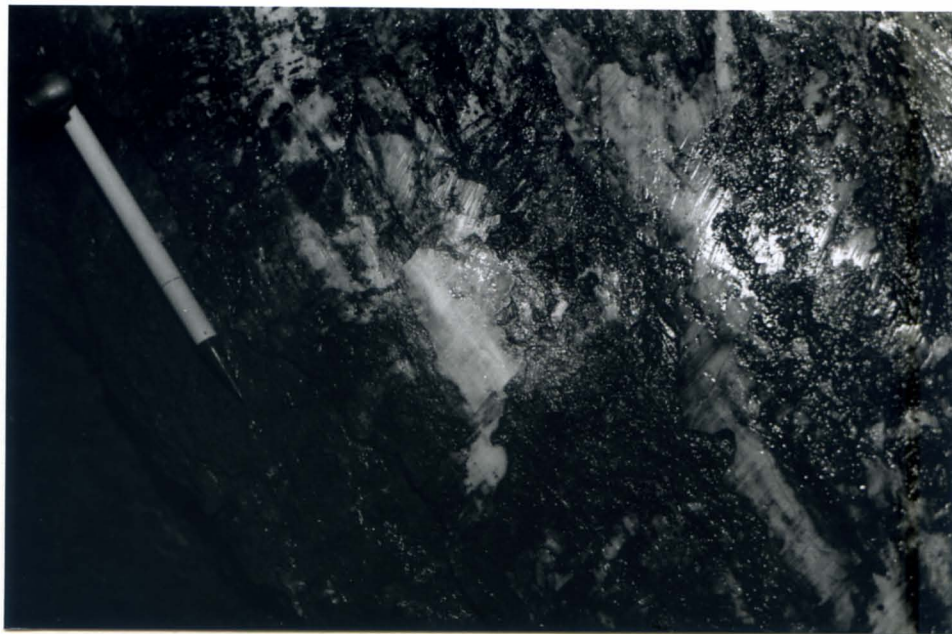


Figure 3.16: Two generations of striations in a fault plane in the Klipwal Mine. The pencil is parallel to the early southeast plunging striations. View is upwards towards the northeast.



Figure 3.17: Steeply dipping late fault. Photograph taken on 9-3 sub-level looking north.

Associated gold mineralization

The Klipwal Gold Mine is located within the Klipwal shear zone. The mine operated sporadically from 1898 until 1974 when Lonrho South Africa Ltd. acquired the property. Mining on a small scale has since then been undertaken continuously.

The largest concentration of gold is associated with the main shear zone² where it is associated with syntectonic quartz and carbonate veins. Gold and sulphide mineralization is also found within the altered (silicified and sericitized) wall-rocks.

² *No zones of mineralization are shown as this data is confidential.*

Minor ore bodies occur in secondary fractures and faults in the hanging wall, the orientations of which vary considerably. The pattern of veining is complicated by the sequential development and distortion of the veins during progressive deformation.

Ore mineralogy of the Klipwal deposit

A detailed mineralogical study of the gold mineralization by Russell (1985) on levels 4 to 6 (prior to the development of any of the lower levels) showed that 7 vol% of the gold occurs as free gold, 12 vol% is associated with the gangue and an unidentified sulphide, 52 vol% is associated with pyrite, 22 vol% is associated with arsenopyrite, and 7 vol% is associated with cracks in pyrite or arsenopyrite grains. She concluded that the ore was deposited from hydrothermal solutions introduced into the shear zone as suggested by (i) an association with quartz-veining, (ii) wall-rock alteration, and (iii) the decrease in the ore grade away from the shear zone and from the association of arsenopyrite-pyrite-pyrrhotite that the temperature of formation of the gold mineralization was in the order of 350°C to 400°C (i.e. mesothermal).

Both disseminated- and vein-type mineralization are found (Figure 3.18). Broad, generally barren, pyrite veins cross-cut the shear fabric of the host rock whereas narrower veins of pyrite are concordant with it. Due to the intimate textural relationship of gold mineralization and sulphides, it is clear that they were deposited contemporaneously.

Possible models for the gold mineralization

The source of the gold still remains unresolved. Neall (1987) and Romberg (1990) propose epigenetic models for the formation of Archaean hydrothermal gold in which gold can be leached from source rocks during metamorphic devolatilization reactions. The gold

is then transported in a low salinity, near to slightly alkaline fluid, as a reduced-sulphur complex of the form $\text{Au}(\text{HS})_2^-$. Interaction of this fluid with Fe-rich rocks (high total Fe and/or high $\text{Fe}/(\text{Fe}+\text{Mg})$), such as dolerite and banded iron-formation, in the temperature range 300°C to 400°C , is believed to cause sulphidation of the wallrocks and destabilization of the thiocomplexes due to the loss of sulphur from solution. This reaction results in precipitation of gold simultaneously with pyrite (and/or pyrrhotite), thus accounting for their common association of gold, particularly within pyrite-rich wallrock-altered zones in the Archaean gold deposits.



Figure 3.18: Vein- and disseminated-pyrite within a mudstone from level 4 in the Klipwal Gold Mine.

Sericite, quartz and pyrite (all present in the Klipwal gold deposit) are characteristic of sericitic alteration in hydrothermal deposits (Stanton, 1972; *cited in* Russell, 1985). The breakdown of orthoclase and chlorite to sericite is induced by reactions with H^+ , whereas the sulphur combines with iron from iron-bearing silicates to form pyrite. It would appear that the style of mineralization found in the hanging wall of the Klipwal deposit is the result of such a process with the dolerite providing the iron necessary to induce the precipitation of sulphides from a solution migrating along the tectonic contact between the dolerite and the sedimentary rocks.

The Klipwal gold deposit also fits Boyle's (1979) classification of "auriferous veins, lodes, fractures, shear and crushed zones, essentially occurring in sedimentary terranes". These deposits range in age from Precambrian to Tertiary. The most favourable rocks for this type of deposit are slate, phyllite, sandstone and greywacke predominantly of marine origin. Boyle (*op. cit.*) proposed that wall rock alteration can be minimal, but silicification, sericitization and pyritization are commonly found. The gold is commonly reported as being found in the native state, or as a disseminated form in pyrite and arsenopyrite.

Major regional structures, such as deep-seated faults or ductile shear zones are required to enable the circulation of large volumes of hydrothermal fluids. Efficient valve-action, causing significant hydrothermal precipitation involves massive fluid discharge with a large accompanying drop in fluid pressure. High-angle reverse or reverse-oblique faults represent optimal structures for valve action, capable of giving rise to the greatest fluid pressure fluctuations. Accumulation of fluid pressure is a necessary prelude to failure and causes arrays of subhorizontal hydraulic extension fractures to open up adjacent to rupture nucleation sites on reverse faults, the whole fracture array serving as an overpressure fluid reservoir for rapid postfailure discharge. Such locally induced permeability is a significant aspect of gold mineralization (Harris, 1987). However, such a fault-valve may later be resealed by hydrostatic precipitation (Sibson, 1990).

Whereas lithological controls played a role in the precipitation of gold at Klipwal, economic concentrations could be related to zones of higher permeability in the shear zone. Irregularities in the shear geometry would be ideal loci for repeated slip events and represent zones of enhanced transient permeability which would focus fluid migration. Furthermore, fluid migration would take place only along the active fault segments at the time of fluid production (Robert, 1991). Thus the timing of the active slip relative to fluid production could explain why some segments of the shear zone are mineralized and others not.

In similar Archaean gold deposits in the Lawlers district of Western Australia, Partington (1987) found that a factor common to most of the gold deposits, is their location in structures formed in a wrench tectonic environment at the brittle-ductile interface. Furthermore, in all cases the gold mineralization is located in small-scale structures which were active toward the end of deformation, when vertical movement was dominant. These later extensional movements caused the shear plane to "open" (such as the late transtensional event in the Klipwal shear zone), resulting in zones of intense pressure reduction. Any fluids in the system at this time would migrate towards this zone.

Russell's (1985) investigation of the Klipwal deposit showed that gold mineralization occurred during a number of phases in the shear zone as hydrothermal fluids were introduced at different times. This is confirmed by the presence of sheared and faulted mineralized quartz and carbonate veins on the deeper levels not examined by Russell (i.e. levels 8 to 11, and Figure 3.19).

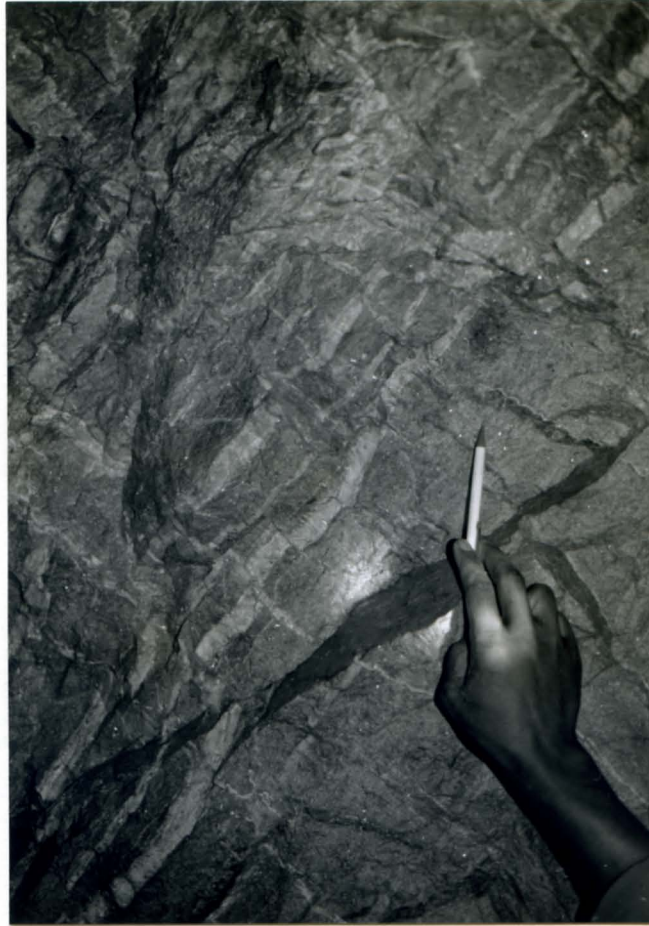


Figure 3.19: Carbonate veins cross-cut by later quartz and carbonate veins. The earlier set extend from the bottom left to top right of the photograph. 9-1 sub level, the earlier carbonate veins dip towards the left of the photograph.

Meander Shear Zone

The northeasterly striking Meander shear zone exposed immediately to the north of the Pongola River is sub-vertical with lineations plunging towards the south-southwest (Map 1B). The shear zone is very poorly exposed within the study area and can be traced for ~ 1 km. To the northwest of the shear zone, the eastern limb of the Ngwenya syncline is overturned (Map 2).

The relationship of this shear zone to the Klipwal shear zone is uncertain, but maybe a footwall splay.

South-southeast directed normal faulting and associated folding

Gunsteling Fault

The Gunsteling fault was originally identified by Humphrey and Krige (1931) as a steep normal fault with a displacement towards the southeast. It runs above the Sinqeni Formation sandstone parallel to the Izermijn shear zone. The age relationship between the Izermijn shear zone and this fault is thus uncertain. The fault has an arcuate northeast trace swinging eastwards towards the east, and possibly southeastwards joining up with the Qumeni shear zone (Map 1B). It is cut by the northwest-trending set of faults and shear zones in this area. The fault has a moderate southeast dip along most of its length.

On the Gunsteling farm (Figure 3.20 northeastern corner) the fault cuts down through the 650 m thick Sinqeni Formation and the stratigraphically highest beds of the hanging wall abut against Nsuze volcanics. As the observed hanging-wall stratigraphy of the Kulphiso Formation has a thickness of 800 m and the Sinqeni Formation is not represented, a minimum displacement of 1450 m is inferred.

The fault varies from a discrete discontinuity 40 cm in width to a wide fault zone of ~ 200 m just north of the Ntombe river where it incorporates a large fault-bounded sandstone sliver (Figure 3.20). Broad breccia zones, up to 40 m wide, made up of fragments of sandstone, conglomerate, dolerite and subordinate shale are present. Fault drag and s-c relationships indicate a normal sense of movement.

Synthetic listric and planar faults are present in the footwall Sinqeni sandstone immediately below the fault zone (Figure 3.21). These floor faults cut back towards the undeformed footwall and may develop as a result of unloading of the footwall (Gibbs, 1984).

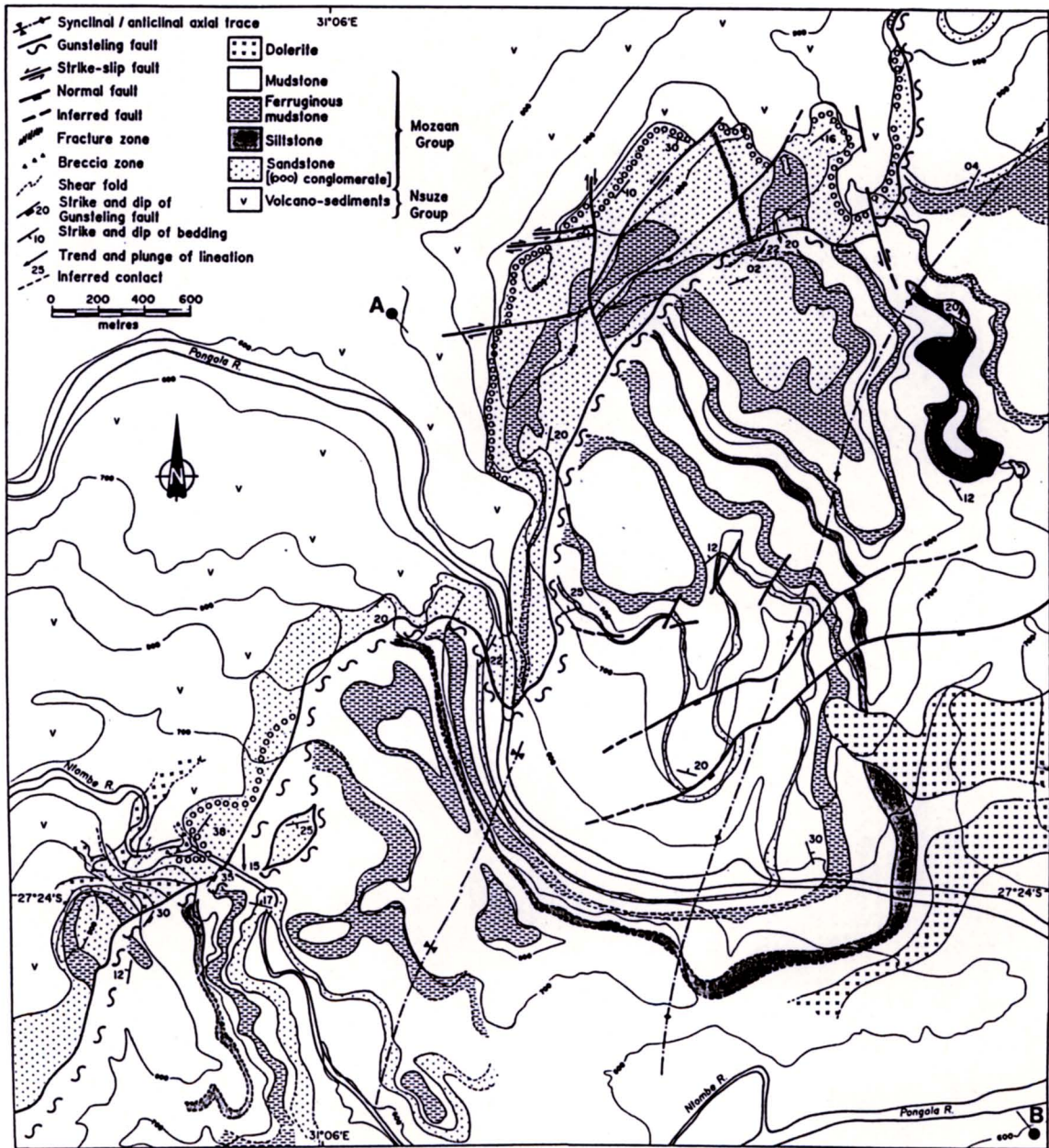


Figure 3.20: Map of the Gunsteling fault. A and B mark the end points of the cross-section line shown in Figure 3.26.

The sandstone in the footwall is highly fractured. The orientations of these fractures are relatively scattered although a large proportion of them appear to be extensional fractures that formed at a high angle to the fault and the direction of slip (Figure 3.22).

Most of the subsidiary faulting in the hanging wall and footwall is bedding-parallel. The lineations measured in the hanging wall have a shallower plunge than those in the footwall due to the attitude of the bedding in the hanging wall being towards the west (Figure 3.23). The orientation of the lineations indicate oblique net slip with transport of the hanging wall to the south-southeast.

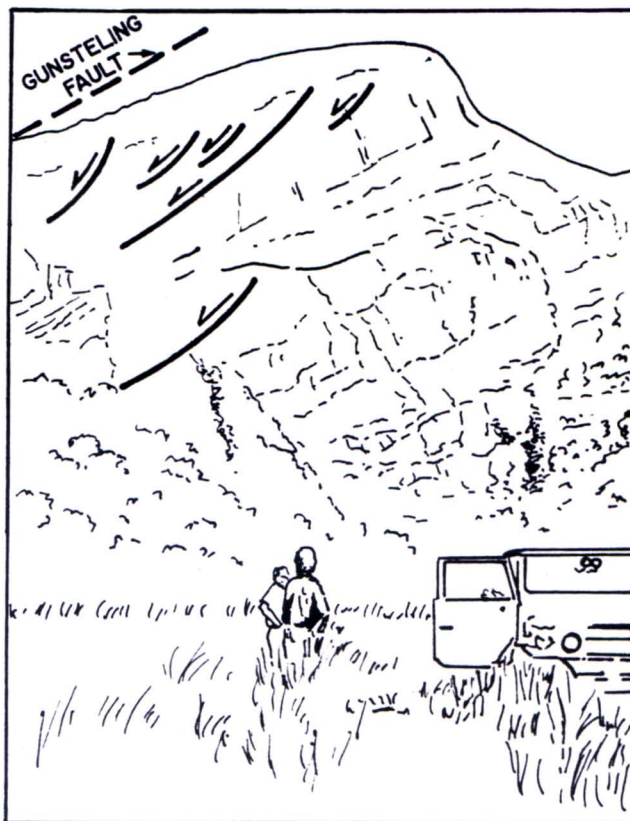


Figure 3.21: Annotated photograph showing faulting in the footwall of the Gunsteling fault. View looking south across the Ntombe River valley.

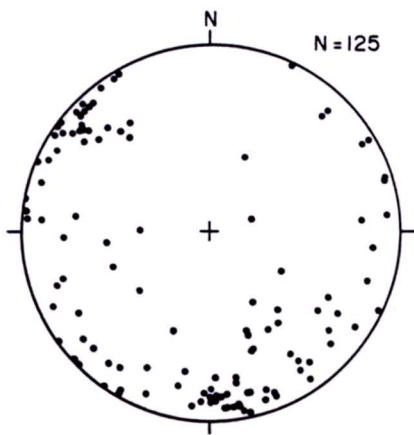


Figure 3.22: Pi plot of fractures in the Gunsteling fault footwall.

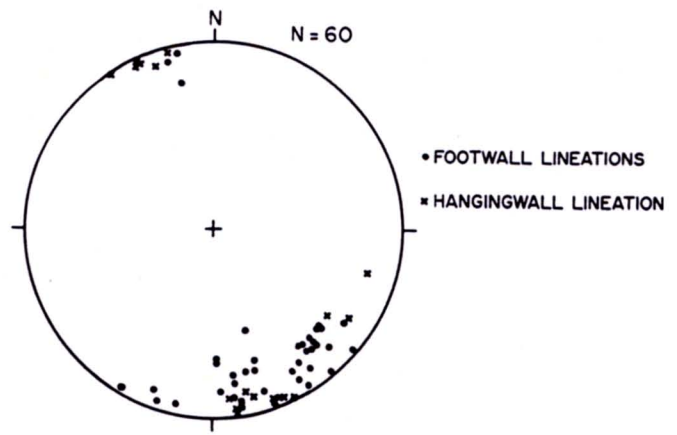


Figure 3.23: Lineations on bedding-parallel faults in the footwall and hanging wall of the Gunsteling fault.

Northeast striking synthetic faults formed in the hanging wall to accommodate space problems caused by the movement of the hanging wall beds down the curved trajectory or over ramps of the fault.

The geometry of the poorly exposed northeastward extension of the Gunsteling fault is problematical. In view of the large displacements associated with the fault to the southwest it is unlikely that it dies out before the Qumeni shear zone is reached. The fault is thus either displaced by the Qumeni/Altona/Sinqeni shear zone system and now continues above the basal sandstone to the east of the Sinqeni mountain, or it swings into a southeast strike to become a sinistral lateral ramp or tear fault that was reactivated as the dextral Qumeni shear zone. Due to the apparent absence of any normal faulting to the east of the Sinqeni mountain, the latter interpretation is favoured. Normal faulting above the Sinqeni Formation does however occur further north. A schematic representation of the possible sequence of deformation events is shown in Figure 3.24.

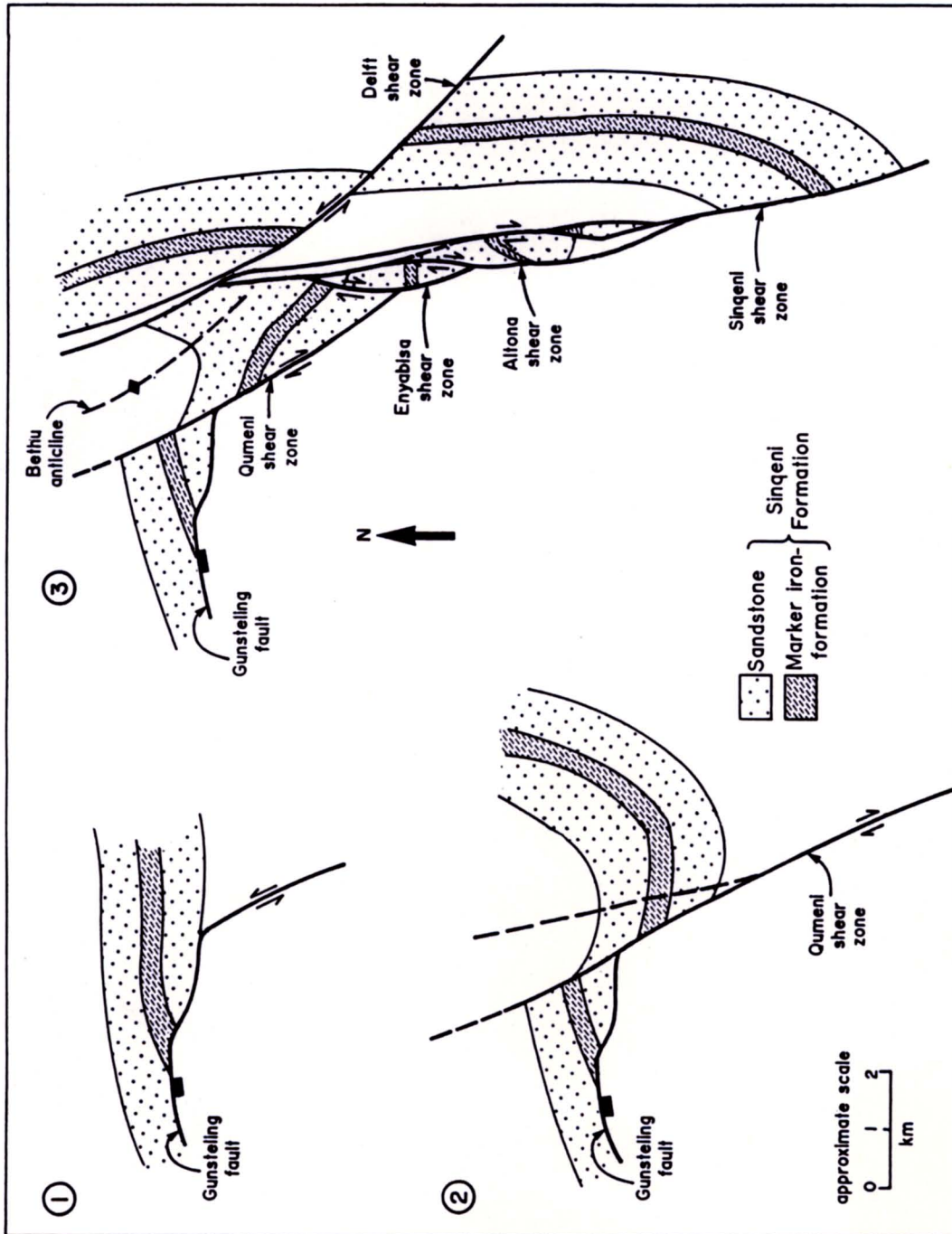


Figure 3.24: Schematic plan showing the relationship of the Gunsteling fault to the strike-slip duplex structure.

Also indicating the shearing out of an anticlinal fold closure by the strike-slip shear zones.

Gunsteling anticline and syncline

The arcuate trace of the fault in plan view (Map 1B) implies a listric shape in profile. A roll-over anticline (the Gunsteling anticline) is clearly developed in the hanging wall (Figures 3.25 and 3.26). A peculiarity of the fold is its monoclinical character with the hanging-wall bedding being sub-horizontal adjacent to the fault while the footwall bedding dips toward the southeast (Map 1C). This is due to a southeastward tilt of the strata in the hanging wall of the IZermijn shear zone prior to the faulting or due to the later regional folding. A synclinal structure is developed in the hanging wall of the Gunsteling fault to the south of the Pongola River. This fold is possibly the result accommodation of hanging wall extension associated with a ramp/flat detachment fault geometry (Figure 3.27; Ellis and McClay, 1988). It is possible, if the IZermijn compression preceded the Gunsteling extension, that early ramp structures were utilized by the later extension giving rise to both anticlines and synclines as the hanging wall was transported south-southeastwards relative to the footwall.

North-northwesterly trending folds

Upright folds with south-southeasterly plunging axes appear to have formed both prior to and contemporaneous with north-south dextral and northwest sinistral shearing. They fold the IZermijn shear zone and Gunsteling fault. These folds occur on all scales (e.g. Bethu anticline, Mfeno syncline and anticline, Nombela anticline and Prudentie syncline; see Maps 1C, 2 and 3).

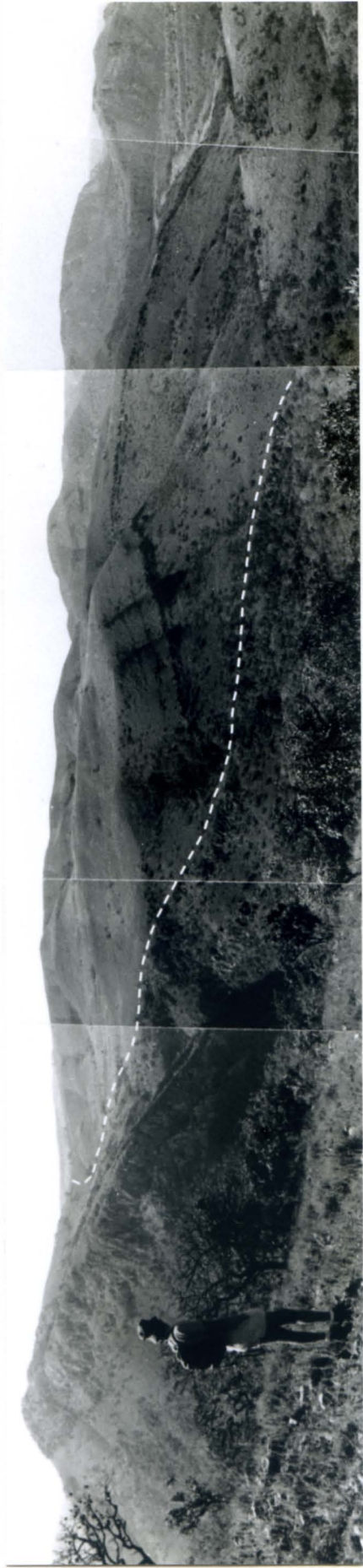


Figure 3.25: Panoramic view of the Gunsteling fault (dashed line) and the roll-over anticline in its hanging wall. View to the north.

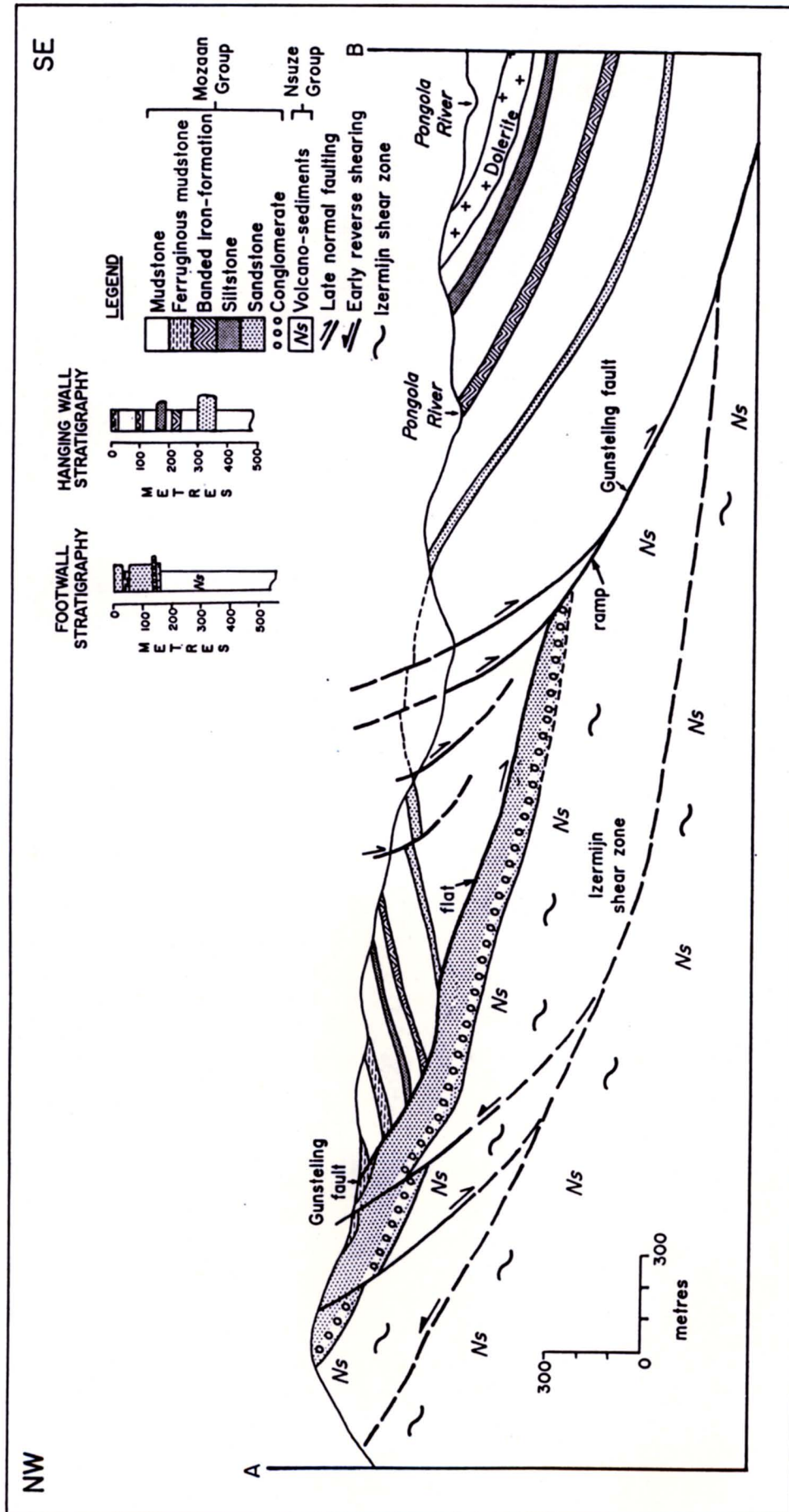


Figure 3.26: Cross-section through the Gunsteling fault. See Figure 3.20 for section line.

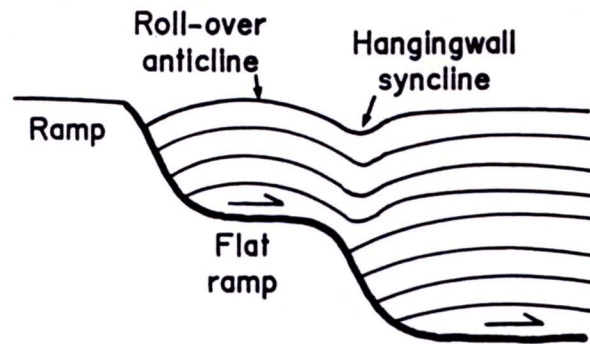


Figure 3.27: Necessary folds in the hanging wall above the footwall ramps and flats explaining the development of hanging-wall synforms in relation to fault geometry (after Gibbs, 1984).

Bethu Anticline

The Bethu anticline which is situated between the Sinqeni and Qumeni shear zones (Figure 3.28 and Map 1C) plunges shallowly towards the southeast and has a steep axial plane which dips steeply towards the northeast. The fold predates the shearing as the fold closure is extensively disrupted by the Altona-Sinqeni shear zone system.

Mfeno Syncline and Anticline

A close overturned fold, the Mfeno syncline, occurs in a fault-bounded block between the Duduka fault, the Sinqeni shear zone and the Dwaleni fault (Figure 3.29 and Map 1C). The northeastern limb dips steeply towards the northeast and the southwestern one towards the southwest. The fold axis plunges shallowly to the southeast and the axial plane dips at $\sim 30^\circ$ towards the northeast.

On the northern side of the Duduka fault the beds have been folded into an open northwest-southeast oriented anticline, the Mfeno anticline (Map 3).

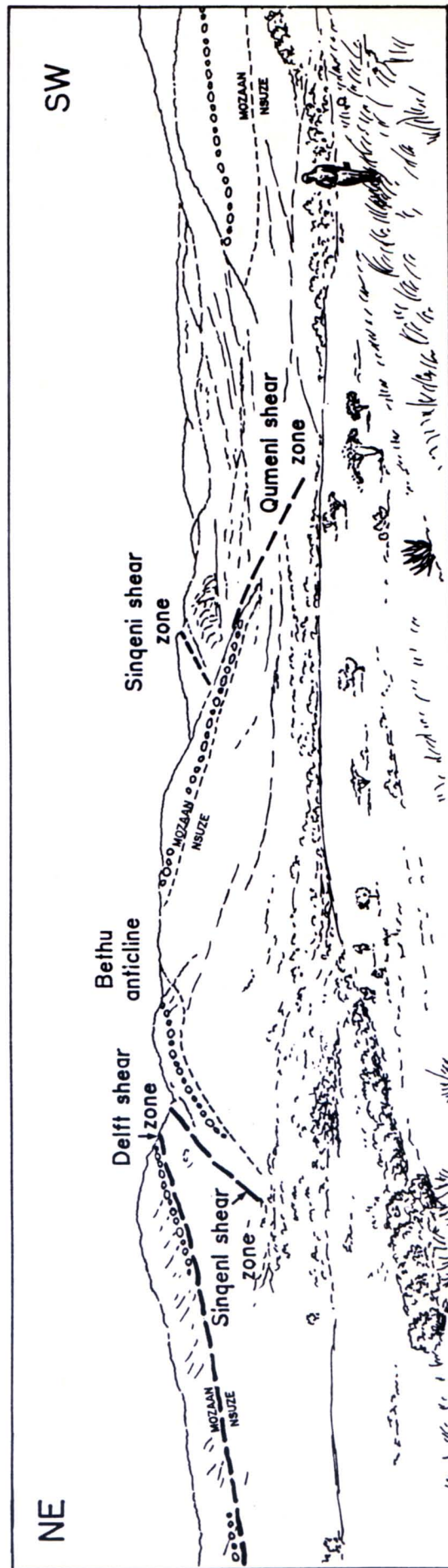


Figure 3.28: Annotated sketch looking southeast towards the Bethu anticline and the Delft Singeni and Qumeni shear zones.

These folds are interpreted as being the result of dextral movement along the Sinqeni shear zone before the initiation of the Duduka fault. A restraining bend in the Sinqeni shear zone may have induced folding and overturning of the Mfeno syncline prior to southward displacement of the block containing this fold.

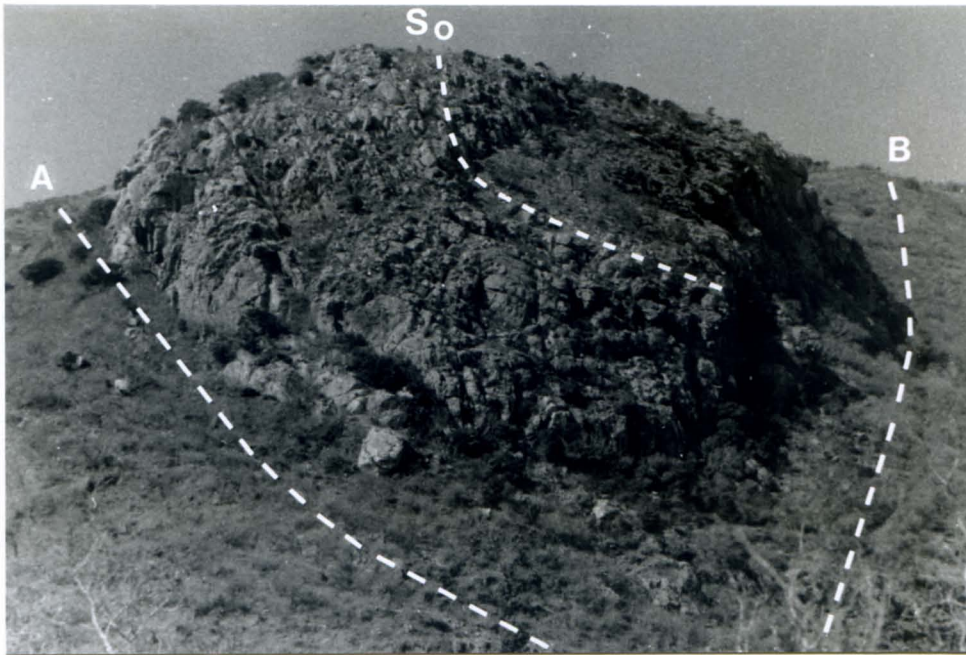


Figure 3.29: View of the Mfeno syncline looking southeastward showing the fold-closure and its southwestern limb. The fold is bounded by the Duduka fault (A) and the Sinqeni shear zone (B). Bedding is indicated by the line with shorter dashes. The sandstone displays an intense vertical jointing.

Nombela Anticline

The northwest-trending Nombela anticline developed late during the shearing event as it folds the Sinqeni shear zone (Map 3). The fold axis plunges towards the southeast (157/12; Figure 3.30).

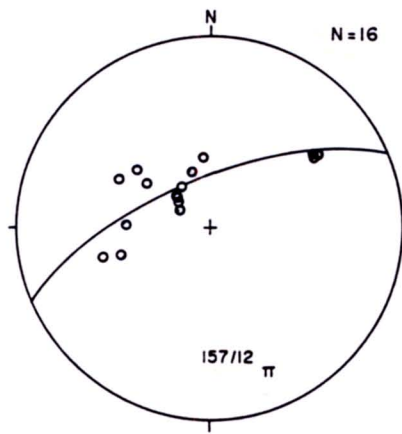


Figure 3.30: Stereoplot of poles to bedding in the Nombela anticline.

Prudentie Syncline

The Prudentie syncline is located between the Gunsteling fault and the Altona shear zone (Map 1C). The fold axis plunges towards the south within the study area. Watchorn (1978, 1979b) states that the fold is a periclinal structure with the axis plunging towards the north further south. The footwall to the Gunsteling fault has also been folded and has an axis which plunges towards the south-southeast (160/19; Map 1C). The arcuate shape of the Gunsteling fault is related to this folding.

Northerly trending dextral shear zones and faults

Eight of these shear zones and faults are exposed within the study area namely the Mkhuzwa, Altona, Sinqeni, Qumeni, Enyabisa, Nkolotsheni and Bumbeni shear zones as well as the Khuphulangwenya fault (Map 1B). Many of them are developed in incompetent mudstone and phyllite units and have bedding-parallel strikes. The Mkhuzwa, Altona, Sinqeni and Enyabisa shear zones splay southwards but appear to join again south of the Pongola River, thus defining a large-scale strike-slip duplex.

Mkhuzwa Shear Zone

This north-south oriented shear zone is very poorly exposed, except in a banded iron-formation unit in the Mkhuzwa stream (Map 3). A series of sub-vertical north-south trending shear zones up to 10 m in width and mesoscopic tight folds are developed here. A dextral sense of movement is inferred inter alia from en échelon tension gashes (Figure 3.31).

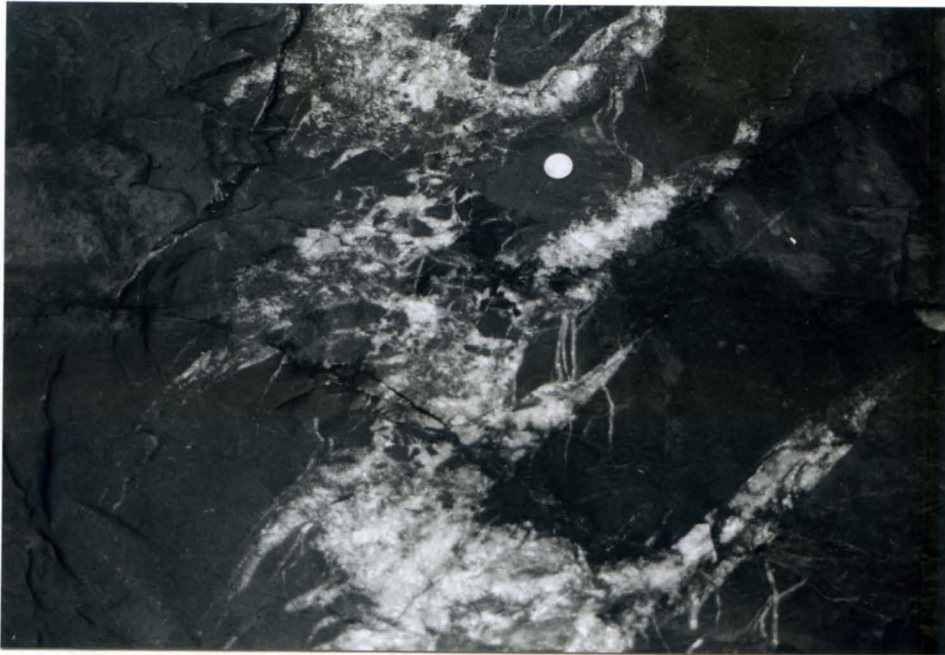


Figure 3.31: Complex quartz-filled en échelon tension gashes in a mudstone in the Mkhuzwa shear zone indicating a dextral sense of shear. North is at the top of the photo (coin diameter is 20 mm).

Horizontal stretching lineations are present on quartz veins which are parallel to bedding. The fold axes lie in the plane of the shear zone with plunges varying from sub-horizontal, parallel to the stretching lineations to sub-vertical. This variation in plunge is probably the result of progressive deformation with fold axes initially developing at a high angle to the shear direction but then rotating into parallelism with the stretching direction.

Northwards the Mkhuzwa shear zone swings in strike and joins the northwest striking Qumeni shear zone.

Qumeni Shear Zone

The Qumeni shear zone, which is very poorly exposed, is interpreted as initially forming part of the arcuate Gunsteling fault possibly developing into a strike-slip shear zone further south. After the Bethu anticline was formed, it was reactivated as the Qumeni shear zone which it propagated in a dextral sense northwards into the Gunsteling fault footwall (Figure 3.32). The Enyabisa shear zone cuts and displaces the Qumeni shear zone southwards to the south (Map 3).

Altona Shear Zone

The Altona shear zone is well exposed in the Mkhuzwa stream where typical shear-related small scale structures indicating right lateral strike-slip displacement can be seen within the banded siltstone of the Nsuze Group. The shear zone is terminated in the north by the northwest-trending Delft shear zone. Strike-slip movement along this northern part was accompanied by a component of normal displacement as the Sinqeni Formation sandstone to the east is downthrown against the Nsuze siltstone to the west. Further south the Altona shear zone displays a reverse component of movement as the Nsuze siltstone overlies the Sinqeni Formation sandstone implying a rotational movement.

A ~2200 m dextral strike separation can be determined from the offset of the marker iron-formation. Phyllitic siltstone interpreted as belonging to the Nsuze Group (Chapter 2) are found within the shear zone. The siltstone displays a well-developed foliation, which is also present to a lesser extent within dolerite in the zone of shearing. The

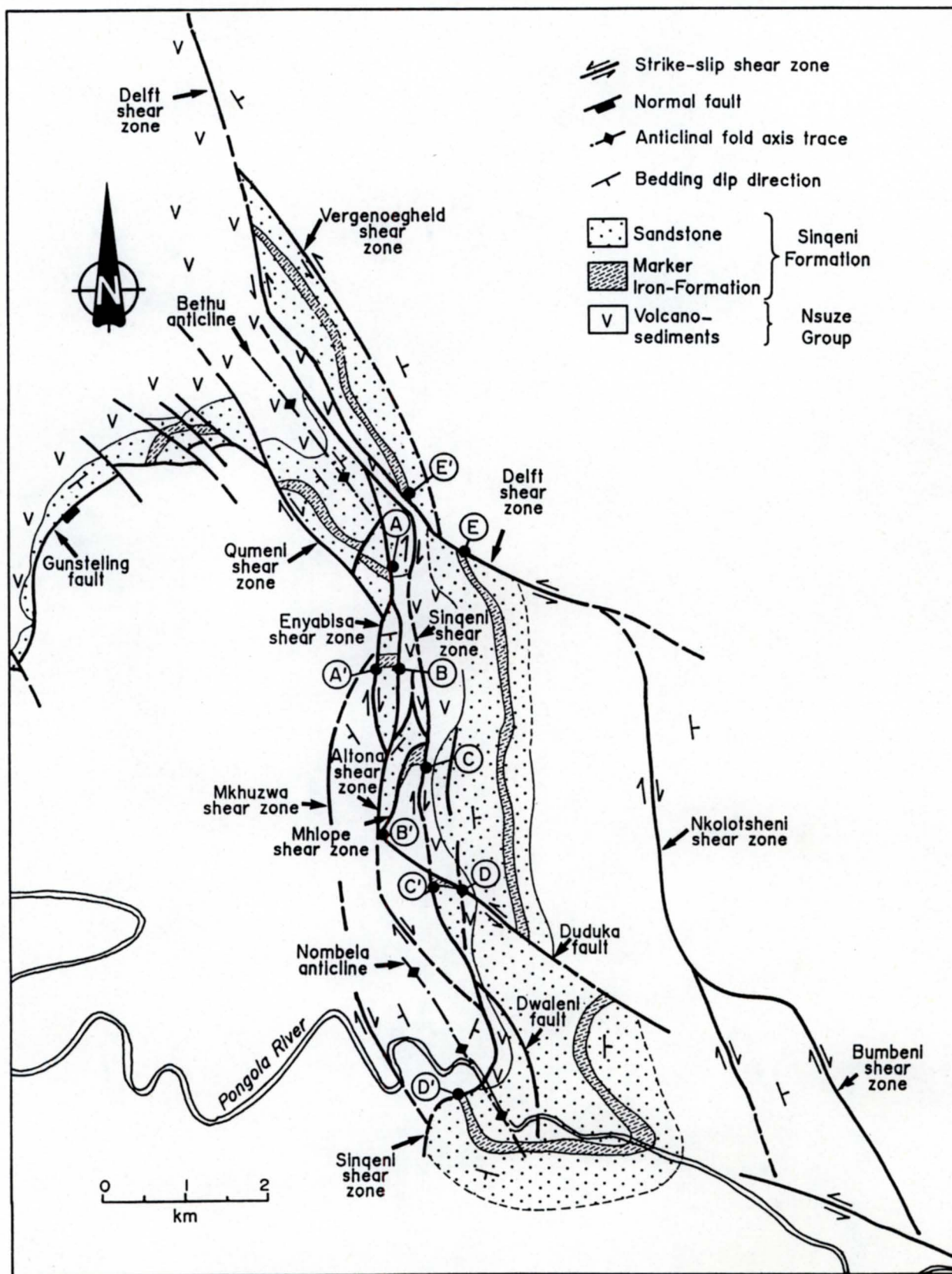


Figure 3.32: Schematic map showing the strike-slip separations along the shear zones: from A to A' along the Enyabisa shear zone, B to B' for the Altona shear zone, C to C' and D to D' for the Sinqeni shear zone and E to E' along the Delft shear zone.

foliation is sub-vertical and varies in strike from north-northeast to northwest (Map 1B). A well defined s-c fabric confirming the dextral displacement is often developed and drag folding (Figure 3.33) and rotation of fault blocks (Figure 3.34) is also observed. Quartz-fibre lineations and striated slickensides have a sub-horizontal attitude and typically plunge gently north-northwest and south-southeast (Map 1B).



Figure 3.33: Sectional view looking obliquely down towards the south through a drag fold developed in the Altona shear zone. The axis plunges southwards.



Figure 3.34: Northwest-trending rotational faults adjacent to the Altona shear zone. Plan view with north to the left.

The dip and younging direction of bedding changes from westwards in the west to eastwards in the east across the shear zone so that the shear zone marks an early sheared out fold closure (Figure 3.35). The sandstone along the shear zone is deformed by brittle faulting and fracturing and has subsequently been extensively recrystallized. The lack of ductile deformation in the sandstone is evident where the basal conglomerate is present, as the clasts have not undergone any apparent change in shape.

In the field strike orientations, namely north-south and northwest strike directions, are found in close association with the north-south set being better developed. These can clearly be seen in the detailed plan view of an outcrop of the shear zone in the Mkhuzwa stream (Figures 3.36 and 3.37) despite their anastomosing character. The north-trending faults and shear zones generally truncate the northwest-trending ones but locally the latter displace the former, indicating contemporaneous development.

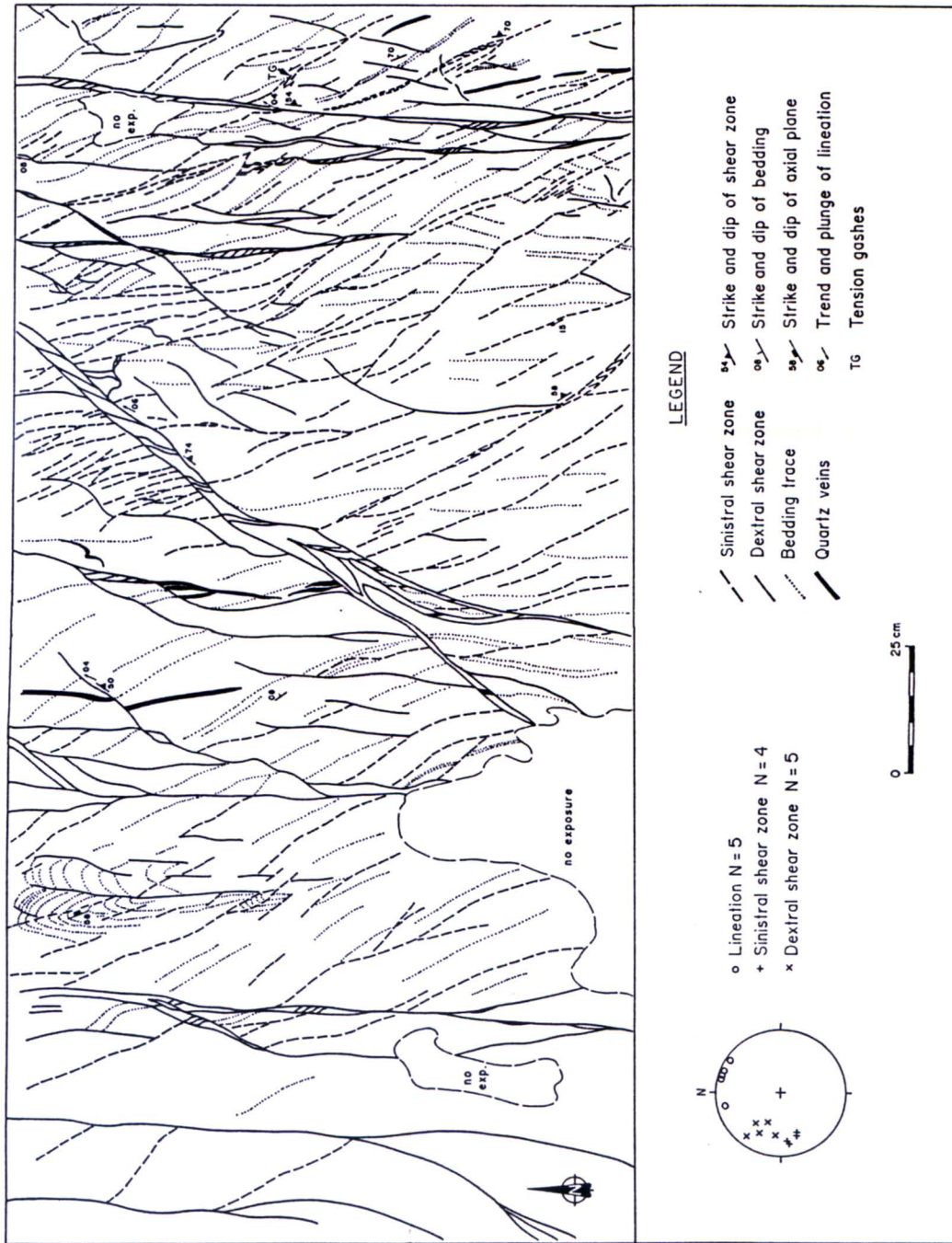


Figure 3.36: Detailed plan view of an outcrop within the Altona shear zone showing small-scale north-south and northwest-trending faults and shear zones. The discontinuities are typically 0.5 to 2.5 cm in width and have sub-horizontal stretching lineations.



Figure 3.37: Intersecting dextral and sinistral faults in the Altona shear zone. Note the conflicting age relationships of cut-offs. North is to the left.

In the Nsuzi siltstone, the folds associated with the shearing show thickening in the hinge zone (class 2 and 3 folds; Ramsay's 1967 classification). The hinges often occur in the zone bounding the acute angle between conjugate faults or shear zones with the axial planes bisecting the faults (Figure 3.38).

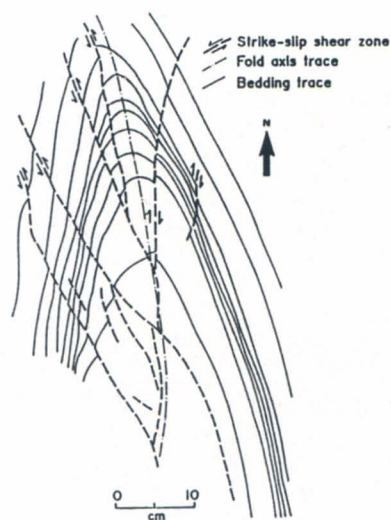


Figure 3.38: Plan view sketch of a fold in the Altona shear zone.

Sinqeni Shear Zone

The Sinqeni shear zone is the most prominent of the north-south striking dextral shear zones, and has a strike length of ~7500 m across the study area. It displaces Nsuze siltstone as is the case with the Altona and Enyabisa shear zones. Unlike the Altona shear zone, the throw of the Sinqeni shear zone does not change along strike and it displays only right-lateral reverse oblique slip. The result is that Nsuze siltstone now overlies the Sinqeni sandstone. In the north, the strike of the shear zone swings around to the northwest, but Nsuze rocks are still present to the east. The Sinqeni shear zone is not as well exposed as the Altona and the sheared Nsuze rocks along it weather easily. The shear zone forms a well defined valley between prominent ridges of the bounding Sinqeni Formation sandstone.

The Sinqeni shear zone was originally described by Humphrey and Krige (1931, pages 27-30) as being situated within the core of a "sharp anticlinal fold". They postulated that a thrust fault could be present between the two prominent sandstones. They also mentioned that shales, which are "white and light-grey in colour... and which weather to a bright red colour" are found in the Itala and Bivane River valleys along strike from the Sinqeni shear zone to the south of the present study area. This suggests that the Nsuze Group siltstone is still preserved within the shear zone some 9 km farther southwards. This would give the shear zone a total strike length of at least 16 km.

The shear zone has tectonically duplicated the Sinqeni Formation. It is parallel to east-dipping bedding to the east, but oblique to it on the western side. This is demonstrated by the truncation of the marker iron-formation in the fault-bounded block between the Altona and Sinqeni shear zones. The bedding within this block is gently deformed by an anticlinal fold, the axis of which plunges gently towards the south-southeast (π axis 172/13; Map 1C). The iron-formation V's upstream in the valley in this block because the stream gradient is greater than the fold plunge. South of the Duduka fault is a fault bounded

block of sandstone which includes the marker iron-formation. This block is displaced ~ 1200 m southwards by the Sinqeni shear zone.

A small Nsuze siltstone exposure in the shear zone south of the Duduka fault provides a good example of the contemporaneity of the two sets of shear zones even though it is surrounded by dolerite and may not be in situ. On the western side of Figure 3.39 three small-scale sinistral shear zones with a northwesterly trend are seen to be terminated by a broader, better developed northeast-trending dextral shear zone. In contrast the most southwesterly of the three sinistral faults truncates a northeast-trending dextral fault.

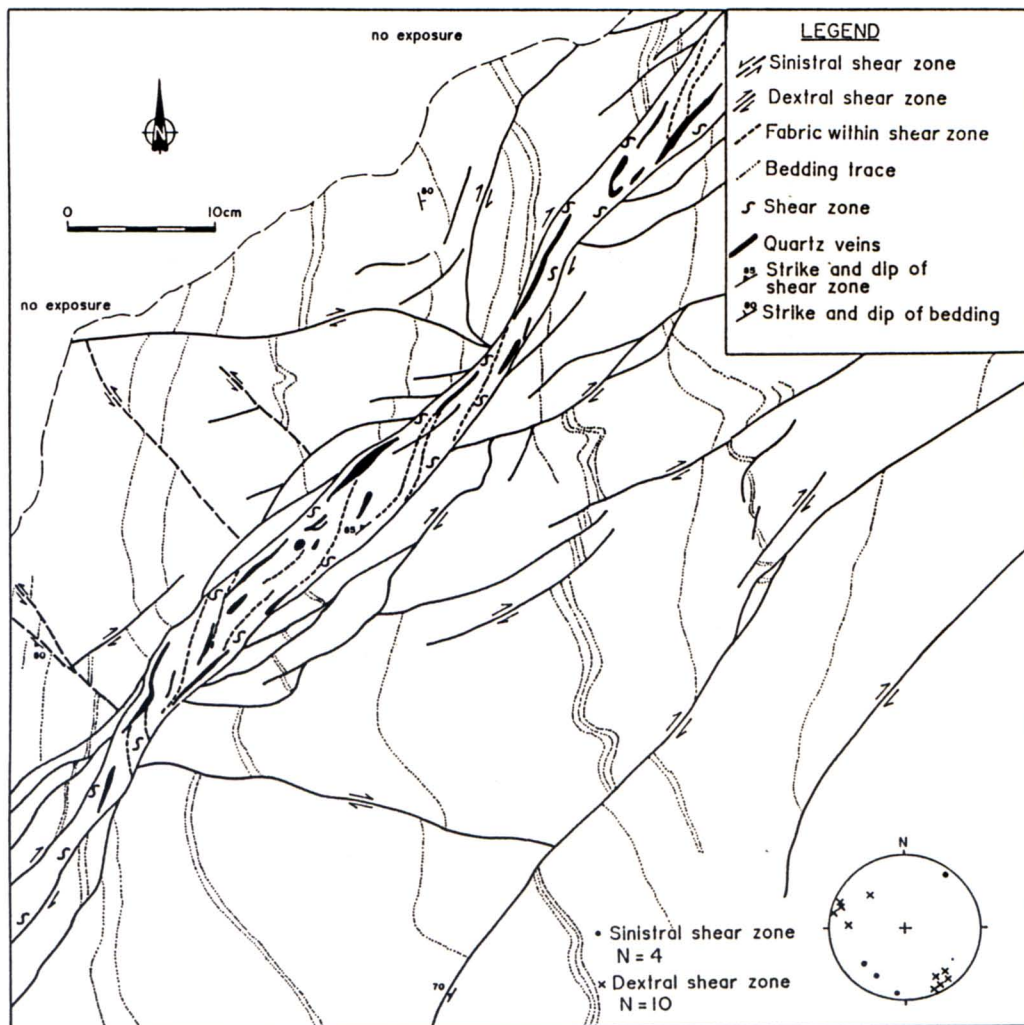


Figure 3.39: Detailed plan view of an exposure within the Sinqeni shear zone to the south of its intersection with the Duduka fault.

The shear zone is very poorly exposed on the western side of Sinqeni mountain in the Pongola River valley. Where it crosses the river, it becomes folded by the north-northwesterly trending Nombela anticline so that its dip shallows and it swings into an east-west strike. It resumes its north-south strike again further to the south.

The total lateral displacement along the Sinqeni shear zone is in the order of 5000 m (C to D'; Figure 3.32) and the cumulative dextral displacement along the north-south trending Sinqeni-Altona-Enyabisa shear zone system is at least 8800 m (A-D').

Mhlope Shear Zone

The Mhlope shear zone is developed within the fault bounded block between the Altona and Sinqeni shear zones (Map 1B). The shear zone dips at $\sim 25^\circ$ to the southeast and strikes northeast and is truncated to the east by the north-south oriented Sinqeni shear zone. It does not appear to continue in the marker iron-formation outside of this block and is thus probably related to the dextral shearing along the Sinqeni shear zone. The shear zone is developed sub-parallel to bedding stratigraphically below the marker iron-formation, but eliminates this hanging-wall unit to the southwest, indicating a normal fault relationship. It was subsequently folded together with the bounding sedimentary rocks. Poles to the shear foliation plot along a partial girdle, the π pole of which has a trend and plunge of $172 \setminus 13$ (Map 1B), and conforms roughly with the axis of the Bethu anticline, confirming a pre-folding age for the shearing. Lineations measured on north-south trending part of the shear are sub-horizontal and are oriented north-south (Map 1B). A right-lateral sense of movement is given by small-scale structures (Figure 3.40).



Figure 3.40: Small-scale folds of bedding in the Mhlope shear zone showing a dextral asymmetry. Note the minor faults with dextral offsets to the right, view looking obliquely down towards southeast.

Dwaleni Fault

The Dwaleni fault, which is mostly bedding-parallel, splays southwards off the Sinqeni shear zone into its hanging wall. It is situated near the base of the Sinqeni cliff and dips towards the east (Figure 3.41 and Map 3). The fault is transpressional with hanging wall transport to the south. A reverse sense of movement is indicated by poorly developed s-c fabrics and detachment folding in the hanging wall (Figure 3.42). The folds plunge shallowly southeastwards. The fault has duplicated the lower parts of the Sinqeni Formation including the basal conglomerate so that it has a greater thickness at Sinqeni mountain.

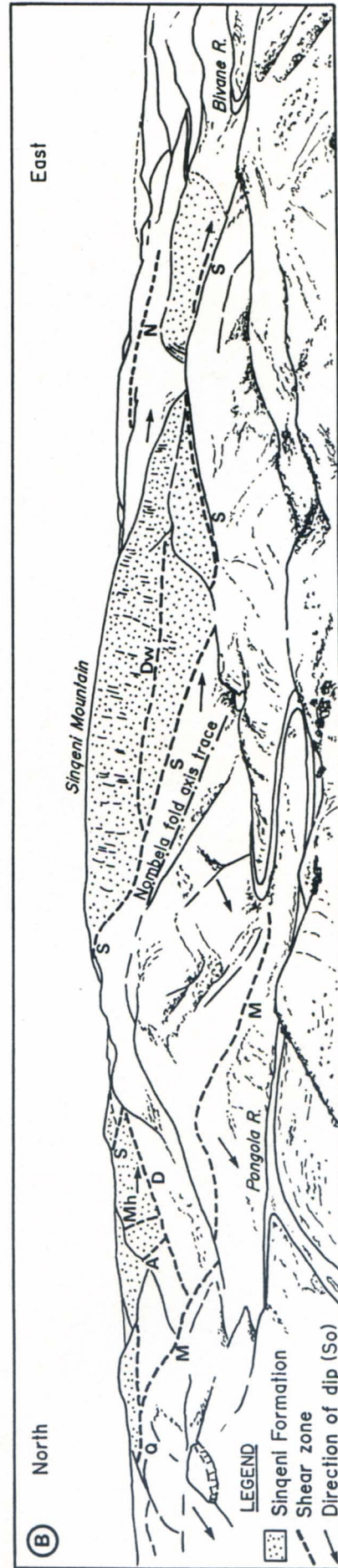
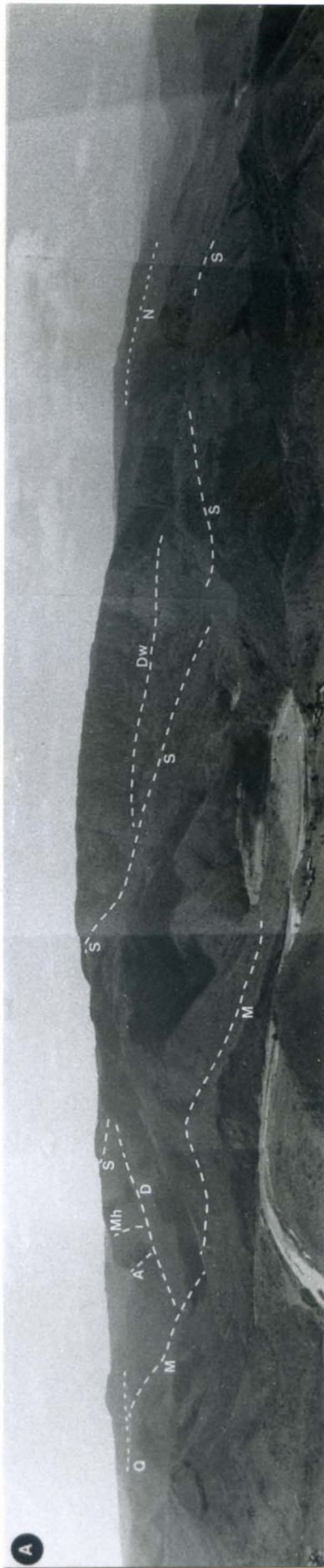


Figure 3.41: A). Panoramic view of the various shear zones and their respective relationships. Shear zones: Q - Qumeni, A - Altona, M - Mkhuzwa, Mh - Mhlope, S - Singeni, Dw - Dwaleni, D - Duduka. B). Annotated sketch of A).

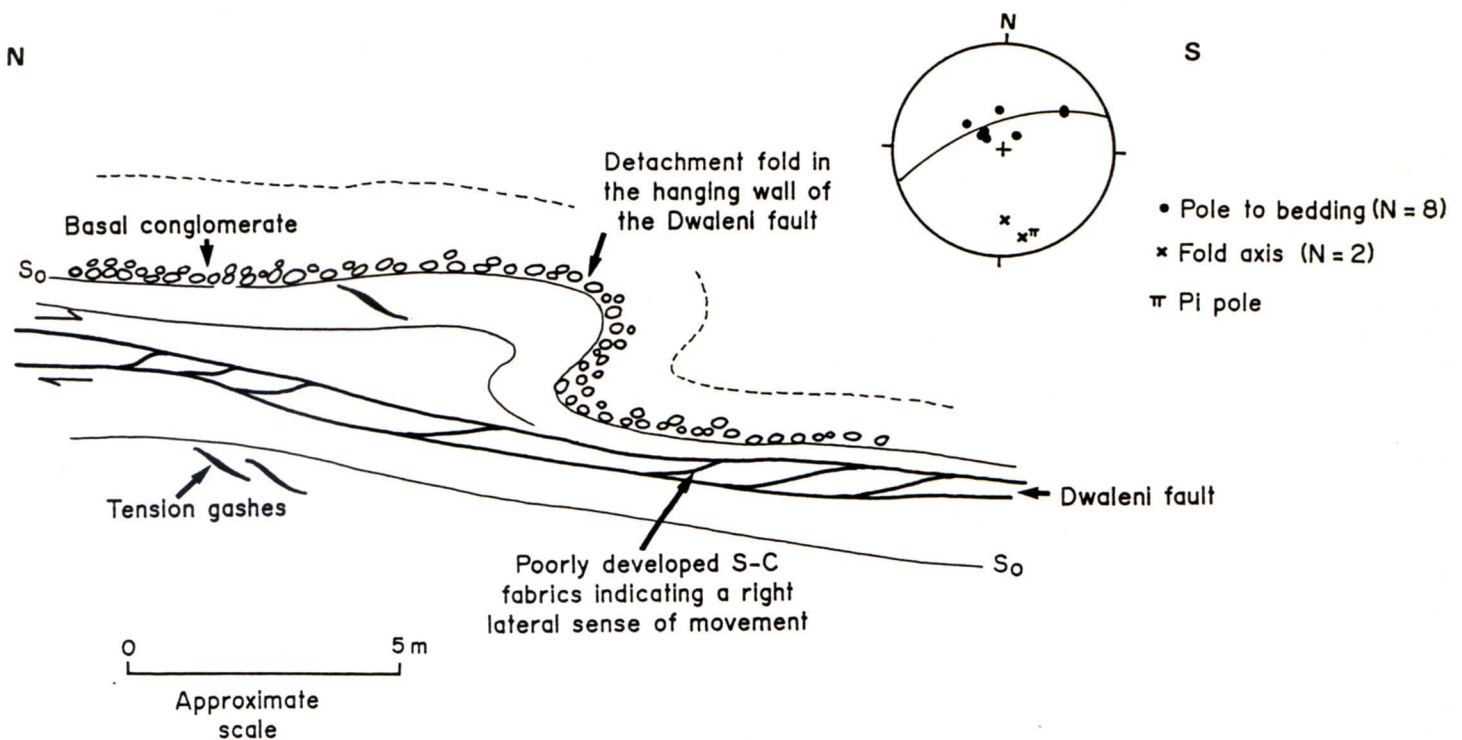


Figure 3.42: Schematic plan view of the Dwaleni fault showing associated folding.

Nkolotsheni-Bumbeni Shear Zone System

The previously unrecognized Nkolotsheni-Bumbeni shear zone system is situated about 2,5 km east of the Altona and Sinqeni shear zones in higher stratigraphic units. Due to their bedding-parallel nature the displacements along them are indeterminable.

Nkolotsheni Shear Zone

The Nkolotsheni shear zone is up to 50 m wide and is generally situated within poorly exposed mudstone of the Thalu Formation. Northwards, it is located between two competent sandstone units, adjacent to a sheared banded iron-formation. The shear zone

strikes north-northwest and contains a steep east-northeast dipping foliation and stretching lineations that plunge very gently towards the north-northwest (Map **1B**). The northern extension of the shear zone is poorly exposed and may terminate before the northwest-striking Delft shear zone is reached or it may be displaced by it (Map **3**). It continues southwards across the Pongola River into the Itala Game Reserve. The best exposure is to the west of the Bumbeni stream, where the Bumbeni shear zone branches off to the southeast. Immediately south of this splay, the Nkolotsheni shear zone widens significantly to about 100 m. The sandstone units to the east have been attenuated and boudinaged with large-scale boudins up to 100 m in length being represented here.

The banded iron-formation to the west has been subjected to both brittle and ductile deformation particularly towards the south. The unit is displaced in a right-lateral sense by a minor splay. Asymmetric z-shaped shear folds have axial planes sub-parallel to the shear zone. The axes typically plunge very gently towards the southeast.

Bumbeni Shear Zone

The Bumbeni shear zone, which is also very poorly exposed, is developed in the Bumbeni stream valley. Shearing has occurred predominantly within dolerite as well as mudstone which has behaved in a ductile manner. It dips steeply to the east-northeast or northeast (Map **1B**). Locally the shear zone is intruded by several phases of dolerite, the earlier ones of which are syn-tectonic.

Subhorizontal slickenside striations and quartz-fibre lineations trending north-northwest are commonly developed on bedding surfaces adjacent to the zone of shearing. Tension gashes indicate a dextral sense of movement. An 80 m thick sandstone unit to the west of the shear zone may be a tectonic correlative of the thick Hlashana Formation sandstone to the east.

The shear zone continues southwards into the Itala Game Reserve where it appears to host the mineralization at the defunct Wonder Gold Mine.

Khuphulangwenya Fault

The Khuphulangwenya fault (Map 2) is the most easterly of the northerly-trending dextral shear zones and faults in the study area. It is not as well developed as the other shear zones and has a more north-northeasterly trend. A dextral displacement is apparent from the ~ 1 km offset of stratigraphic units and the sense of drag of a ~ 50 m thick sandstone on the western side of the fault immediately northeast of the Khuphulangwenya stream.

The faulted zone is discrete, particularly where both the footwall and hanging wall consist of sandstone, but it widens up to 50 m where it passes through mudstone, as for example in a road-cutting west of the Klipwal Gold Mine. The fault cuts a thick dolerite intrusion at its northern extremity although most of the displacement on the fault appears to predate the intrusion (Map 2).

The foliation in the fault plane dips steeply towards the east or east-southeast. Lineations are oriented north-south and typically plunge towards the south, although there is significant variation in the plunge (Map 1B).

Several major northeast-striking sub-vertical faults with orientations similar to the Khuphulangwenya fault occur in the hanging wall of the Klipwal shear zone. The displacement of lithological units indicates downthrow to the southeast with a local component of dextral movement. The variation in plunge of lineations along these faults indicate that their movement history is complex.

Northwesterly trending sinistral shear zones and faults

The set of northwest-southeast shear zones are not as well developed as the north-south trending ones and data from them is limited due to their poor exposure. They differ in style from the north-south set because of their general obliquity to bedding. The most prominent of these structures are the Delft, Mzamba and Nkosetsha shear zones and the Duduka fault.

Delft Shear Zone

The Delft shear zone is situated in the northwestern portion of the study area (Map 3) and is very poorly exposed. As the Delft shear zone approaches the hinge zone of the Bethu anticline it swings into a north-northwest azimuth parallel to its axial trace. The marker iron-formation is displaced sinistrally by about 1 km. Sinistral drag of east-dipping bedding adjacent to the shear zone has produced drag folds plunging at about 55° towards the east-northeast (Figure 3.43). The shear zone is not exposed east of the Duduka stream. The Nkosetsha shear zone to the southeast lies along strike from and is probably a continuation of the Delft shear zone.

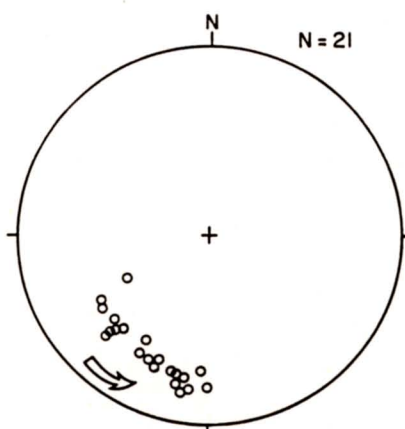


Figure 3.43: Rotation of poles to bedding adjacent to the Delft shear zone (arrow indicates sense of rotation).

A prominent northeast-dipping and a local north-striking cleavage occur within the shear zone, particularly in the Nsuze siltstone. Corresponding to these two foliation orientations are two sets of lineations that plunge shallowly towards the southeast and the north respectively (Map 1B).

Northeast of the Bethu anticline, it assumes an attitude parallel to the Sinqeni shear zone. The two zones do not join and the Delft shear zone is located in the Nsuze siltstone to the northeast of the Sinqeni shear zone.

Nkosetsha Shear Zone

This ~ 60 m wide shear zone (Map 1B and Map 2) in the northeastern part of the study area is very poorly exposed and can only be followed over a distance of about 200 m. It dips steeply towards the northeast and truncates the Klipwal shear zone. A sinistral sense of movement is inferred from drag folding of footwall lithologies.

Vergenoegheid Shear Zone

On the farm Vergenoegheid (Map 1A), the Sinqeni Formation is confined as a fault-bound block between the Delft and Vergenoegheid shear zones. The latter shear zone, which is very poorly exposed, strikes northwest-southeast, is sub-parallel to bedding, and typically dips towards the northeast. The Vergenoegheid shear zone is truncated by the Delft shear zone in the northwest and in the southeast where it is displaced by about 1 km. The shear zone continues south of the Delft shear zone but cuts down through the upper part of the Sinqeni Formation in the vicinity of Sinqeni Mountain. This shear zone, like the Altona shear zone, has a rotational component. Northeast of the Bethu anticline, there is loss of ground across the shear zone while in the south the marker iron-formation has been duplicated (Map 3).

Mzamba Shear Zone

The Mzamba shear zone adjacent to the Piet Retief-Klipwal Mine road is the most poorly exposed of the northwest-trending shear zones (Maps **1B** and **3**). The sense of movement is difficult to determine but a sinistral sense seems likely from its northwest orientation.

Duduka Fault

The northwest-trending Duduka fault appears to have negligible sinistral strike-slip displacement where it crosses the Nsuze-Mozaan contact, increasing to a few hundred metres further to the southeast. It is cut by the Altona shear zone in the northwest. A parallel fault to the south has offset the marker iron-formation sinistrally by 300 m. Quartz-fibre lineations and slickenside striations are oriented sub-horizontally (Map **1B**).

The Duduka fault cannot be followed along strike towards the northwest, but small-scale northwest-striking faults are exposed in the Mkhuzwa stream. They have displacements in the order of several centimetres and cross-cut the north-trending Mkhuzwa shear zone.

Enigma of the conjugate shear zones

It is apparent from the relationships described above that the north-south dextral and northwest sinistral shearing occurred contemporaneously and that folding occurred prior to, during and after the shearing.

The relative senses of movement along the respective shear zones and the orientations of the large-scale fold axes indicates that the maximum principal compressive stress axis, σ_1 , bisects the obtuse angle between the shear zones and trends east-northeast ($\sim 067^\circ$).

The σ_3 axis appears to plunge shallowly northwest to give rise to a normal component of movement of sinistral northwest shear zones and a reverse component of the north-south ones.

The relationship of the shear zones to σ_1 contrasts with the orientations predicted by the Mohr-Coulomb theory (Jaeger and Cook, 1979; Thatcher and Hill, 1991) which states that σ_1 will bisect the acute angle between conjugate faults whereas the obtuse angle is bisected by σ_3 (Figure 3.44). As this relationship holds for synthetic and antithetic faults in a simple shear regime (Figure 3.45), the north-south and northwest shear zones cannot be interpreted simply as Riedel and conjugate Riedel shears.

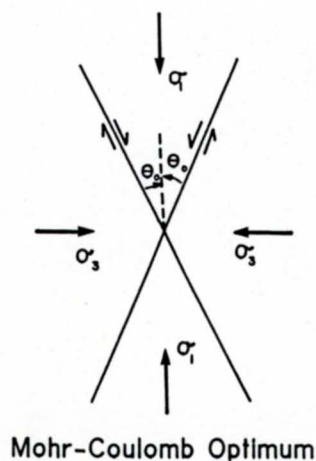


Figure 3.44: Conjugate fault planes generated under tri-axial stress conditions ($\sigma_1 > \sigma_2 > \sigma_3$). Arrows show orientations of maximum and minimum principal stresses (after Thatcher and Hill, 1991).

Conjugate shear zones in which the obtuse angle (generally between 90° and 130°) between shear zones reflects the greatest shortening direction have been reported from some weak or semi-ductile rocks (Becker, 1893; Wellman, 1954; Ramsay 1980; Ramsay and Huber, 1987; Sylvester, 1988; Price and Cosgrove, 1990). Becker (*op. cit.*) pioneered attempts to explain the development of obtuse conjugate relationships on the basis of the strain ellipse concept. These shear zones described as "ductile shears" were reported to occur in rocks which exhibit considerable strain. According to Price and

Cosgrove (*op. cit.*) this "ductile shear" concept was widely used for almost half a century, but that it contains many fundamental errors although they did not elaborate. Becker's (*op. cit.*) "erroneous" concept was gradually abandoned. As a consequence, observations regarding such structures have almost completely disappeared from the literature, although, as Price and Cosgrove (*op. cit.*) mention, these structures have not disappeared from the outcrop.

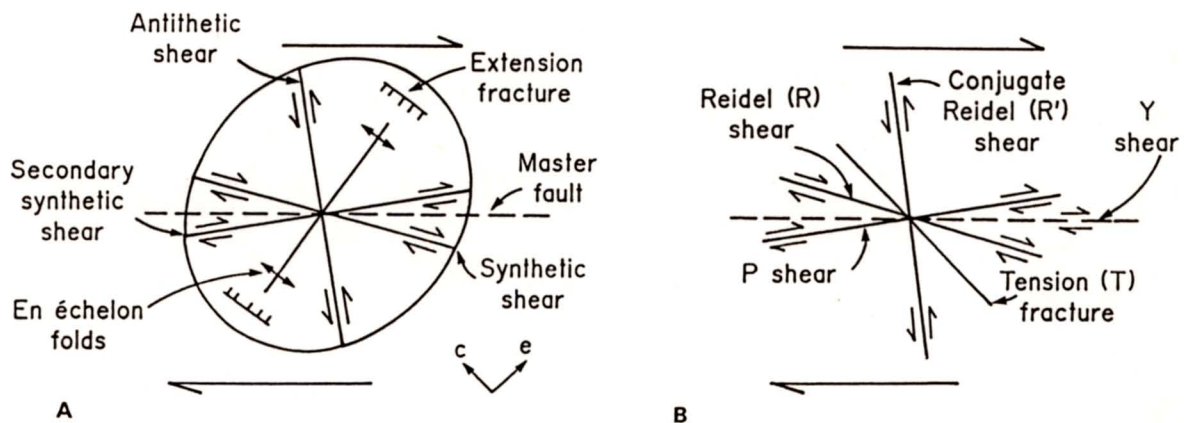


Figure 3.45: The angular relationships between structures that form in an idealized right-lateral simple shear (after Wilcox *et al.*, 1973; Christie-Blick and Biddle, 1985; Allen and Allen, 1990). c is the vector of compression and e is the vector of extension.

- (A) Fractures and folds superimposed on a strain ellipse for overall deformation.
- (B) Riedel shear terminology.

Models for the conjugate relationship

Four alternative models to account for the obtuse relationship of the shear zones can be considered:

Separate deformation events

Although the small-scale structures in the Altona and Sinqeni shear zones suggest that they are contemporaneous (e.g. Figures 3.36 and 3.39) the prevalence of northwest-southeast shear zones truncating north-south shear zones within the study area (e.g. the Delft shear zone terminates the Altona and the Duduka cuts the Sinqeni shear zone; Hunter, 1968) suggest that the northwest strike-slip shearing event may have been later. A similar relationship mapped by Leedal and Walker (1954) in northwestern Ireland was attributed to two different tectonic events since their orientations did not agree with Coulomb fracture angles. On a regional scale, however, the north-south shear zones tend to truncate the northwest-southeast shear zones (Hatfield, 1990; Verbeek, 1991).

It is also of relevance that the post-Pongola Usushwana Complex is displaced by a north-south right-lateral shear zone (Sleigh, 1988; Hatfield, 1990; Verbeek, 1991). The complex is believed to have intruded into a northwest-southeast striking rift-like structure (Hunter, 1970b; Hammerbeck, 1977; Hunter and Wilson, 1988; Riganti, 1991). This suggests that at least some of the northwest-southeast structures predate the north-south shear zones and supports the suggestion that the present displacement pattern is best explained by deformation along a conjugate set of shear zones.

Rotation of shear zones

Conjugate strike-slip shear zones formed in clay model experiments are not fixed in orientation through time, but rotate as deformation proceeds (Freund, 1970; Davis, 1984).

There are two possible types of rotation:

1. With simple shear deformation, external rotation of the conjugate faults accompanies rotation of the axes of the strain ellipse (Figure 3.46A). There is no effect on the conjugate angle.
2. For both simple and pure shear deformation, an internal rotation of the conjugate faults with a consequent change in conjugate angle may occur (Figure 3.46B).

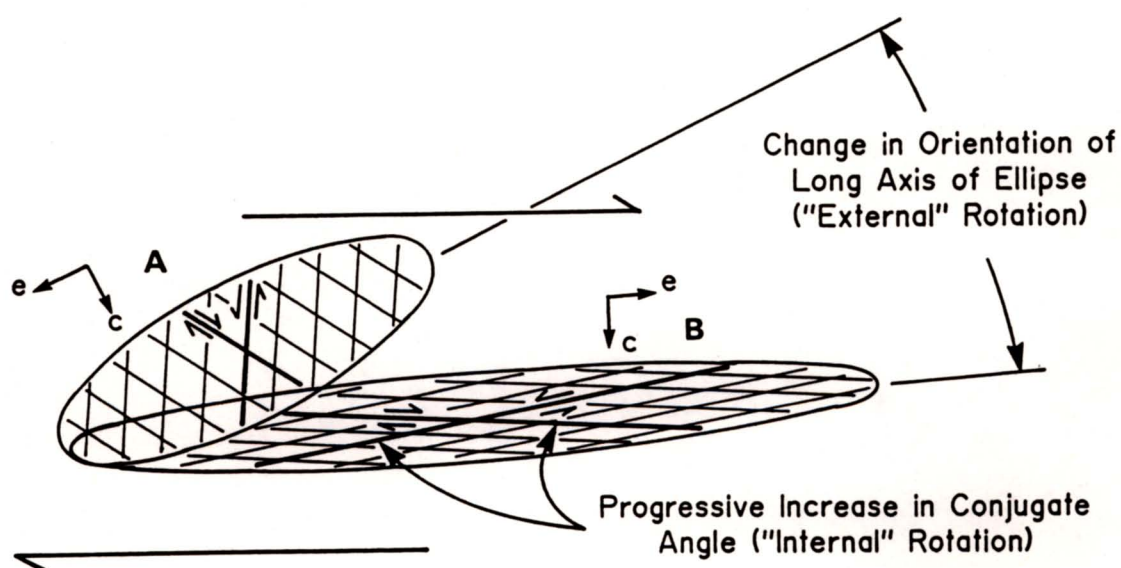


Figure 3.46 A: Progressive external rotation of conjugate faults during simple shear deformation.
B: Internal rotation increases the conjugate angle facing the bulk shortening direction (c). After Davis (1984), *e* is the vector of extension.

To achieve the present orientations, they would have had to be rotated through $\sim 45^\circ$ (Figure 3.47), the sinistral shear zones moving clockwise and the dextral shear zones anti-clockwise. The maximum obtuse angle after rotation given by Davis (1984) is 120° from an initial angle of 60° (i.e. a rotation of 60°), while Nur *et al.* (1986) report that large rotations leading to angles between shear zones of 100° can occur in crustal blocks. These values are less than the 135° (or a rotation of 90°) observed for the strike-slip shear zones in this study.

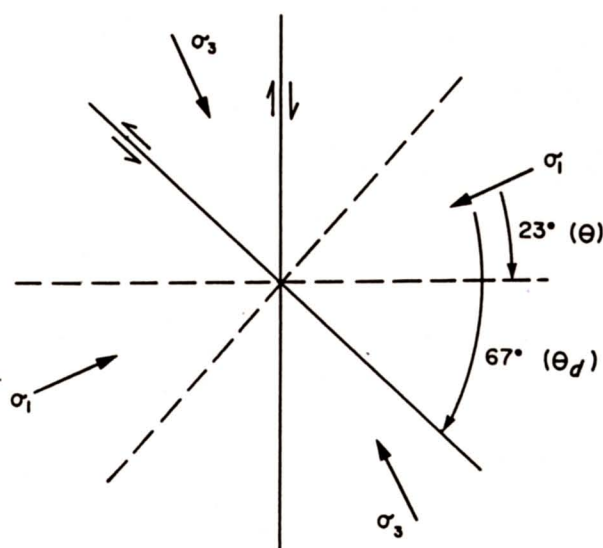


Figure 3.47: Required rotation of conjugate shear zones in the study area.

A rotation of this magnitude would cause considerable shortening. The strain ratio or ellipticity (R_s) can be calculated using Wettstein's equation (Ramsay and Huber, 1983, page 294):

$$R_s = \frac{\tan\theta}{\tan\theta_d}$$

where Θ is the original angle between the shear zone and a line which becomes the principal extension in the undeformed state, and Θ_d is the angle in the deformed state (Figure 3.48).

Substituting the values given in Figure 3.47 into the equation gives a value for $R_s = 5.550$, corresponding to an extension $e=0.18$ and therefore a percentage shortening of 82%. Wood (1974) showed that cleavages in slates commonly develop from shortening values above 40%. No cleavage fabric is identified beyond the limits of the shear zones, and furthermore, the original sedimentary structures are commonly very well preserved. It would also be reasonable to expect that compressional structures, such as reverse faults and isoclinal folds, would accompany shortening of such magnitude. In addition, during rotation the old strike-slip faults would lock and new conjugate faults could form at the expected Coulomb angles. This would result in a large spread of orientations of strike-slip faults in the field (Freund, 1970). The lack of these features militates against rotation accounting for the observed shear zone geometry.

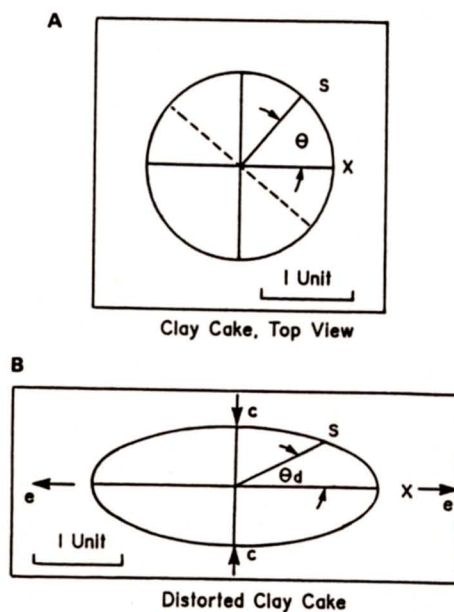


Figure 3.48: Deformation of a hypothetical clay cake that is forced to distort in an ideally homogeneous way showing the rotation of planar structures.

- (A) Undeformed state.
- (B) Deformed state.

Reactivation of zones of weakness in the cover

This model assumes that the north-south-trending dextral shear zones were initiated as sinistral shear zones, while the northwest-southeast ones originally had a dextral sense of displacement (i.e. the opposite sense to what is now observed in the field). These orientations would be consistent with Coulomb fractures that occurred during an earlier phase of compression in which σ_1 was oriented north-northwest. The subsequent reversal of σ_1 and σ_3 would have resulted in a reactivation of pre-existing zones of weakness with movement along shears now being in the opposite direction.

No evidence was found to suggest that the strike-slip shear zones had an opposite sense of movement originally. It can be argued that this pre-existing shearing is not well developed and that the structures had only just been initiated when this deformational episode terminated or that the earlier structures were overprinted during subsequent re-activation.

Reactivation of zones of weakness in the basement

A further possibility is that the orientations of the shear zones reflect structural trends that formed in the Archaean basement rocks prior to or during the deposition of the Pongola Sequence and were subsequently reactivated. Northwest-trending structures in the granitoid-greenstone terrain to the west of the study area have been reported by Smith (1987), Sleight (1988), and Verbeek (1991). Both Smith and Sleight found evidence for the existence of pre-Pongola northwest oriented strike-slip shear zones (Smith's D₄, and Sleight's D₃). Some of these structures are however described as being of post-Usushwana and thus also post-Pongola age (Smith, *op. cit.*; Sleight, *op. cit.*; and Verbeek, *op. cit.*).

Hunter (1970a) reported north-south wrench-faults which dip steeply towards the east within the Ancient Gneiss Complex in Swaziland north of the study area. He also described discontinuities which are oriented northwest-southeast.

It is therefore possible that north-south and northwest-trending conjugate shear zone sets existed in the basement rocks prior to the development of the conjugate shear system in the Pongola basin. Following the Pongola deposition compression from the east-northeast could have led to reactivation of these shear zones which then cut up through the overlying Pongola rocks. Pre-existing structures with appropriate orientations in the cover may also have been were reactivated.

CHAPTER 4: SUMMARY AND CONCLUSIONS

GEODYNAMIC SYNTHESIS

The Pongola Sequence represents the earliest known supracrustal succession on the Kaapvaal Craton. Burke *et al.* (1985) and Matthews (1990) proposed that it accumulated in a rift environment. The Nsuze Group was seen to represent a initial phase of subsidence and filling of a rift as a result of uplift and crustal extension caused by lithospheric heating. This assumption was based on the recognition of characteristics similar to those of more recent initial phase rift deposits including large variations in lateral thickness of sedimentary facies, syndepositional basement faulting and irregular basement topography, thick sequences of shallow water facies deposits, immature basement derived deposits and (at least locally) faulted margins and bimodal volcanic rocks. The considerable variation in thickness of the Nsuze Group (10 000 m west of the present study area, and 1800 m in the White Mfolozi inlier) is attributed to differential subsidence during deposition. The immature nature of the fluvial deposits at the base of the Nsuze Group indicates that they were derived, at least in part, from a local, rapidly uplifted, source terrane. Hobday and Von Brunn (1976) have demonstrated a dominantly granitic source for the arenites and argillites interbedded with the Nsuze lavas. In places the arenites wedge out against palaeotopographic basement highs (Matthews, 1967) that may have been induced by syndepositional basement faulting (Button, 1981). Normal faulting of pre-Mozaan age has locally been demonstrated in the Nkandla area (Matthews, 1967).

The accumulation of the nearly 5000 m of sedimentary rocks with only a minor component of volcanic rocks during Mozaan deposition was attributed by Burke *et al.* (1985) and Matthews (1990) to a thermal subsidence phase. Broad crustal downwarping resulted from thermal cooling and contraction of the subcrustal lithosphere.

A subsequent resurgence of crustal extension and thermal activity in the northern parts of the basin is evidenced by several volcanic events. A late Mozaan episode of volcanism is represented by the amygdaloidal basalts of the Nkoneni Formation, the emplacement of the mafic to ultramafic Usushwana intrusive complex and the intrusion of several extensive granitoid plutons which deformed and disrupted the northern and eastern part of the main Pongola basin. Hunter (1970b) suggested that the Usushwana complex was preferentially emplaced along faults that were initiated during an episode of rifting.

Following these events the basin was subjected to several phases of deformation, of which three are recognized in the present study area. The first involved compression from the southeast, the second was the development of extensional faults to the southeast (the Gunsteling fault) and to the northeast (along the Klipwal shear zone). The third, and most intensely developed, resulted in the formation of northwest oriented folds, north-trending dextral and northwest-striking sinistral shear zones. The cause of these events is unknown. The latest event was the development of northeasterly aligned upright folds which are related to the emplacement of large-scale post Pongola granites (Matthews, 1990).

The northeasterly orientation of the principal stress direction during the development of the conjugate strike-slip shear zones which disrupt the Pongola Sequence may be related to the same event that caused the Nsuzi nappe immediately north of the Natal Mobile Belt. The structural trends swing northwestwards to the west along the rim of the basin. This nappe was probably transported by gravitational gliding from an up-arched region situated to the south (Matthews, 1990). Plate tectonics involving a continent-continent or a continent-island arc collision are discounted by Matthews (*op. cit.*) because of the absence of rocks older than ~ 1500 Ma within the adjacent sector of the Natal Mobile Belt. He instead envisages that the geological evolution of the Pongola Sequence took place along the southern margin of the Kaapvaal Craton while this margin was situated along part a transform plate boundary with a major ocean basin.

The deformation of the main Pongola basin could also be related to the Limpopo Orogeny along the northern boundary of the Kaapvaal Craton. The Limpopo Belt, which has a minimum age of 2.6 Ma (McCourt and Van Reenen, 1992), extensively reworked the craton which was still made up of a relatively thin and unstable crust. McCourt and Vearncombe (1987, 1992) suggested that the Limpopo belt was emplaced from the northeast. The corresponding axis of maximum compression would thus coincide with that required for the formation of the major northwest-trending folds and the conjugate shear zones in the Pongola basin. The late syn-tectonic Usushwana Igneous Suite intruded the Pongola Sequence at ~2870 Ma (Hegner *et. al.*, 1984), making the deformation histories of the two areas roughly contemporaneous.

SUMMARY

Stratigraphy

The Study Area

The study area, straddling the Prudentie and Tobolsk synclines of the main Pongola basin, is underlain predominantly by sediments of the Mozaan Group. The upper Nsuzi Group stratigraphy is present in the northwest and is marked by an upward transition from pyroclastic volcanics to reworked tuffaceous sediments. The transition to the clastic sediments of the overlying the Mozaan Group is gradational and the contact is defined here to occur at the lower contact of the first thick sandstone. The Mozaan stratigraphy is subdivided into six formations. The lowermost Sinqeni Formation, comprising a ~650 m thick sandstone, and the overlying Ntombe Formation, a ~900 m thick unit made up predominantly of mudstone, together constitute an upward fining succession. The Thalu Formation is made up of alternating mudstone and sandstone, the upper parts which is characterized by a series of upward coarsening cycles. The overlying 500 m thick

Hlashana Formation is composed almost entirely of siltstone and sandstone. The topmost Odwaleni Formation is composed of sandstone, mudstone and ferruginous mudstone and includes four distinctive diamictite horizons.

The stratigraphic position of the Kulphiso Formation in the Prudentie pericline is unclear as it overlies a major normal fault and cannot be equated with confidence with any of the other formations. It may correlate with the upper Ntombe and lower Thalu Formations. A lower stratigraphic position than the Mozaan sediment in the adjacent Tobolsk pericline (e.g. Matthews, 1990) is however discounted.

Regional correlations

Due to the complexity of the structures, in particular the evidence presented in this study for normal and reverse fault displacements affecting the Pongola basin, correlations of stratigraphic units on a regional basis should be made with great caution. Only two stratigraphic packages in the Mozaan Group can be used as markers with any degree of confidence, namely the basal Sinqeni Formation, comprising a prominent sandstone with an interbedded marker iron-formation and the uppermost Nkoneni Formation containing basaltic lavas.

Apart from the study area, the Sinqeni Formation is found in the main Pongola basin, on the eastern and western flanks of the Spekboom granite, to the south in the White Mfolozi inlier and in the Amsterdam area to the northwest. The Sinqeni Formation does not appear to be developed in Swaziland.

The uppermost basaltic units occur in the central parts of the main Pongola basin in the core of the Tobolsk syncline, in the Magudu area to the east of the main basin, and in the Kubuta area, to the east of the Mooihoek pluton.

Depositional setting

Following the final phases of Nsuze volcanism, the Pongola depository underwent substantial subsidence with the development of a broad, relatively shallow, epeiric sea.

The accumulation of the Mozaan Group sediments was initiated by the deposition of the sandstone of the Sinqeni Formation as a response to transgression into the basin. The thick succession of overlying mudstone of the Ntombe Formation indicates continued deepening of the basin and/or a decrease in sediment input into the Mozaan basin. During the accumulation of the Thalu and Hlashana Formations, the Pongola epeiric sea must have been relatively shallow again as implied by the increased accumulation of sandstone. Evidence for storm-induced conditions is abundant in these arenites.

The basin was then subjected to rapid subsidence or decrease in sediment input when the predominantly argillaceous sediments of the Odwaleni Formation were deposited in deep relatively quiet water. Intermittent influx of coarser grained material resulted from storm-induced activity. The interlayered diamictite units are interpreted as having a glacial origin, and thus representing the earliest known glacial event on earth.

Structure

The Study Area

The structures within the study area have resulted from three deformational events. An early compressional phase resulted in the formation of zones of north-northwest-directed bedding-parallel slip (the Izerlijn shear zone) and oblique ramping (the Klipwal shear zone). The latter structure curves into a frontal ramp northwards.

An extensional phase followed during which time the Klipwal shear zone was reactivated in a normal sinistral sense. The Gunsteling fault, a major normal listric fault, with downthrow towards the south-southeast, probably formed during this time. It cannot be traced eastwards and may die out or develop into a lateral ramp or tear fault.

The main phase of deformation produced early shallow north-northwest oriented subhorizontal upright folds (e.g. Prudentie syncline, Bethu anticline, Tobolsk syncline), followed by conjugate shear zones. A north-trending set of shear zones display a sinistral or sinistral reverse sense of movement. The most important of these is the Altona-Sinqeni shear zone system which defines a duplex structure and has a strike-slip displacement of ~5 km. It follows and disrupts the hinge zone of the Bethu anticline. A contemporaneous northwest-trending set has dextral or dextral normal displacements.

Four models are considered to account for the obtuse relationship of the conjugate shear zones to the principal compression direction: the shear zones formed during two separate events; shear zones with acute relationships were rotated into obtuse orientations; the shear zones were initiated as Coulomb fractures in an earlier phase of northwest-trending compression; and pre-existing north- and northwest-trending shear zones structures were reactivated and then cut up into the cover sequence.

Regional structure

Similar structural trends to those associated with the main phase of deformation in the study area occur on a regional scale within the Pongola Sequence as well as within the basement granites and gneisses. The largest and most intensely developed of these shear zones is the northwest-striking zone which extends from east of Piet Retief to the present study area. A later phase of upright folding (F_2 of Matthews, 1990) related to granite intrusions refolded the early northwest trending F_1 folds into basins and domes. This

phase is not represented in the study area which is well removed from the granite intrusions.

Concluding Statement

The present study, representing detailed work on a small area in the main Pongola basin, has demonstrated the complexity of structures within it and has highlighted the need for many more studies of this nature before the stratigraphy and structural evolution can be satisfactorily resolved.

REFERENCES

- Aigner, T., 1982. Calcareous tempestites: Storm-dominated stratification in Upper Muschelkalk limestones (Middle Triassic, S.W. Germany). **IN**; Cyclic and event stratification. Einsele, G. and Seilacher, A. (eds). Springer-Verlag, New York, 248-261.
- Alexander, J., Nichols, G.J. and Leigh, S., 1990. The origins of marine conglomerates in the Pindus foreland Basin, Greece. *Sed. Geol.*, **66**, 243-254.
- Allen, J.R.L., 1973. Features of cross-stratified units due to random and other changes in bed forms. *Sedimentology*, **20**, 189-202.
- , 1980. Sand waves: A model of origin and internal structure. *Sed. Geol.*, **26**, 281-328.
- , 1984. Sedimentary structures. Their character and physical basis, **2**. *Developments in sedimentology*, **30**. Elsevier, Amsterdam, 663p.
- Allen, P.A. and Allen, J.R.L., 1990. Basin analysis. Principles and applications. Blackwell Scientific Publications, Oxford, 451p.
- Anderson, J.B. and Molnia, B.F., 1989. Glacial-marine sedimentation. Short course in Geology: Vol **9**. American Geophysical Union, 28th Internatl Geol. Cong. Washington, 127p.
- Anderton, R., 1976. Tidal-shelf sedimentation: An example from the Scottish Dalradian. *Sedimentology*, **23**, 429-458.
- Armstrong, N.V., 1980. The geology and geochemistry of the Nsuze Group in northern Natal and the southeastern Transvaal. Unpubl. PhD. thesis, **1**, Univ. Natal, Pietermaritzburg, 386p.
- , Hunter, D.R., and Wilson, A.H., 1982. Stratigraphy and petrology of the Archaean Nsuze Group, northern Natal and southeastern Transvaal, South Africa. *Precambrian Res.*, **19**, 75-107.
- , Wilson, A.H. and Hunter, D.R., 1986. The Nsuze Group, Pongola Sequence, South Africa: Geochemical evidence for Archaean volcanism in a continental setting. *Precambrian Res.*, **34**, 175-203.
- Armstrong, R.A., Bristow, J.W. and Cox, K.G., 1984. The Rooi Rand dyke swarm, southern Lebombo. **IN**; Petrogenesis of the volcanic rocks of the Karoo Province. Erlank A.J. (ed). *Spec. Publ. Geol. Soc. S. Afr.*, **13**, 77-86.

- Barton, J.M., Jr., Hunter, D.R., Jackson, M.P.A. and Wilson, A.C., 1983. Geochronologic and Sr-isotopic studies of certain units in the Barberton granite-greenstone terrane, Swaziland. *Trans. Geol. Soc. S. Afr.*, **86**, 71-80.
- Becker, G.F., 1893. Finite homogeneous strain, flow and rupture of rocks. *Geol. Soc. Am. Bull.*, **4**, 13-90. *Cited in* Price, N.J. and Cosgrove, J.W., 1990. *Analysis of geological structures*. Cambridge Univ. Press, Lond., 502p.
- Beukes, N.J., 1973. Precambrian iron-formations of southern Africa. *Econ. Geol.*, **68**, 960-1004.
- , 1983. Palaeoenvironmental setting of iron-formations in the depositional basin of the Transvaal Supergroup, South Africa. **IN**; *Iron-formation: Facts and problems*. *Developments in Precambrian geology*; **6**. Trendall, A.F. and Morris, R.C. (eds). Elsevier, Amsterdam, 131-210.
- and Cairncross B., 1991. A lithostratigraphic-sedimentological reference profile for the Late Archaean Mozaan Group, Pongola Sequence: application to stratigraphy and correlation with the Witwatersrand Supergroup. *S. Afr. J. Geol.*, **94**, 44-69.
- Boggs, S. (Jr.), 1987. *Principles of sedimentology and stratigraphy*. Merrill, Columbus, Ohio, 784p.
- Boulton, G.S., 1978. Boulder shapes and grain-size distributions of debris as indicators of transport paths through a glacier and till genesis. *Sedimentology*, **25**, 773-799.
- Boyle, R.W., 1979. The geochemistry of gold and its deposits. *Geol. Surv. Canada Bull.*, **280**, 584p.
- Burger, A.J. and Coertze, F.J., 1973. Radiometric age measurements on rocks from southern Africa to the end of 1971. *Bull. Geol. Surv. S. Afr.*, **58**, 46p.
- Burke, K., Kidd, W.S.F. and Kusky, T.M., 1985. The Pongola structure of southeastern Africa: The world's oldest rift? *J. of Geodynamics*, **2**, 35-49.
- Button, A., 1981. The Pongola Group. 501-510. **IN**; *Precambrian of the southern hemisphere*. D.R. Hunter (ed). Elsevier Scientific Publishing Co., Amsterdam, 882p.
- Carey, St.N. and Sigurdsson, H., 1980. The Roseau Ash: Deep-sea tephra deposits from a major eruption on Dominica, Lesser Antilles Arc. *J. Volcanol. Geotherm. Res.*, **7**, 67-86. *Cited in* Heinrichs, T. 1984. The Umsoli Chert, turbidite testament for a major phreatoplinian event at the Onverwacht/Fig Tree transition (Swaziland Supergroup, Archaean, South Africa). *Precambrian Res.*, **24**, 237-283.
- Carney, M.D., 1984. An investigation into the banded iron-formation and associated lithologies of the Pongola Sequence, east of Paulpietersburg. Unpubl. Honours project, Univ. Natal. Pietermaritzburg, 64p.

- Carter, N.G., 1964. The geology of an area between the Pongola And Mozaan Rivers, S.E. Transvaal. Unpubl. MSc. thesis. Univ. of Natal. Durban, 144p.
- Christie-Blick, N. and Biddle, K.T., 1985. Deformation and basin formation along strike-slip faults. **IN**; Strike-slip deformation, basin formation, and sedimentation. Biddle, K.T. and Christie-Blick, N. (eds). Spec. Publ. Soc. Econ. Paleont. Mineral., **37**, 1-34.
- Cloud, P., 1983. Banded iron-formation. **IN**; Iron-formation: Facts and problems. Developments in Precambrian geology. Trendall, A.F. and Morris, R.C. (eds). Elsevier, Amsterdam, **6**, 401-416.
- Cluckey, E.C., Kulhawy, F.H., Liu, P.L-F. and Tate, G.B., 1985. The impact of wave loads and pore-water pressure generation on initiation of sediment transport. *Geomarine Letters*, **5**, 177-183. *Cited in* Hill, P.R. and Nadeau, O.C. 1989. Storm domination on the inner shelf of the Canadian Beaufort Sea. *J. Sed. Pet.*, **59**, 455-468.
- Collinson, J.D. and Thompson, D.B., 1989. Sedimentary structures. 2nd edition. Unwin Hyman, Lond., 207p.
- Davies, R.D., Allsop, H.L., Erlank, A.J. and Manton, W.I., 1970. Sr-isotopic studies on various layered mafic intrusions in southern Africa. *Spec. Publ. Geol. Soc. S. Afr.*, **1**, 576-593.
- Davis, G.H., 1984. Structural geology of rocks and regions. John Wiley and Sons, New York, 492p.
- Dia, A., Allegre, C.J. and Erlank A.J., 1990. The development of continental crust through geological time: The South African case. *Earth Planet. Sci. Lett.*, **98**, 74-89.
- Duke, W.L., Arnott, R.W.C. and Cheel, R.J., 1991. Shelf sandstones and hummocky cross-stratification: New insights on a stormy debate. *Geology*, **19**, 625-628.
- Eichler, J., 1976. Origin of the Precambrian banded iron-formation. **IN**; Handbook of strata-bound and stratiform ore deposits. **7**, Wolf, K.H. (ed). Elsevier, New York, 157-201.
- Ellis, P.G. and McClay, K.R., 1988. Listric extensional fault systems - results of analogue model experiments. *Basin Research*, **1**, 55-70.
- Eriksson, K.A. and Soegaard, K., 1985. The petrology and geochemistry of Archaean and Early Proterozoic sediments: Implications for crustal compositions and surface processes. *Geol. Surv. Finland*, **331**, 7-32.
- Fraser, G.S., 1989. Clastic depositional sequences. Processes of evolution and principles of interpretation. Prentice Hall. Eaglewood Cliffs, New Jersey, 459p.

- Freund, R., 1970. Rotation of strike slip faults in Sistan, southeast Iran. *J. Geol.*, **78**, 188-200.
- Gadow, S. and Reineck, H-E., 1969. Ablandiger Sandtransport bei Sturmfluten. *Senckenbergiana Maritima*, **50**, 63-78.
- Galloway, W.E. and Hobday, D.K., 1983. Terrigenous clastic deposits. Applications to petroleum, coal, and uranium exploration. Springer-Verlag, New York, 423p.
- Geological Survey, Swaziland, 1968. 1:50 000 geological series, 2nd edition. Sheets 2631 BA, CC, CD, DA, DC. Crown copyright.
- , 1980. 1:50 000 geological series, 3rd edition. Sheets 2631 CA, CD and 2731 AA, AB. Government of Swaziland, Mbabane.
- , 1982. 1:250 000 geological map of Swaziland. Government of Swaziland, Mbabane.
- Gibbs, A.D., 1984. Structural evolution of extensional basin margins. *J. Geol. Soc. Lond.*, **141**, 609-620.
- Gold, D.J.C., 1991. Strike-slip shearing (D3) in the Pongola Sequence, east of Paulpietersburg. Extended Abst; Conference on Precambrian sedimentary basins of southern Africa. Terra abst supplement 3 to Terra Nova volume 3. Blackwell Scientific Publications, Oxford, 34p.
- Grandstaff, D.E., Edelman, M.J., Foster, R.W., Zbinden, E. and Kimberly, M.M., 1986. Chemistry and mineralogy of the Precambrian palaeosols at the base of the Dominion and Pongola Groups (Transvaal, South Africa). *Precambrian Res.*, **32**, 97-131.
- Gravenor, C.P., Von Brunn, V. and Dreimanis, A., 1984. Nature and classification of water lain glaciogenic sediments, exemplified by Pleistocene, Late Paleozoic and Late Precambrian deposits. *Earth-Science Reviews*, **20**, 105-166.
- Groenewald, P.B., 1984. The lithostratigraphy and petrogenesis of the Nsuze Group, northwest of Nkandla, Natal. MSc. thesis. Unpubl. Univ. Natal, Pietermaritzburg, 333p.
- Hammerbeck, E.C.I., 1977. The Usushwana Complex in the southeastern Transvaal, with special reference to its economic mineral potential. Unpubl. PhD. thesis, Univ. Pretoria, 226p.
- Harris, L.B., 1987. A tectonic framework for the Western Australian shield and it's significance to gold mineralization: A personal view. **IN**; Recent advances in understanding Precambrian gold deposits. Ho, S.E. and Groves, D.I. (eds). Univ. Western Australia publ., **11**, 1-27.

- Hatfield, R.A., 1990. The geology and structure of the Pongola Sequence east of Piet Retief, southeastern Transvaal. Unpubl. MSc. thesis. Univ. Natal, Pietermaritzburg, 109p.
- Heckel, P.H., 1972. Recognition of ancient shallow marine environments. 226-286. **IN**; Recognition of ancient sedimentary environments. Rigby, J.K. and Hamblin, W.K. (eds). Soc. Econ. Paleontologists and Mineralogists Spec. Publ. **16**, 340p.
- Hegner, E., Kröner, A. and Hofmann, A.W., 1984. Age and isotope geochemistry of the Archaean Pongola and Usushwana suites in Swaziland, southern Africa: A case for crustal contamination of mantle-derived magma. *Earth Planet. Sci. Lett.*, **70**, 267-279.
- Heinrichs, T., 1984. The Umsoli Chert, turbidite testament for a major phreatoplinian event at the Onverwacht/Fig Tree transition (Swaziland Supergroup, Archaean, South Africa). *Precambrian Res.*, **24**, 237-283.
- Hepworth, J.V., 1973. A photogeological investigation of the Ancient Gneiss Complex and the Mozaan of Swaziland. Institute of Geological Sciences, Overseas Division, Swaziland. Report **20**, 23p.
- Hill, P.R. and Nadeau, O.C., 1989. Storm-dominated sedimentation on the inner shelf of the Canadian Beaufort Sea. *J. Sed. Pet.*, **59**, 455-468.
- Hobday, D.K. and Von Brunn, V., 1976. Evidence for anomalously large tidal ranges in the early Precambrian Pongola Supergroup. *S. Afr. J. Sci.*, **72**.
- Humphrey, W.A. and Krige, L.J., 1931. The geology of the country south of Piet Retief: An explanation of sheet No. 68 (Piet Retief). *Geol. Surv. of S. Afr.*, Govt printer, Pretoria, 72p.
- Hunter, D.R., 1953. **IN**; Ann. Rep. Geol. Surv. Dept., Swaziland, 26p.
- , 1961. The geology of Swaziland. *Geol. Surv. and Mines Dept, Swaziland*, 104p.
- , 1963. The Mozaan Series in Swaziland, 5-16. **IN**; *Geol. Surv. and Mines Dept, Swaziland. Bulletin*, **3**, 53p.
- , 1968. The Pre-Cambrian terrain in Swaziland with particular reference to the granite rocks. Unpubl. PhD thesis, Univ. Witwatersrand, Johannesburg, 273p.
- , 1970a. The Ancient Gneiss Complex in Swaziland. *Trans. Geol. Soc. S. Afr.*, **LXIII**, 107-150.
- , 1970b. The Usushwana Complex in Swaziland. *Spec. Publ. Geol. Soc. S. Afr.*, **1**, 645-660.

- , 1974. Crustal development in the Kaapvaal Craton, Part II, the Proterozoic. Econ. Geol. Res. unit, Univ. Witwatersrand, Info. Circ., **74**, 25p.
- , 1991. Excursion guide for the Pongola Sequence. Conference on Precambrian sedimentary basins of southern Africa. Sedimentology division, Geol. Soc. S. Afr., 17p.
- ✓----- and Wilson, A.H., 1988. A continuous record of Archaean evolution from 3.5 Ga to 2.6 Ga in Swaziland and northern Natal. S. Afr. J. Geol., **91**, 57-74.
- Isherwood, C.H.J., 1979. An interpretation of a portion of the central Mozaan basin, south east Transvaal. Unpubl. Honours project, Univ. of Natal, Pietermaritzburg, 41p.
- Jaeger, J.G. and Cook, N.G.W., 1979. Fundamentals of rock mechanics. 3rd edition. Chapman and Hall, Lond., 585p.
- Jensen, J.S., 1976. A new cation plot for classifying subalkaline volcanic rocks. Ontario Division Mines, Misc. Pap., No. **66**.
- Johnson, M.R., 1987. Guidelines for standardised lithostratigraphic descriptions. Circular **1**. South African Committee for Stratigraphy (SACS). Geological Survey, Department of Mineral and Energy Affairs, 19p.
- Kamo, S.L., Davis, D.W. and de Wit, M.J., 1990. U-Pb geochronology of Archaean plutonism in the Barberton region, S. Africa: 800 Ma of crustal evolution (abst): 7th International Conference on Geochronology, Cosmochronology and Isotope Geology, Abst, Canberra, 53p.
- Klein, G. de V., 1982. Probable sequential arrangement of depositional systems on cratons. Geology, **10**, 17-22.
- Lapidus, D.F., 1990. Collins dictionary of geology. Collins, Lond., 565p.
- Laskowski, N. and Kröner, A., 1985. Geochemical characteristics of Archaean and Late Proterozoic to Palaeozoic fine-grained sediments from southern Africa and significance for the evolution of the continental crust. Geologische Rundschau, **74**, 1-9.
- Leedal, G.P. and Walker, G.P.L., 1954. Tear faults in the Barensmore area, Donegal. Geol. Mag., **91**, 116-120.
- Linström, W., 1987. Die geologie van die gebied Vryheid. Toeligting van blad 2730. Department van Mineraal- en Energiesake. Pretoria, Rep. S. Afr., 48p.
- Lowe, D.R., 1982. Sediment gravity flows, II. Depositional models with special reference to the deposits of high density turbidity currents. J. Sed. Pet., **52**, 279-297.

- Maitre, R.W., 1976. The chemical variability of some common igneous rocks. *J. Pet.*, **17**, 589-637.
- Martin McB, D., Stanistreet, I.G. and Camden-Smith, 1989. The interaction between tectonics and mudflow deposits within the Main Conglomerate Formation in the 2.8-2.7 Ga Witwatersrand basin. *Precambrian Res.*, **44**, 19-38.
- Matthews, P.E., 1967. The pre-Karoo formations of the White Umfolozi Inlier, northern Natal. *Trans. Geol. Soc. S. Afr.*, **70**, 39-64.
- , 1985. Archaean post-Pongola granites in the southeastern Kaapvaal Craton. *S. Afr. J. Sci.*, **81**, 479-484.
- , 1987. Tectonic evolution of a Late Archaean Pongola aulocogen and deformed epicratonic basin in southeastern Africa. Abst: The annual congress of the tectonics division of the Geological Society of South Africa. Rand Afrikaans Univ. (Johannesburg), 95-96.
- , 1990. A plate tectonic model for the Late Archaean Pongola Supergroup in southeastern Africa. **IN**; *Crustal Evolution and Orogeny*. Sychanthavong S.P.H. (ed). Oxford Publ., New Delhi, 41-73.
- , 1991. A transpressional tectonic model for regional deformation and emplacement of granites within the Late Archaean Pongola aulocogen in southeastern Africa. Extended Abst; Conference on Precambrian sedimentary basins of southern Africa. Terra abst supplement **3** to Terra Nova volume **3**. Blackwell Scientific Publications, Oxford, 34p.
- and Scharrer, R.H., 1967. A graded unconformity at the base of the early Precambrian Pongola system. *Trans. Geol. Soc. S. Afr.*, **71**, 257-271.
- McCourt, S. and van Reenen, D., 1992. Structural geology and tectonic setting of the Sutherland greenstone belt, Kaapvaal Craton, South Africa. *Precambrian Res.*, **55**, 93-110.
- and Vearncombe, 1987. Shear zones bounding the central zone of the Limpopo mobile belt, southern Africa. *J. Struct. Geol.*, **9**, 127-137.
- and -----, 1992. Shear zones of the Limpopo belt and adjacent granitoid-greenstone terranes: Implications for late Archaean collision tectonics in southern Africa. *Precambrian Res.*, **55**, 553-570.
- McKay, J.C., 1991. Personal communication, Lonrho head office, Parktown, Johannesburg.
- McLennan, S.M. and Taylor, S.R., 1983. Geochemical evolution of Archaean shales from South Africa. **1**. The Swaziland and Pongola Supergroups. *Precambrian Res.*, **22**, 93-124.

- Mel'nik, Y.P., 1982. Precambrian banded iron-formations: Physiochemical conditions of formation. *Developments in Precambrian geology*; **5**. Elsevier, Amsterdam, 310p.
- Mendonidis, P., 1979. A structural study of a portion of the central Mozaan basin in the vicinity of the Klipwal mine, southeastern Transvaal. Unpubl. Honours project, Univ. of Natal, Pietermaritzburg, 77p.
- Miall, A.D., 1977. A review of the braided river depositional environment. *Earth Sci. Rev.*, **13**, 1-62.
- Monaco, P., 1992. Hummocky cross-stratified deposits and turbidites in some sequences of the Umbria-Marche area (central Italy) during the Toarcian. *Sed. Geol.*, **77**, 123-142.
- Moore, J.G. and Peck, D.L., 1962. Accretionary lapilli in volcanic rocks of the western continental United States. *J. Geol.*, **70**, 182-193.
- Neall, F.B., 1987. Sulphidation of iron-rich rocks as a precipitation mechanism for large Archaean gold deposits in Western Australia: Thermodynamic confirmation. 265-269. **IN**; Recent advances in understanding Precambrian gold deposits. Ho, S.E. and Groves, D.I. (eds). Univ. Western Australia publ., 368p.
- Nelson, C.H., 1982. Modern shallow water graded sand layers from storm surges, Beiring Shelf: A mimic of Bouma sequences and turbidite systems. *J. Sed. Pet.*, **52**, 537-545.
- Nesbitt, H.W., Young, G.M., 1982. Early Proterozoic climates and plate motions inferred from major element chemistry of lutites. *Nature*, **299**, 715-717.
- Nio, S.D. and Nelson, C.H., 1982. The North Sea and northeastern Beiring Sea: A comparative study of the occurrence and geometry of sand bodies of two shallow epicontinental shelves. *Geol. en Mijnbou*, **61**, 105-114.
- Nur, A., Ron, H. and Scotti, O., 1986. Fault mechanics and the kinematics of block rotations. *Geology*, **14**, 746-749.
- Partington, G.A., 1987. The tectonic environments of gold deposition and intrusion of rare metal pegmatites: Implications for Au, Sn and Ta exploration in the Yilgarn Block, Western Australia. **IN**; Recent advances in understanding Precambrian gold deposits. Ho, S.E. and Groves, D.I. (eds). Univ. Western Australia publ., 67-83.
- Preston, V.A., 1987. The geology and geochemistry of the Mpongoza inlier, northern Natal. Unpubl. MSc. thesis. Univ. Natal, Pietermaritzburg, 282p.
- Price, N.J. and Cosgrove, J.W., 1990. Analysis of geological structures. Cambridge Univ. Press, Lond., 502p.

- Ramsay, J.G., 1967. Folding and fracturing of rocks. McGraw Hill, Lond., 568p.
- , 1980. Shear zone geometry: a review. *J. Struct. Geol.*, **2**, 83-99.
- and Huber, M.I., 1983. The techniques of modern structural geology. 1. Strain Analysis. Academic Press, Lond., 308p.
- and -----, 1987. The techniques of modern structural geology. 2. Folds and fractures. Academic Press, Lond., 309-700.
- Reineck, H-R and Singh, I.B., 1972. Genesis of laminated sand and graded rhythmites in storm-sand layers of shelf mud. *Sedimentology*, **18**, 123-128.
- and -----, 1980. Depositional sedimentary environments. 2nd edition. Springer-Verlag, New York, 549p.
- Riganti, A., 1991. The geology of the north-western portion of the Usushwana Complex, south-eastern Transvaal. Unpubl. MSc thesis, Rhodes Univ., 133p.
- Robert, F., 1991. Greenstone gold and crustal evolution. GAC NUNA Research Conference. *Geoscience Canada*, **18**, 83-86.
- Roering, C.R., 1968. Non-orogenic granites and the age of the Precambrian Pongola Sequence. *Econ. Geol. Res. Unit, Univ. Witwatersrand, Johannesburg, Info. Circ. No. 46*.
- Romberg, S.B., 1990. Transport and deposition of gold in hydrothermal systems. **IN**; NUNA conference on Greenstone gold and crustal evolution. Robert, F., Sheahan, P.A. and Green, S.B. (eds). *Geol. Assoc. of Canada Min. Dep. Div. 61-66*.
- Russell, J.A., 1985. A mineralogical investigation of the gold ore of the Klipwal Mine near Piet Retief. Unpubl. MSc thesis, Rand Afrikaans University, Johannesburg, 112p.
- SACS (South African Committee for Stratigraphy), 1980. Stratigraphy of South Africa. Part 1 - (Comp. L.E. Kent). Lithostratigraphy of the Republic of South Africa, Southwest Africa/Namibia and the Republics of Bophuthatsawana, Transkei and Venda. *Handb. Geol. Surv. S. Afr.*, **8**.
- Schemerhorn, L.J.G., 1974. Late Precambrian mixtites: Glacial and/or nonglacial? *Am. J. Sci.*, **274**, 673-824.
- , 1975. Tectonic framework of Late Precambrian supposed glaciers. **IN**: Ice Ages: Ancient and modern. 241-274. Wright, A.E. and Mosely, F. (eds). *Geol. J. Spec. Issue 6*, Seel House Press, Liverpool.

- Sibson, R.H., 1990. Fault structure and mechanics in relation to greenstone gold deposits. **IN**; NUNA conference on Greenstone gold and crustal evolution. Robert, F., Sheahan, P.A. and Green, S.B. (eds). Geol. Assoc. of Canada Min. Dep. Div., 54-60.
- Sleigh, D.W.W., 1988. The geology of the Archaean terrane in the Piet Retief district, Transvaal. Unpubl. MSc. thesis, Univ. Natal, Pietermaritzburg, 208.
- Smith, R.G., 1987. Geochemistry and structure of the Archaean granitoid-supracrustal terrane, southeastern Transvaal and northern Natal. Unpubl. PhD. thesis, Univ. Natal, Pietermaritzburg, 305p.
- Squyres, S.W., Anderson, D.W., Nedell, S.S. and Whorton, R.A., 1991. Lake Hoare, Antarctica: Sedimentology through a thick perennial ice cover. *Sedimentology*, **38**, 363-379.
- Stanistreet, I.G., Martin McB, D., Spencer, R. and Beneke, D., 1988. The importance of diamictites in the understanding of the tectonics and sedimentology of the Witwatersrand basin. 22nd Earth Sci. Cong. of the Geol. Soc. S. Afr., Abst, Durban, 607-610.
- Stanton, R.L., 1972. Ore petrology. McGraw Hill Publishers, 710p. *Cited in* Russel, J.A., 1985. A mineralogical investigation of the gold ore of the Klipwal Mine near Piet Retief. Unpubl. MSc thesis, Rand Afrikaans University, Johannesburg, 112p.
- Stride, A.H., Belderson, R.H., Kenyon, N.H. and Johnson, M.A., 1982. Offshore tidal deposits: Sandsheet and sand bank facies. **IN**; Offshore tidal sands. Processes and deposits. Stride, A.H. (ed). Chapman and Hall, Lond., 95-125.
- Swift, D.J.P., 1975. Tidal sand ridges and shoal-retreat massifs. *Marine Geol.*, **18**, 105-134.
- , 1976. Coastal sedimentation. **IN**; Marine sediment transport and environmental management. Stanley, D.J. and Swift, D.J.P. (eds). John Wiley and Sons, New York. 255-310.
- , Stanley, D.J. and Curray, J.R., 1971. Relict sediments on continental shelves: A recommendation. *J. Geol.*, **79**, 322-346.
- and Field, M.E., 1981. Evolution of a classic sand ridge field: Maryland sector, North American inner shelf. *Sedimentology*, **28**, 461-482.
- Sylvester, A.G., 1988. Strike-slip faults. *Geol. Soc. Am. Bull.*, **100**, 1666-1703.
- Talbot, C.J., Hunter, D.R. and Allen, A.R., 1987. Deformation of the Assagai supracrustals and adjoining granitoids, Transvaal, South Africa. *J. Struct. Geol.*, **9**, 1-12.

- Tazieff, H., 1970. Mechanisms of ignimbrite eruption. **IN**; Mechanism of igneous intrusion. Newall, G. and Rast, N. (eds). Gallery Press, Liverpool, 157-164.
- Thatcher, W. and Hill, D.P., 1991. Fault orientations in extensional and conjugate strike-slip environments and their implications. *Geology*, **19**, 1116-1120.
- Trumbull, R.B., 1990. The age, petrology and geochemistry of the Archean Sinceni pluton and associated pegmatites in Swaziland: A study of magmatic evolution. Unpubl. PhD thesis, Technical University of Munich, 147p.
- Van Vuuren, C.J., 1965. Die geologie van 'n gebied suid van Amsterdam - Oos Transvaal. Unpubl. MSc thesis, Univ. of the Orange Free State, Bloemfontein. *Cited in* Weilers, B.F., 1990. A review of the Pongola Supergroup and its setting on the Kaapvaal Craton. Econ. Res. Unit, Univ. Witwatersrand, Info. Circ., **228**, 69p.
- Verbeek, J.A., 1991. The geology and geochemistry of the Archaean terrane, southeast of Piet Retief, Transvaal. Unpubl. PhD. thesis. Univ. Natal, Pietermaritzburg, 261p.
- Visser, H.N., Krige, L.J. and Truter, F.C., 1947. The geology of the area south of Ermelo. An explanation of sheet 64 (Ermelo). *Geol. Surv. S. Afr.*, 102p.
- Visser, J.N.J., 1983. Glacial-marine sedimentation in the Late Palaeozoic Karoo Basin, southern Africa. **IN**: Glacial marine sedimentation, 667-701. Molnia, B.F. (ed.), Plenum Press, New York.
- , 1989. The Permo-Carboniferous Dwyka Formation of southern Africa: deposition by a predominantly subpolar marine ice shelf. *Palaeogeog., Palaeoclim., Plaeoecol.*, **70**, 377-391.
- Von Brunn, V., 1974. Tidalites of the Pongola Supergroup (Early Precambrian) in the Swart-Mfolozi area, northern Natal, 108-122. **IN**; Precambrian Research Unit, Bull. **15**. Kröner A. (ed), 213p.
- , 1981. Sedimentary facies related to late Paleozoic (Dwyka) deglaciation in the eastern Karoo Basin, South Africa. **IN**; Gondwana Five: Selected papers and abstracts of papers presented at the fifth International Gondwana Symposium. Cresswell, M.M. and Vella, P. (eds). Balkema, Rotterdam, 117-124.
- , 1987. A facies analysis of Permo-Carboniferous glacial deposits along a paleoscarp in northern Natal, South Africa. **IN**; Gondwana six: Stratigraphy, sedimentology, and paleontology. McKenzie, G.D. (ed). Geophysical monograph, **41**, 113-122.
- and Hobday, D.K., 1976. Early Precambrian tidal sedimentation in the Pongola Supergroup of South Africa. *J. Sed. Pet.*, **46**, 670-679.

- and Mason, T.R., 1977. Siliciclastic-carbonate tidal deposits from the 3000 Ma Pongola Supergroup, South Africa. *Sedim. Geol.*, **18**, 245-255.
- and Gold, D.J.C., 1992. Diamictite in the Archaean Pongola Sequence southeast of Piet Retief. Extended abst, 24th Congress of the Geological Society of South Africa.
- and -----, 1993. Diamictite in the Archaean Pongola Sequence of southern Africa. *J. Afr. Earth Sci.*, **16**, 367-374.
- Walker, R.G., 1984. Shelf and shallow marine sands. **IN**; Facies models, 2nd edition. R.G. Walker (ed). Geoscience Canada reprint Ser. 1, 141-170.
- Watchorn, M.B., 1978. Sedimentology of the Mozaan Group in the southeastern Transvaal and northern Natal. Unpubl. MSc. thesis. Univ. Natal, Pietermaritzburg, 111p.
- , 1979a. Fluvial and tidal sedimentation in the Mozaan basin of the Pongola Supergroup. *Econ. Res. Unit, Univ. Witwatersrand, Info. Circ.*, **138**, 16p.
- , 1979b. A reappraisal of the geology of the western Mozaan basin. *Econ. Res. Unit, Univ. Witwatersrand, Info. Circ.*, **141**, 7p.
- , 1980. Fluvial and tidal sedimentation in the 3000 Ma Mozaan basin, South Africa. *Trans. Geol. Soc. S. Afr.*, **13**, 27-42.
- and Armstrong, N.V., 1980. Contemporaneous sedimentation and volcanism at the base of the early Precambrian Nsuzze Group, South Africa. *Trans. Geol. Soc. S. Afr.*, **83**, 231-238.
- Weilers, B.F., 1990. A review of the Pongola Supergroup and its setting on the Kaapvaal Craton. *Econ. Res. Unit, Univ. Witwatersrand, Info. Circ.*, **228**, 69p.
- Wellman, H.W., 1954. Angle between the principal horizontal stress and transcurrent faults. *Geol. Mag.*, **91**, 407-408.
- Wilcox, R.E., Harding, T.P. and Seely, D.R., 1973. Basic wrench tectonics. *Am. Ass. Pet. Geol. Bull.*, **57**, 74-96.
- Winn, R.D., 1991. Storm deposition in marine sand sheets: Wall Creek Member, Frontier Formation, Powder River Basin, Wyoming. *J. Sed. Pet.*, **61**, 86-101.
- Wolmarans, L.G., 1988. Sheet 2730, Vryheid. 1:250 000 Geological Series, Dept. Min. Energy Affairs, Pretoria.
- Wood, D.S., 1974. Current views of the development of slaty cleavage. *Ann. Rev. Earth and Plan. Sci.*, **2**, 369-400.

Wronkiewicz, D.J. and Condie, K.C., 1987. Geochemistry of Archaean shales from the Witwatersrand Supergroup, South Africa: Source area weathering and provenance. *Geochim. Cosmochim. Acta*, **51**, 2401-2416.

----- and -----, 1989. Geochemistry and provenance of sediments from the Pongola Supergroup, South Africa: Evidence for a 3.0 Ga continental craton. *Geochim. Cosmochim. Acta.*, **53**, 1537-1549.

Zeissink, H.E., 1971. Trace element behaviour in two nickeliferous laterite profiles. *Chem. Geol.*, **7**, 25-36.

APPENDIX 1: Representative thin section descriptions of sedimentary rocks.

ROCK TYPE	SAMPLE N ^o .	MAJOR MINERALS	MINOR MINERALS	COMMENT
Sandstone	ALTQ2	Quartz.	Fe oxide.	Quartz grains are highly strained and are totally re-crystallized. Fe oxide is found at the quartz grain boundaries. The original well rounded shape of the detrital grains are occasionally preserved.
Sandstone	QA 30	Quartz.	White mica, zircon, opaques.	Quartz grains are re-crystallized. There are zones of deformation where quartz has been crushed (there is a high mica concentration in these zones). Fine-grained opaque grains are concentrated around the quartz grain boundaries.
Sandstone	QA 34	Quartz.	Muscovite, opaques, sphene.	Re-crystallization of quartz. Elongate muscovite grains are aligned parallel defining a foliation.
Conglomerate	CC 2	Quartz, chert.	Opagues, Fe oxide, sphene.	Quartz and chert grains are very well rounded with a high degree of sphericity. Some of the quartz grains are highly strained. Very fine-grained matrix of quartz and Fe-rich minerals. Fe oxide found along quartz grain boundaries.
Conglomerate	OG 1	Quartz, chert.	Opagues, white mica, Fe oxide, sphene.	Quartz grains are re-crystallized. Chert grains are very well rounded. Some quartz grains are highly strained.
Diamictite	MS 5b	Quartz.	Chlorite, opaques, lithic fragments.	Grains range in shape and size from very well rounded to very angular. Large range in grain shape. Matrix very fine-grained and is predominantly dark (Fe-rich).
Diamictite	DMS 1	Quartz, chlorite.	Opagues, lithic fragments.	Euhedral opaque grains. Large range in size and shape of grains. Matrix is very fine-grained and comprises of quartz and chlorite.

Thin section descriptions of intrusive rocks.

ROCK TYPE	SAMPLE N ^o .	MAJOR MINERALS	ACCESSORY MINERALS	COMMENT
Dolerite	DB 1	Quartz, clinopyroxene, plagioclase.	Sericite, opaques, chlorite, calcite penninite, carbonate.	Myrmekitic textures and alteration rims of clinopyroxene to chlorite.
Dolerite	DB 2	Clinopyroxene, quartz.	Leucoxene, penninite, chlorite, calcite, white micas, opaques, carbonate.	Saussurite replacement of plagioclase.
Dolerite	DB 3	Orthopyroxene, plagioclase, olivine.	Carbonate, opaques, biotite, antigorite.	Relict plagioclase grains, and alteration of olivine to antigorite.
Dolerite	DB 5	Carbonate, clinopyroxene, quartz, plagioclase.	Calcite, opaques, sericite, chlorite.	Alteration of clinopyroxene grains to carbonate, and of plagioclase to sericite myrmekitic textures.
Dolerite	DB 7	Clinopyroxene, chlorite, quartz.	Epidote, serpentinite, leucoxene, opaques, carbonate, relict plagioclase.	Alteration of clinopyroxene to serpentinite and of relict plagioclase to saussurite.
Dolerite	DB 8	Clinopyroxene, quartz, plagioclase.	Calcite, opaques, carbonate, sericite.	Extensive re-crystallization of quartz and alteration of plagioclase to sericite.
Dolerite	DB 10	Clinopyroxene, carbonate, quartz, chlorite.	Opaques, calcite.	Relict clinopyroxene grains altered to carbonate, myrmekitic textures.
Dolerite	DB 11	Clinopyroxene, quartz, plagioclase, chlorite.	Opaques, white micas, serpentinite, carbonate, orthopyroxene, sericite.	Alteration of plagioclase to saussurite, re-crystallization of quartz, and myrmekitic textures.
Dolerite	DB 15	Clinopyroxene, quartz, chlorite.	Sericite, calcite, epidote, penninite, white micas.	Alteration of clinopyroxene to tremolite, re-crystallization of quartz, myrmekitic textures, relict plagioclase.
Dolerite	DB 16	Clinopyroxene, quartz, plagioclase.	Calcite, carbonate, leucoxene, white micas.	Cross-cutting quartz and brown epidote veins.

Thin section descriptions of intrusive rocks (continued).

ROCK TYPE	SAMPLE N°.	MAJOR MINERALS	ACCESSORY MINERALS	COMMENT
Dolerite	DB 17	Clinopyroxene, chlorite, quartz, plagioclase, carbonate.	Sericite, penninite, leucoxene.	Relict feldspar and myrmekitic textures.
Dolerite	DB 18	Quartz, clinopyroxene.	Carbonate, sericite, leucoxene, epidote, calcite.	Relict feldspar.
Dolerite	DL 1	Plagioclase, clinopyroxene, quartz.	Opagues, epidote, carbonate, sericite.	Anheral and euhedral opaques, minor alteration of clinopyroxene to carbonate.
Dolerite	DL 2	Plagioclase, clinopyroxene, quartz.	Opagues, sericite, biotite.	Rock is very fresh. Myrmekitic textures.
Dolerite	DL 3	Clinopyroxene, plagioclase, quartz.	Opagues, sericite.	Rock is very fresh. Myrmekitic textures, some of the quartz grains show a high degree of strain.
Dolerite	DL 4	Plagioclase, quartz, clinopyroxene.	Sericite, carbonate, opaques.	Re-crystallization of quartz.
Dolerite	DL 5	Plagioclase, clinopyroxene, quartz, orthopyroxene.	Opagues, sericite, white, micas.	Rock is very fresh.
Dolerite	DL 6	Clinopyroxene, plagioclase, quartz.	Opagues, sericite, biotite.	Rock is very fresh, orthopyroxene is intercumulus.
Dolerite	DL 7	Clinopyroxene, plagioclase.	Opagues.	Rock is very fresh.
Sheared dolerite	DB 9.2	Chlorite, quartz, white micas, carbonate, penninite.	Zoisite, opaques, calcite.	Highly strained quartz and re-crystallization of quartz. Rock is phyllonitised.
Sheared dolerite	DB 9.A	Chlorite, quartz, white micas.	Opagues, zoisite, calcite.	Quartz not as strained as DB 9.2, quartz grains are elongated parallel to the shear fabric.

Thin section descriptions of intrusive rocks (continued).

ROCK TYPE	SAMPLE N°.	MAJOR MINERALS	ACCESSORY MINERALS	COMMENT
Sheared dolerite	DB 9.B	Quartz, white mica, carbonate, chlorite.	Calcite, zoisite, opaques.	Quartz is extremely fine grained and granoblastic - some of which is highly strained.
Ultramafic	DB 13	Olivine, orthopyroxene, clinopyroxene, chlorite.	Penninite, opaques, carbonate, white mica, serpentinite.	Alteration of orthopyroxene to serpentinite. Olivine altered to carbonate. Cumulus olivine crystals enclosed in post-cumulus clinopyroxene.
Ultramafic	DB 14	Olivine, orthopyroxene, antigorite.	Opaques, serpentinite, carbonate, mica (white and biotite), serpentinite.	Olivine enclosed in clinopyroxene oikocrysts. Olivine outside the oikocrysts altered to carbonate. Cumulate textures with olivine representing the first cumulus phase. Antigorite replaces olivine crystals.
Altered dolerite	DB 4	Quartz, clinopyroxene, actinolite	Opaques, leucoxene, epidote.	Actinolite alteration from pyroxene (but still retains clinopyroxene in the centre of the crystal).
Altered dolerite	DB 6	Clinopyroxene, actinolite/tremolite, chlorite, quartz.	Penninite, epidote, serpentinite.	Alteration of clinopyroxene to actinolite/tremolite.
Altered dolerite	DB 9	Quartz, carbonate, white micas.	Opaques, epidote, chlorite, penninite.	Re-crystallization of quartz, extensive carbonitization. Presence of well developed fabric which is cross-cut by chlorite/penninite/quartz stringers. Elongate quartz grains are aligned parallel to the fabric.
Altered dolerite	DB 12	Amphiboles (actinolite/tremolite??).	Relict plagioclase phenocrysts.	Rock is too fine grained to allow a detailed analysis.

APPENDIX 2: GEOCHEMISTRY ANALYSES

Major element analyses for the sedimentary rocks in weight percent.

	SiO ₂	Al ₂ O ₃	FeO	MnO	MgO	CaO	Na ₂ O	K ₂ O	TiO ₂	P ₂ O ₅	TOTAL
MS1	50.56	11.54	29.64	0.38	3.3	0.08	0.11	0	0.45	0.07	99.78
MS2	40.81	2.39	45.53	0.92	2.61	0.19	0.11	0.47	0.05	0.11	98.81
MS3	64.32	1.62	28.5	0.42	1.08	0.50	0.04	0.03	0.02	0.04	100.17
MS7	56.30	7.06	27.74	0.11	3.41	0.31	0.44	0.81	0.23	0.05	99.88
MS8	64.95	14.08	12.59	0.03	3.89	0.59	0.01	2.82	0.55	0.04	99.56
MS9	60.50	2.05	29.77	3.27	0.24	0.04	0	0.32	0.05	0.07	99.98
MS10	57.89	17.11	0.04	3.98	0.53	0.9	0.90	2.03	0.65	0.08	99.41
MS11	74.28	10.82	0.01	2.74	0.78	0.02	0	2.38	0.37	0.02	99.55
DMS1	63.48	8.71	19.02	0.10	2.95	0.73	1.07	1.39	0.34	0.04	100.17
DMS5	63.40	8.60	18.99	0.11	2.88	0.62	1.02	1.48	0.34	0.04	99.83
DMS8	60.54	9.07	20.65	0.14	3.15	1.25	0.75	1.76	0.36	0.04	100.27
BIF1	45.60	1.26	46.19	0.09	0.11	0.02	0	0.01	0.02	0.05	99.05

Trace element analyses for the sedimentary rocks in ppm.

Sample	Nb	Y	Rb	Zr	Sr	U	Th	Zn	Cu	Ni	Cr	V	La	Ba	Sc	L.O.I.
MS1	4	21	1	89	3	2	8	70	3	95	338	114	26	0	21	4
MS2	0	15	31	12	5	0	5	6	0	0	70	20	1	400	4	3
MS3	0	6	2	10	10	0	0	6	0	4	41	8	5	62	2	2
MS7	1	10	22	48	29	0	0	31	15	88	273	73	7	122	10	2
MS8	5	17	95	167	26	1	7	35	5	199	682	135	22	450	23	
MS9	1	6	23	13	111	0	2	4	1	20	112	18	2	323	4	1
MS10	9	24	77	136	58	3	13	65	43	168	547	181	35	337	29	
MS11	5	11	72	98	34	1	3	24	5	95	378	79	21	298	15	
DMS1	3	11	86	86	117	1	3	37	20	107	353	84	20	150	12	2
DMS5	3	10	91	88	114	1	3	37	24	111	350	82	20	169	11	2
DMS8	3	11	42	82	137	2	4	38	20	114	363	92	11	300	16	3
BIF1	0	11	4	12	5	0	0	0	0	0	48	14	0	31	2	1

Major element analyses for the intrusive rocks in weight percent.

	SiO ₂	Al ₂ O ₃	FeO	MnO	MgO	CaO	Na ₂ O	K ₂ O	TiO ₂	P ₂ O ₅	TOTAL	Mg/ Mg+Fe
DB1	54.35	14.17	7.74	0.16	9.08	10.78	1.93	0.01	0.41	0.08	99.66	67.64
DB2	56.56	14.39	8.95	0.18	5.17	8.95	3.03	0.67	0.63	0.13	99.77	50.72
DB5	56.12	7.06	9.66	0.25	17.22	5.57	1.3	0.51	0.45	0.08	99.41	76.06
DB7	54.67	13.75	9.59	0.17	5.88	9.79	2.57	1.02	0.95	0.2	99.77	52.21
DB8	55.34	13.10	8.60	0.17	8.61	9.76	2.02	0.52	0.47	0.09	99.74	64.08
DB10	55.18	13.17	10.81	0.18	4.80	8.80	2.75	1.19	1.18	0.26	99.66	44.17
DB11	54.95	13.89	8.45	0.17	7.33	11.12	1.54	0.87	0.31	0.05	99.72	60.72
DB15	55.07	13.81	10.53	0.17	6.98	10.41	1.88	0.34	0.38	0.05	99.61	56.87
DB16	52.53	12.40	12.93	0.18	7.77	9.31	2.63	0.61	0.85	0.13	99.64	54.46
DB17	56.70	13.82	11.69	0.16	4.94	5.97	4.84	0.16	0.80	0.15	99.22	45.70
DB18	53.65	14.97	10.47	0.19	6.76	9.80	1.77	1.31	0.48	0.09	99.49	56.24
DL1	47.81	12.92	14.64	0.22	5.91	9.44	2.69	0.60	3.47	0.36	99.89	41.84
DL2	52.03	13.97	10.95	0.19	6.02	10.11	2.83	0.48	1.48	0.18	99.58	49.49
DL3	52.03	13.78	10.95	0.19	6.24	10.15	2.54	0.47	1.48	0.16	99.35	50.38
DL4	52.08	13.99	10.84	0.18	6.03	10.08	2.56	0.52	1.46	0.17	99.27	49.78
DL5	47.04	13.61	13.24	0.19	9.57	9.05	2.38	0.27	1.96	0.20	99.95	56.29
DL6	47.03	13.42	13.27	0.19	9.29	9.06	2.42	0.27	2.11	0.21	99.46	55.51
DL7	48.41	13.62	12.05	0.18	7.40	11.00	2.50	0.30	2.28	0.22	99.57	52.52
DB3	51.75	13.72	12.00	0.21	5.59	10.39	2.67	0.47	1.38	0.19	99.85	45.36
DB-8L	49.26	15.11	12.96	0.19	5.05	9.76	1.78	2.86	1.04	0.14	98.15	43.69
DB-9.1	53.36	15.64	12.28	0.18	4.96	7.87	0.04	3.88	1.06	0.17	99.44	44.56
DB-9.2	41.97	26.4	15.25	0.04	6.11	1.24	0.05	6.86	0.85	0.07	98.85	44.38
DB-9A	69.04	12.43	10.64	0.01	3.51	0.57	0.03	2.53	0.45	0.03	99.59	39.62
DB13	46.85	5.65	11.31	0.20	29.73	3.94	0.12	0.78	0.14	0.04	99.11	82.41
DB14	44.28	3.36	10.17	0.17	36.52	2.51	0.23	0.13	0.20	0.05	98.87	86.49
DB4	56.68	11.38	9.73	0.16	6.09	8.78	2.71	1.19	0.86	0.16	99.76	55.82
DB6	56.00	11.08	9.66	0.14	6.03	7.47	4.14	1.14	0.91	0.16	99.10	52.66
DB9	46.89	9.45	9.03	0.17	23.84	7.35	0.80	0.22	0.25	0.05	99.47	82.04
DB12	53.99	13.10	9.06	0.16	8.99	9.16	3.19	0.29	0.52	0.09	99.68	63.88

Trace element analyses for the intrusive rocks in ppm.

	Nb	Y	Rb	Zr	Sr	U	Th	Zn	Cu	Ni	Cr	V	La	Ba	Sc	L.O.I
DB1	2	16	0	61	341	0	0	65	35	229	629	181	8	16	31	3
DB2	4	25	21	102	262	1	5	81	46	83	57	195	12	232	29	2
DB3	4	32	12	105	170	2	3	101	171	47	65	306	6	144	36	1
DB5	1	14	21	56	116	0	0	79	45	476	1725	152	12	115	27	2
DB7	4	33	38	144	263	0	0	85	59	124	185	227	11	243	31	2
DB8	2	18	17	68	180	0	0	70	36	187	380	171	15	254	27	2
DB10	5	43	40	183	250	0	0	96	71	87	25	285	10	233	27	1
DB11	1	14	51	39	200	0	0	61	50	121	198	194	13	119	42	1
DB15	0	17	13	44	121	0	1	66	43	111	138	196	5	65	40	
DB16	3	31	17	125	229	0	4	93	432	258	195	245	92	289	35	
DB17	5	33	5	127	205	0	5	59	57	77	12	242	26	74	32	
DB18	2	19	43	74	225	1	2	66	46	138	128	181	16	239	30	
DL1	8	50	18	212	227	0	1	119	452	102	177	412	16	142	30	0
DL2	3	27	13	111	305	2	4	88	159	76	158	306	4	161	30	0
DL3	4	26	13	105	315	0	0	87	140	74	133	302	10	167	32	0
DL4	4	26	11	108	312	0	0	90	151	77	161	306	8	174	29	0
DL5	4	30	7	111	219	0	0	104	272	224	503	279	15	80	26	1
DL6	3	31	8	116	221	0	5	106	290	218	499	283	6	81	26	0
DL7	4	33	8	123	223	0	0	96	286	129	359	357	1	85	37	0
DB-8L	5	34	84	151	231	0	4	102	161	65	19	202	17	273	31	
DB-9.1	5	34	112	151	132	2	4	86	74	80	33	221	18	365	31	
DB-9.2	10	23	218	209	35	3	13	62	19	234	880	205	34	652	30	
DB-9A	4	11	75	139	20	2	6	41	3	136	525	110	18	317	17	
DB13	0	8	32	32	123	0	1	67	16	1192	3418	75	3	79	22	6
DB14	2	6	6	22	48	2	3	57	19	2435	6765	70	4	9	13	6
DB4	6	36	45	146	350	0	5	94	87	267	618	197	7	234	32	2
DB6	7	36	37	155	423	0	3	94	96	204	422	201	20	293	28	1
DB9	1	15	10	31	48	0	3	54	30	1470	2865	115	1	40	27	4
DB12	1	20	8	70	845	0	0	74	13	318	1126	196	8	317	33	2

APPENDIX 3

LOCALITY SITES

Sedimentary rocks

MS1	27° 22' 37"S	31° 11' 05"E
MS2	27° 23' 02"S	31° 13' 53"E
MS3	27° 23' 26"S	31° 09' 42"E
MS7	27° 24' 52"S	31° 13' 28"E
MS9	27° 18' 19"S	31° 09' 18"E
MS10	27° 26' 02"S	31° 16' 23"E
DMS1	27° 24' 36"S	31° 13' 12"E
DMS5	27° 24' 41"S	31° 13' 19"E
DMS8	27° 25' 16"S	31° 12' 26"E
BIF1	27° 22' 44"S	31° 12' 00"E
MS8	Klipwal Mine, level 8	
MS11	Klipwal Mine, level 9	

Igneous rocks

DB1	27° 22' 36"S	31° 10' 28"E
DB2	27° 23' 08"S	31° 10' 00"E
DB3	27° 23' 05"S	31° 10' 00"E
DB4	27° 25' 00"S	31° 12' 30"E
DB5	27° 25' 37"S	31° 12' 42"E
DB6	27° 25' 37"S	31° 12' 37"E
DB7	27° 24' 47"S	31° 13' 18"E
DB8	27° 25' 05"S	31° 13' 39"E
DB9	27° 25' 14"S	31° 13' 44"E
DB10	27° 25' 00"S	31° 13' 51"E
DB11	27° 25' 11"S	31° 14' 00"E
DB12	27° 23' 52"S	31° 15' 00"E
DB13	27° 26' 44"S	31° 16' 27"E
DB14	27° 27' 57"S	31° 16' 48"E
DB15	27° 26' 08"S	31° 16' 32"E
DB16	27° 26' 00"S	31° 16' 26"E
DB17	27° 26' 15"S	31° 16' 26"E
DB18	27° 26' 24"S	31° 16' 34"E
DL1	27° 24' 52"S	31° 09' 42"E
DL2	27° 24' 13"S	31° 10' 34"E
DL3	27° 24' 31"S	31° 12' 18"E
DL4	27° 24' 18"S	31° 12' 18"E
DL5	27° 25' 42"S	31° 14' 09"E
DL6	27° 25' 14"S	31° 14' 14"E
DL7	27° 24' 11"S	31° 16' 32"E
DB-8L	Klipwal Mine, level 8	
DB-9A	Klipwal Mine, level 9	
DB-9.1	Klipwal Mine, level 9.1	
DB-9.2	Klipwal Mine, level 9.2	

APPENDIX 4

SAMPLE PREPARATION AND ANALYTICAL TECHNIQUES

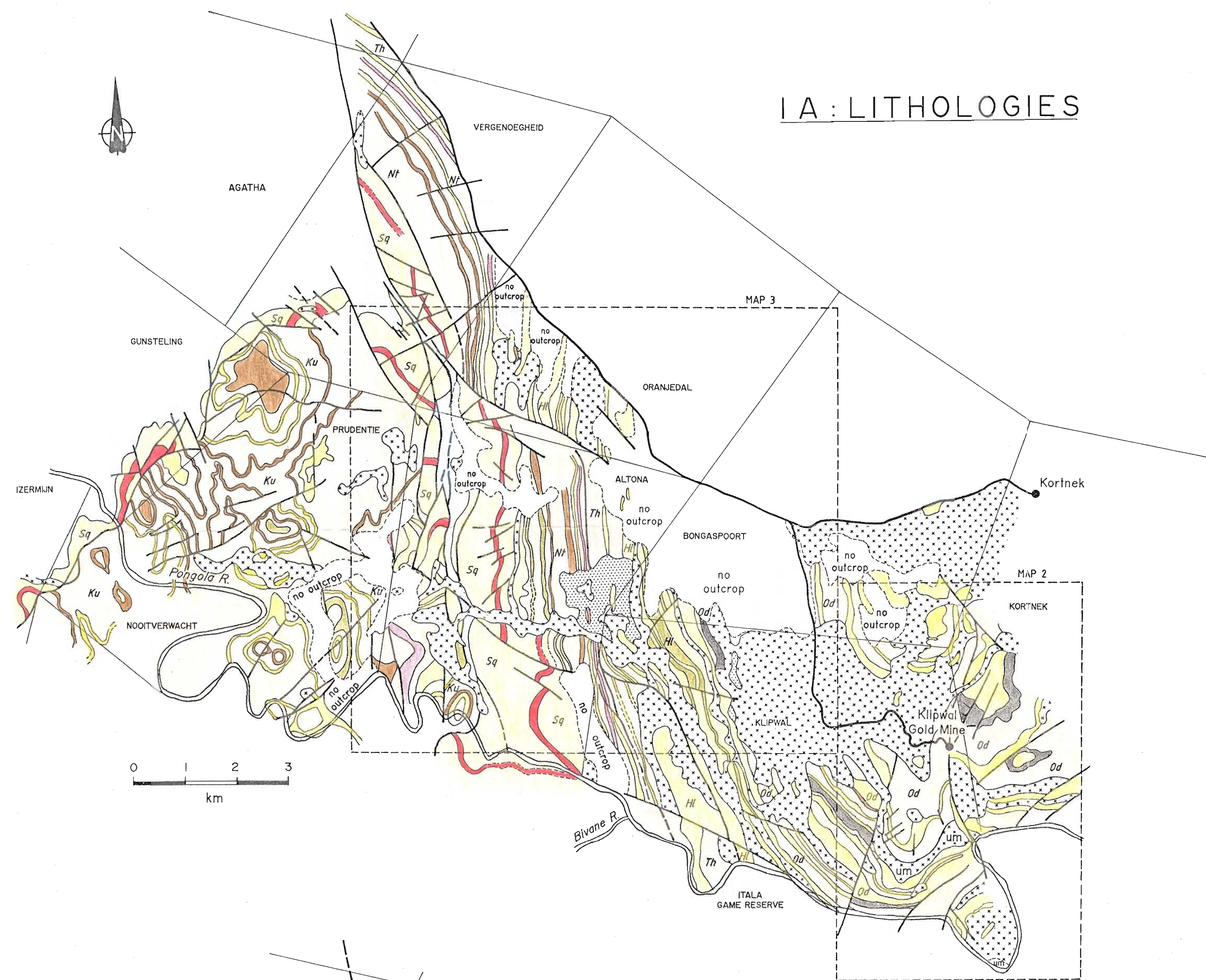
Sixty-two samples from within the study area were collected for analysis by X-ray Fluorescence. For the suite of samples used to chemically constrain the different lithologies an effort was made in the field to collect only fresh material. This was, however, not always possible because of the intensely altered state of the rock types. The sample mass of these samples varied from 2 kg to 10 kg depending on grain-size and the intensity of alteration of the sample. The mass of the samples used to constrain the effects of mineralization and alteration varied between 500 g and 2 kg depending on the thickness of the unit being sampled.

The samples were reduced to fragments of 2 cm to 10 cm in diameter by means of a hydraulic sample splitter. Any weathered or altered portions of the samples were removed as was vein- or joint-plane filling material. The fragments were then scrubbed under running water and cleaned for 2 minutes in an ultrasonic cleaner. They were then rinsed with distilled water and dried in an oven at 100°C for 1 hour. Samples were crushed in a jaw-crusher with hardened steel jaws to fragments smaller than 1 cm in diameter. The jaw-crusher was stripped, scrubbed with a wire brush, vacuumed and washed with acetone between samples. The samples were then reduced to 100 g by the cone-and-quartering technique, and milled to a fine powder in a swing-mill. The swing-mill was cleaned with quartz chips, scrubbed and washed with acetone before each run. This eliminated any form of contamination.

Approximately 8 g of each of the finely milled samples was then mixed with ~0.6 ml Mowiol binding agent and homogenised with an agate mortar and pestle. The samples were pressed into pellets ~5 mm thick under a pressure of 10 tons for ~10 seconds. The pellets were then hardened at 120°C for 4 hours. The milled powders were also fluxed in a platinum crucible at 1000°C for 4 hours to make fusion discs. Approximately 0.4 g of the samples was mixed with ~0.9 g of Spectroflux. The discs were then cast in a brass die and allowed to anneal for ~3 hours at 250°C. The discs were cooled in a desiccation jar.

Major and trace element analyses were undertaken using the Phillips PW 1404 X-Ray Fluorescence Spectrometer in the Department of Geology, University of Natal - Pietermaritzburg. The instrument was calibrated using internationally accepted standards. The detection limits and analytical accuracy of the analyses is as follows;

Element	Tube	KV	Ma	Analysing Line	Analysing Crystal	Collimator	Counter	Peak λ	Count Time Sec.	Background λ	Count Time Sec.	Standard	Blanks	Detection Limits	Analytical Accuracy
SiO ₂	Cr	50	50	Ka	Pet	Coarse	Flow	109.165	60	106.000	30	SiO ₂ 100% NIMD 37.02%		0.004%	0.2%
Al ₂ O ₃	Cr	50	50	Ka	-	-	-	145.040	60	139.160	30	NIML 13.90%	SiO ₂	0.005%	0.5%
Fe ₂ O ₃	Au	50	50	Ka	Lif200	Fine	-	57.525	40	Blank standards used to calibrate background.		NIML 10.28%	SiO ₂ and 60CaO+40SiO ₂	0.001%	0.5%
MnO	Au	50	50	Ka	Lif200	-	-	62.990	40	background.		NIML 0.78%	SiO ₂ and 60CaO+40SiO ₂	0.001%	0.5%
MgO	Cr	50	50	Ka	PX-1	Coarse	-	23.300	60	25.300	30	M-1 6.55%	SiO ₂	0.011%	0.3%
CaO	Cr	50	50	Ka	pet	Fine	-	45.240	40	Blank standards		NIML 3.32%	SiO ₂ and 40Fe ₂ O ₃ 60SiO ₂	0.0003%	0.2%
K ₂ O	Cr	50	50	Ka	Pet	-	-	50.720	40	used to calibrate		M-1 0.65%	SiO ₂ and 60CaO+40SiO ₂	0.0003%	0.2%
TiO ₂	Cr	50	50	Ka	Pet	-	-	36.720	40	background		M-1 1.05%	SiO ₂ and 60CaO+40SiO ₂	0.0004%	0.2%
P ₂ O ₅	Cr	50	50	Ka	Ge	Coarse	-	141.040	60	138.000 143.000	30 30	BR 1.10%	SiO ₂	0.001%	0.2%
Na ₂ O	Cr	50	50	Ka	PX-1	Fine	-	28.170	60	30.000	30	BR 3.12%	SiO ₂	0.018%	2%
Sc	Cr	50	50	Ka	Lif200	-	-	97.730	60	95.850 98.555	30 30	BCR 33 ppm	SiO ₂ and CaCO ₃	0.3 ppm	10%
Ba	Cr	50	50	La	Lif220	-	-	115.275	60	114.500 116.500	30 30	M-1 160 ppm	SiO ₂ and MgO	1 ppm	± 20%
Zn	Au	50	50	Ka	Lif200	-	-	41.795	60	39.65 46.70	30 30	NIMP 100 ppm	SiO ₂ and CaCO ₃	0.3 ppm	± 10%
Cu	Au	50	50	Ka	Lif200	-	-	45.040	50	46.70	30	M-1 110 ppm	SiO ₂ and CaCO ₃	0.2 ppm	± 10%
Ni	Au	50	50	Ka	Lif200	-	-	48.690	60	50.00	30	BR 260 ppm	SiO ₂ and CaCO ₃	0.1 ppm	± 10%
Cr	Au	50	50	Ka	Lif200	-	-	69.375	60	58.10 70.80	30 30	JB1 400 ppm	SiO ₂	0.6 ppm	10%
V	Au	50	50	Ka	Lif220	-	-	123.220	60	117.10 123.80	30 30	M-1 260 ppm	SiO ₂	0.5 ppm	± 10%
La	Au	50	50	Ka	Lif220	-	-	138.920	60	132.60 141.80	30 30	BR 80 ppm	SiO ₂	1.5 ppm	15%
Zr	Rh	50	50	Ka	Lif220	-	Scint	32.045	60	29.30 34.89	30 30	AGV 230 ppm	SiO ₂	0.3 ppm	3%
Sr	Rh	50	50	Ka	Lif220	-	-	35.830	60	34.89 36.90	30 30	M-1 190 ppm	SiO ₂	0.2 ppm	3%
Nb	Rh	50	50	Ka	Lif220	-	-	30.420	60	29.45 34.80	30 30	GSP 23 ppm	SiO ₂	0.1 ppm	3%
Y	Rh	50	50	Ka	Lif220	-	-	33.855	60	29.45 34.80	30 30	NIMG 145 ppm	SiO ₂	0.3 ppm	3%
Rb	Rh	50	50	Ka	Lif220	-	-	37.960	60	34.80 41.10	30 30	NIMG 320 ppm	SiO ₂	0.4 ppm	2%
U	Rh	50	50	Ka	Lif220	-	-	37.300	100	36.50 41.10	30 30	NIMG 15 ppm	SiO ₂	0.1 ppm	20%
Th	Rh	50	50	Ka	Lif220	-	-	39.250	100	36.90 41.10	30 30	GSP 105 ppm	SiO ₂	0.5 ppm	20%



LEGEND

LITHOLOGIES

- Dolerite and ultramafic (um) intrusions
- Diamictite } Dwyka Group
- Diamictite
- Ferruginous mudstone
- Banded iron-formation
- Marker iron-formation
- Mudstone
- Siltstone
- Sandstone
- Volcano-sediments } Nsuze Group

STRUCTURE

- Strike-slip shear zone
- Thrust fault
- Normal fault
- Broad zone of shearing
- Inferred fault
- Antiformal axial trace
- Synformal axial trace
- Overturned fold
- Strike and dip direction of bedding
- Bedding trace
- Lithological contacts

ALTONA

- Farm name
- Road
- River
- Farm boundary

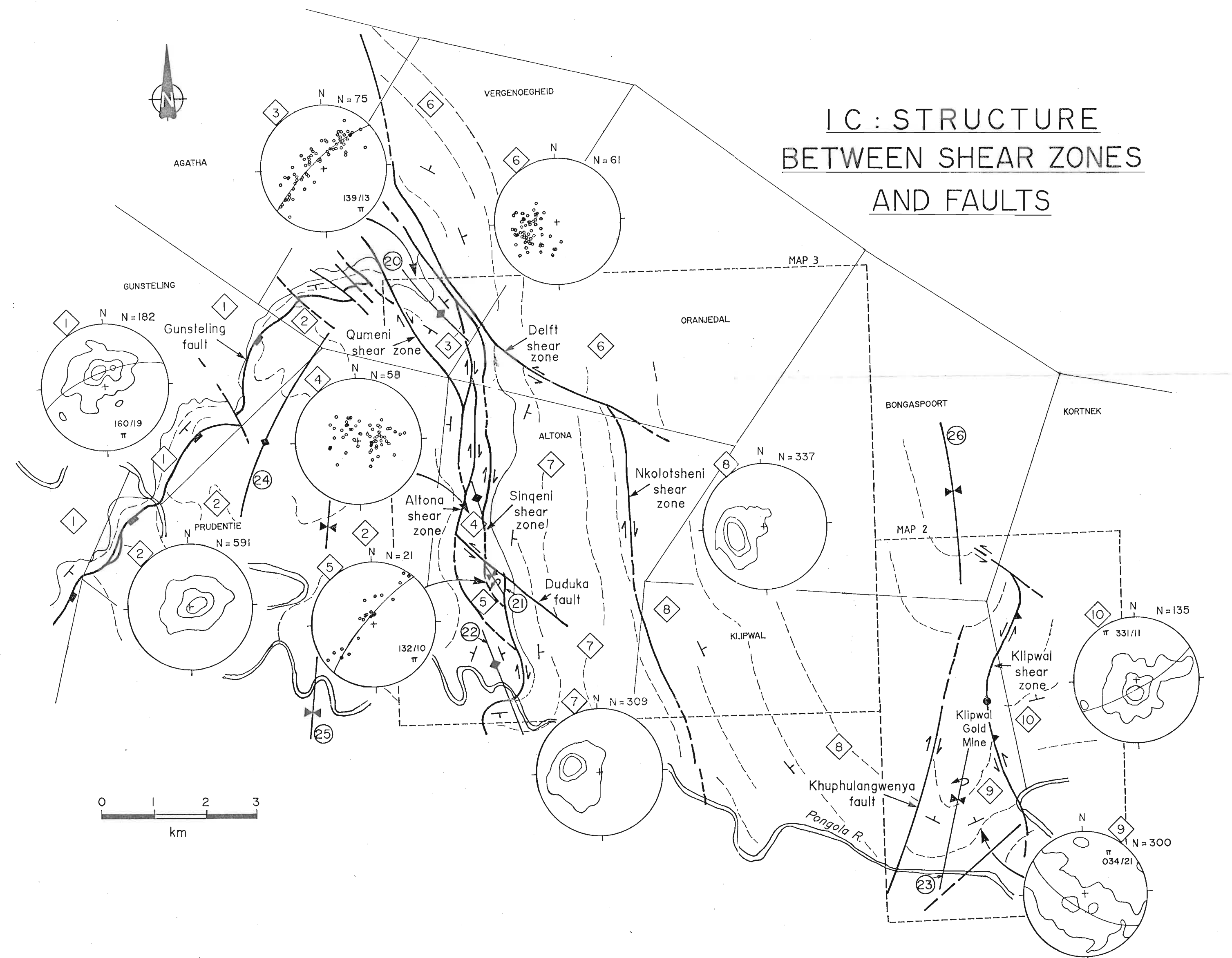
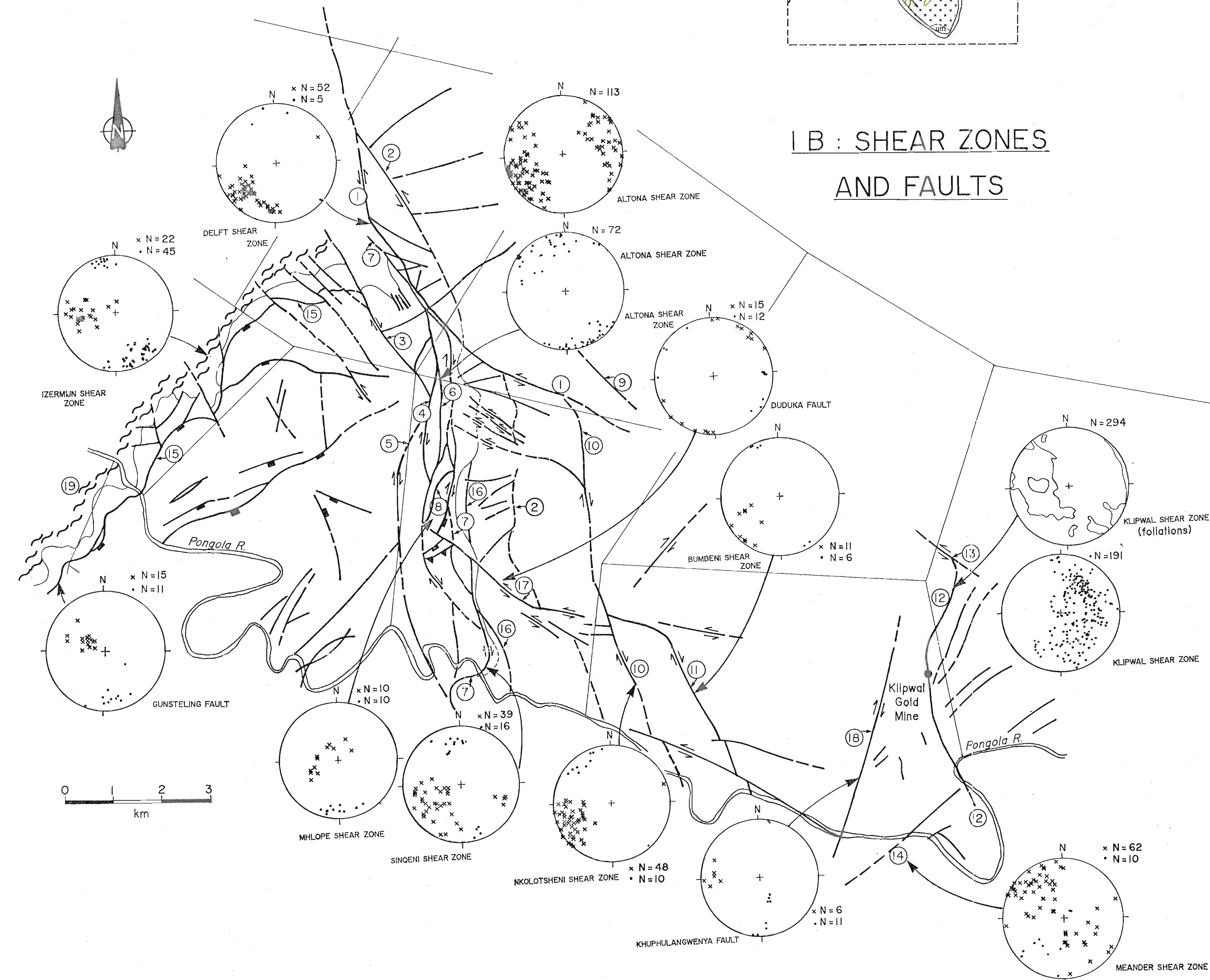
DOMAINS BETWEEN SHEAR ZONES AND FAULTS

- ① Delft shear zone
- ② Vergenoegheid shear zone
- ③ Qumeni shear zone
- ④ Enyabisa shear zone
- ⑤ Mkhuzwa shear zone
- ⑥ Altona shear zone
- ⑦ Sinqeni shear zone
- ⑧ Mhlope shear zone
- ⑨ Mzamba shear zone
- ⑩ Nkolotsheni shear zone
- ⑪ Bumbeni shear zone
- ⑫ Klipwal shear zone
- ⑬ Nkosetsha shear zone
- ⑭ Meander shear zone
- ⑮ Gunsteling fault
- ⑯ Dwaleni fault
- ⑰ Duduka fault
- ⑱ Khuphulangwenya fault
- ⑲ Izermijn shear zone
- ⑳ Bethu anticline
- ㉑ Mfeno syncline
- ㉒ Nombela anticline
- ㉓ Ngwenya syncline
- ㉔ Gunsteling anticline
- ㉕ Prudentie syncline
- ㉖ Tobolsk syncline

STEREOPLOTS

- × Poles to foliation
- Poles to bedding
- Lineation
- π Pi poles
- Contours at 5% intervals
- All contoured stereoplots represent poles to bedding (except where otherwise stated)

<i>Ku</i> Kulphiso Formation	<i>Od</i> Odwaleni Formation
<i>Hl</i> Hlshana Formation	<i>Th</i> Thalu Formation
<i>Nt</i> Ntombe Formation	<i>Sq</i> Sinqeni Formation





LEGEND

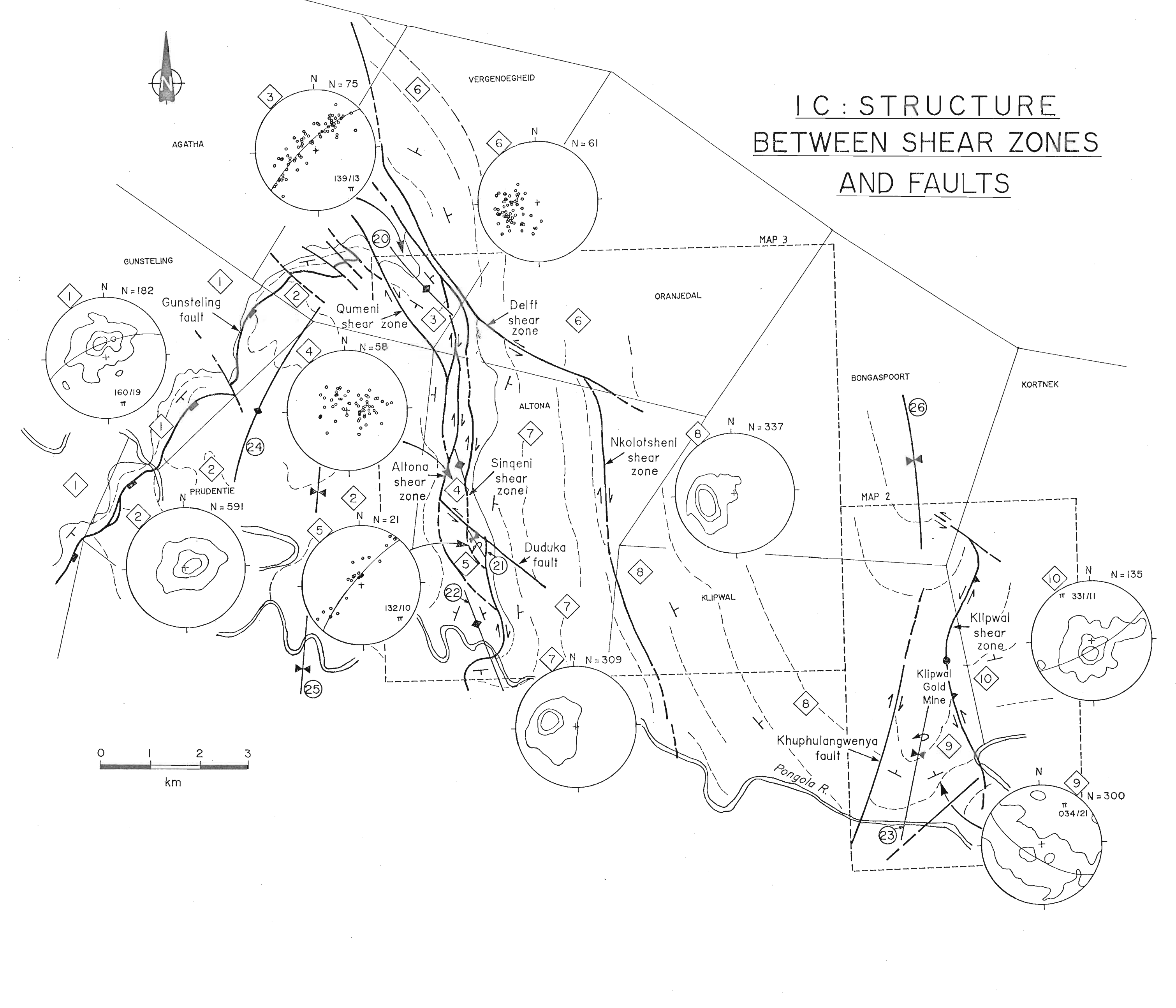
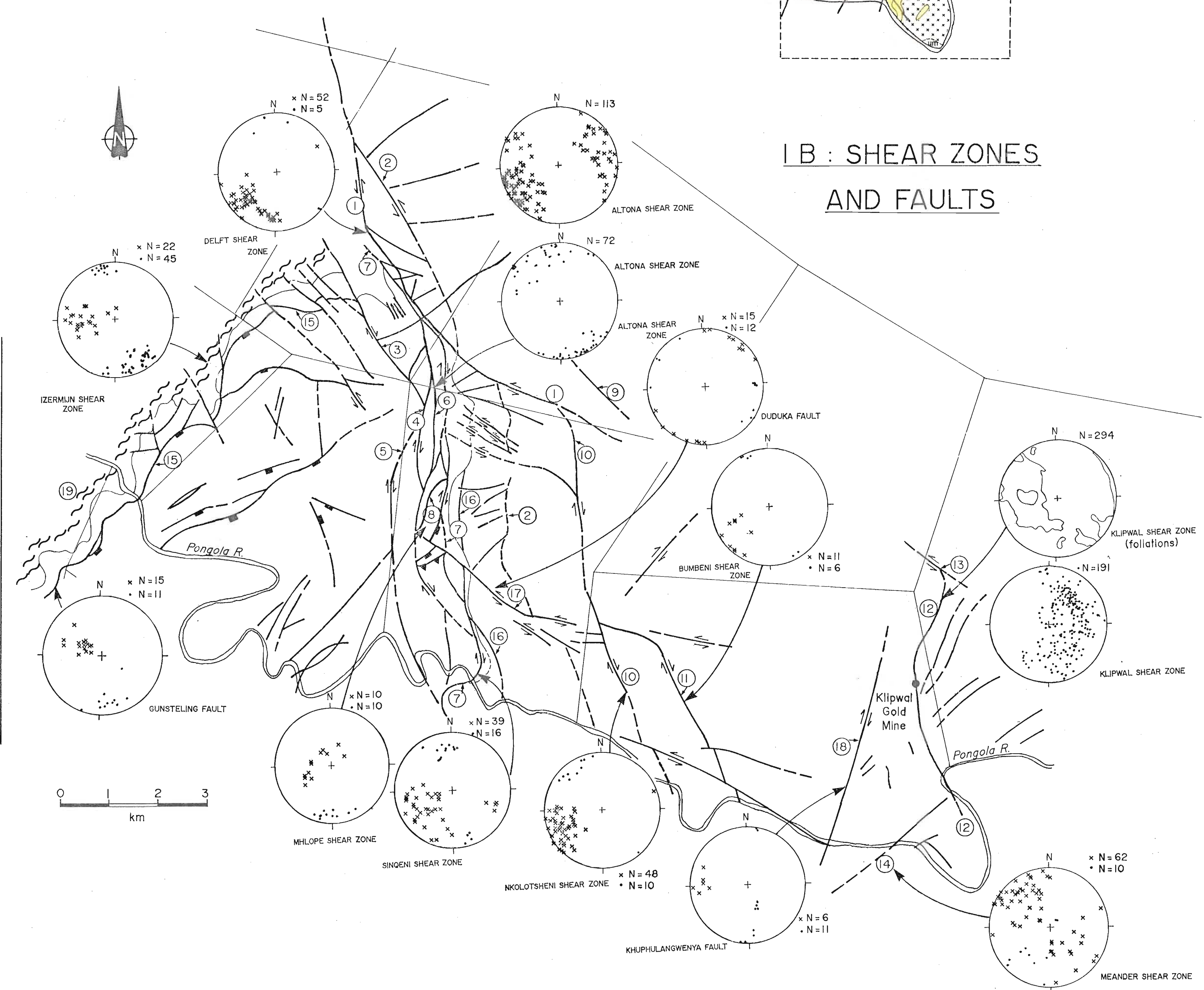
DOMAINS BETWEEN SHEAR ZONES AND FAULTS

- ① West of Gunsteling fault
- ② Between Gunsteling fault and Altona / Qumeni shear zones
- ③ Between Qumeni and Delft and Altona shear zones
- ④ Between Altona and Sinqeni shear zones
- ⑤ Between Sinqeni shear zone and the Duduka and Dwaleni faults
- ⑥ East of Delft shear zone
- ⑦ Between Sinqeni and Nkolotsheni shear zones
- ⑧ Between Nkolotsheni shear zone and Khuphulangwenya fault
- ⑨ Between Khuphulangwenya fault and Klipwal shear zone
- ⑩ East of Klipwal shear zone

STEREOPLOTS

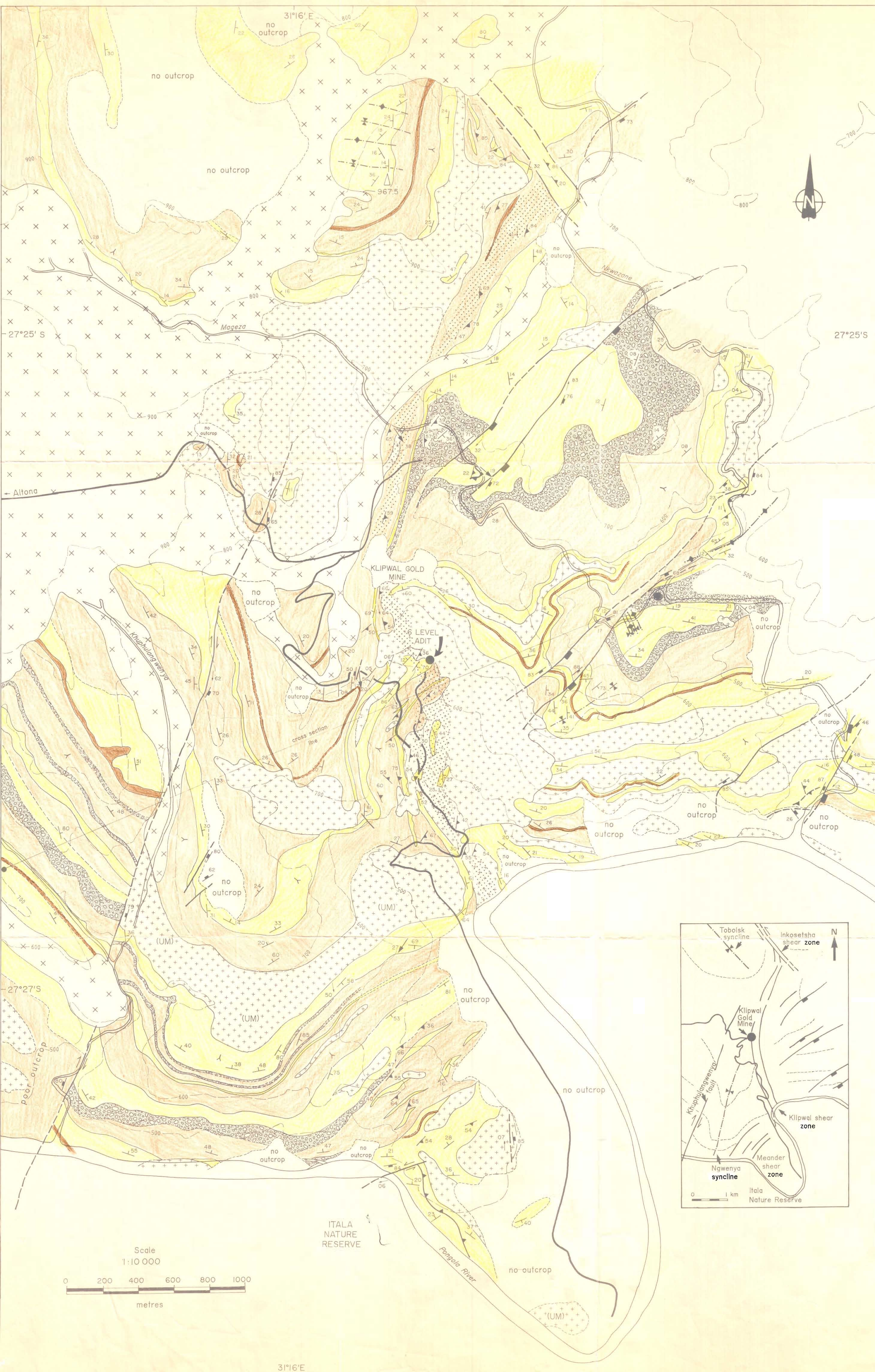
- × Poles to foliation
- Poles to bedding
- π Pi poles
- Contours at 5% intervals
- All contoured stereoplots represent poles to bedding (except where otherwise stated)

Ku Kulphiso Formation
Od Odwaleni Formation
Hl Hlashana Formation
Th Thalu Formation
Nt Ntombe Formation
Sq Sinqeni Formation



MAP 2:

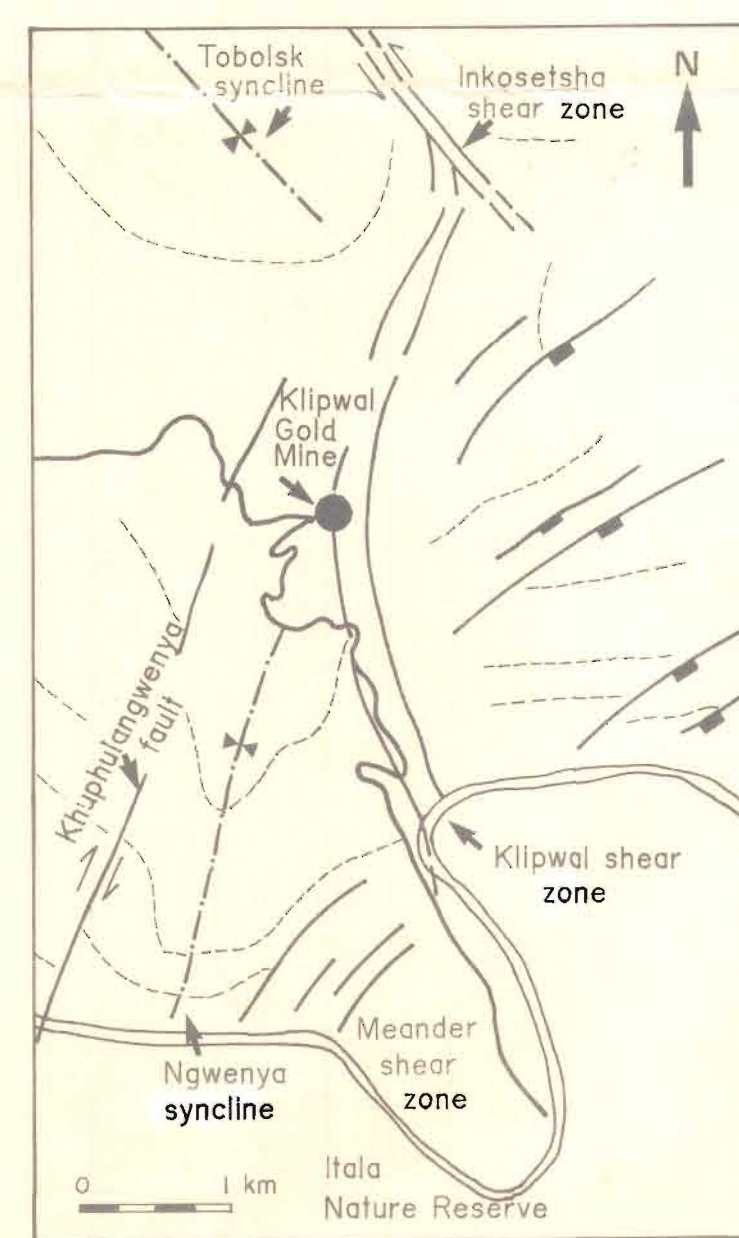
GEOLOGY IN THE VICINITY OF THE KLIPWAL GOLD MINE



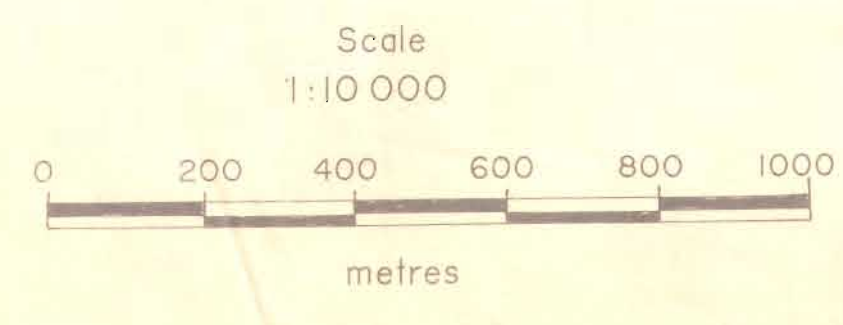
LEGEND

- Dolerites and ultramafic intrusions (UM) of various ages
- Diamictite
- Ferruginous mudstone
- Mudstone
- Sandstone
- Strike-slip shear zone
- Thrust fault
- Normal fault
- Inferred fault
- Antiformal axial trace
- Synformal axial trace
- Strike and dip of bedding
- Strike and dip of fault
- Strike and dip of cleavage in shear zone
- Trend and plunge of lineation
- Trend and plunge of slickenside
- Stratigraphic polarity
- Lithological contact
- Inferred lithological contact
- Rivers and streams
- Roads
- Contours (at 100m intervals)
- Trigonometrical station (with height above sea level)

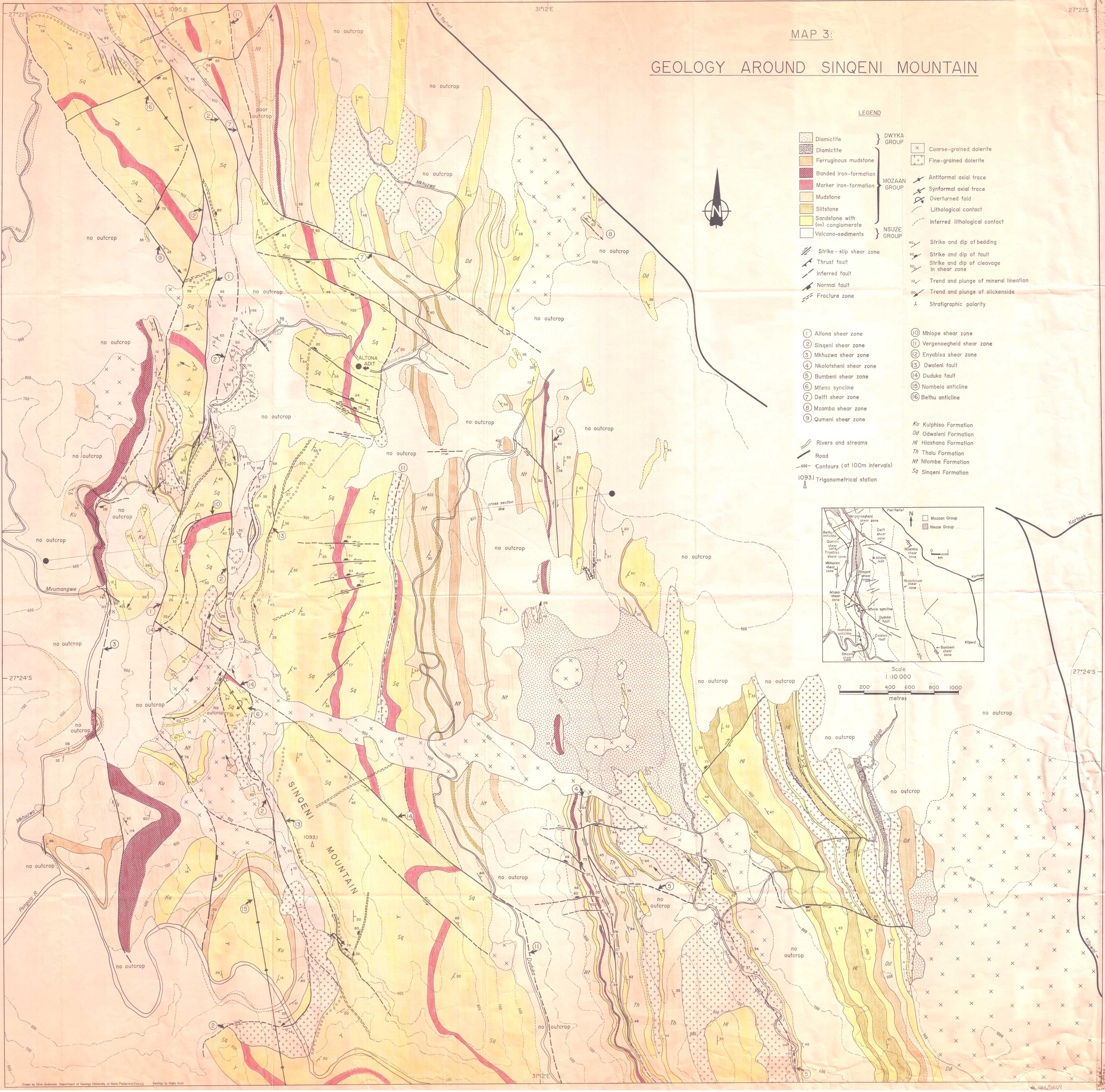
MOZAAN GROUP
(Odwaleni Formation)



Klipwal shear zone



GEOLOGY AROUND SINQENI MOUNTAIN



LEGEND

- | | | | | |
|--|----------------------------------|-----------------|--|-------------------------------|
| | Diamictite | } DWYKA GROUP | | Coarse-grained dolerite |
| | Diamictite | | | Fine-grained dolerite |
| | Ferruginous mudstone | | | Antiformal axial trace |
| | Banded iron-formation | | | Synformal axial trace |
| | Marker iron-formation | } MOZAAAN GROUP | | Overturned fold |
| | Mudstone | | | Lithological contact |
| | Siltstone | | | Inferred lithological contact |
| | Sandstone with (ca) conglomerate | } NSUZE GROUP | | Strike and dip of bedding |
| | Volcano-sediments | | | Strike and dip of fault |
| | Strike-slip shear zone | | Strike and dip of cleavage in shear zone | |
| | Thrust fault | | Trend and plunge of mineral lineation | |
| | Inferred fault | | Trend and plunge of slickenside | |
| | Normal fault | | Stratigraphic polarity | |
| | Fracture zone | | | |

- | | | | |
|--|--------------------------|--|-----------------------------|
| | 1 Altona shear zone | | 10 Mhlope shear zone |
| | 2 Sinqeni shear zone | | 11 Vergenoegheid shear zone |
| | 3 Mkhuzwa shear zone | | 12 Enyabisa shear zone |
| | 4 Nkolotsheni shear zone | | 13 Dwatani fault |
| | 5 Bumbeni shear zone | | 14 Duduka fault |
| | 6 Mfeno syncline | | 15 Nombela anticline |
| | 7 Delft shear zone | | 16 Bethu anticline |
| | 8 Mzamba shear zone | | |
| | 9 Qumeni shear zone | | |
- Rivers and streams
 Road
 Contours (at 100m intervals)
 1093.1 Trigonometrical station
- | | | |
|--|----|--------------------|
| | Ku | Kulphiso Formation |
| | Od | Odwaleni Formation |
| | Hl | Hlshana Formation |
| | Th | Thalu Formation |
| | Nf | Ntombe Formation |
| | Sq | Sinqeni Formation |

